Regulation of Neuroblastoma Malignant Properties by Pannexin 1 Channels: Role of Post-Translational Modifications and Mutations

Stephen Henry Holland

A thesis submitted in partial fulfillment of the requirements for the
Master's degree in Science specializing in Cellular Molecular Medicine

Department of Cellular Molecular Medicine
Faculty of Medicine
University of Ottawa

Abstract

Neuroblastoma (NB) is the most common extracranial solid tumour in childhood. NB is thought to arise from the failed differentiation of neural crest progenitor cells that would normally form tissues of the adrenal gland and sympathetic nervous system. These neural crest progenitors then uncontrollably proliferate forming a tumour. Despite aggressive surgery and chemotherapy, the cure rate of high-risk NB patients remains below 30%. Our laboratory has shown that human NB tumour specimens and high-risk patient derived cell lines express pannexin 1 (PANX1), and that treatment with the PANX1 channel blockers carbenoxolone or probenecid constitute reduce NB progression *in vitro* and *in vivo*. PANX1 is a glycoprotein that forms single membrane channels best known to serve as conduits for ATP release. Interestingly, while PANX1 was also detected in control neurons by western blotting, its banding pattern was strikingly different as a band at around 50 kDa was found in all NB cell lines, but not in neurons. Using shRNA targeting PANX1 and deglycosylation enzymes, I have shown that this band corresponds to a PANX1 glycosylated species. PANX1 has been reported to be phosphorylated in NB at amino acid Y10. PANX1 is also predicted to be glycosylated at N255. In order to study the role of these post-translational modifications, myc-tagged Y10F and N255A PANX1 mutants were engineered by site-directed mutagenesis. Immunolocalization and cell surface biotinylation assays suggest that the localization both mutants at the cell surface is reduced compared to that of myc-PANX1. Dye uptake assays revealed that myc-Y10F has significantly reduced channel activity. Expression of myc-Y10F and myc-N255A in NB cells inhibited cell proliferation and decreased metastatic potential *in vitro*. Further analysis of NB tumour specimens revealed that there is a missense mutation in *PANX1* resulting in the formation of truncated peptide (amino acid 1-99). Interestingly, I have

found that when co-expressed with myc-PANX1, $PANX1^{1-99}$, reduced PANX1 channel activity. Taken together, these findings indicate that phosphorylation on Y10 and glycosylation on N255 regulate PANX1 channel activity and exacerbate NB malignancy, while the expression of $PANX1^{1-99}$ in NB may be beneficial.

Acknowledgments

I would like to thank my supervisor, Dr. Kyle Cowan, as well as Dr. Stéphanie Langlois for providing me with this wonderful opportunity. I am extremely thankful for their excellent leadership throughout my Master's degree, and for sharing their passion of science with me. I would also like to thank my Thesis Advisory Committee, Dr. Marjorie Brand and Dr. Christina Addison, for their guidance and support. Furthermore, I would like to thank all laboratory members, notably Xiao Xiang, Marie-Eve St-Pierre, Anna Blinder, Emily Freeman and Sanaz Karami, for their friendship and constant encouragement. I am grateful to have been part of the amazing community at CHEO Research Institute, which made coming to the lab everyday enjoyable. I would like to extend my gratitude to Lynn Kyte for dealing with all the orders and organizing CHEO RI fundraising events. I would also like to thank Keith for all his help with organizing the lab space, and for our morning daily discussions. Lastly, I would like to thank my family, friends, and girlfriend, Alexa Quarrington, for their love and support throughout my studies.

Table of Contents

List of Figures

List of Table

List of Abbreviations

a.a	Amino Acid
^{10}Panx1	Peptide Based Inhibitor of Pannexin 1
ADAMs	A Disintegrin and Metalloproteinases
ALK	Anaplastic Lymphoma Kinase
ANOVA	Analysis of Variance
AP-2β	Activating Enhancer Binding Protein 2 Beta
Ascl1	Achaete-Scute Family BHLH Transcription Factor 1
ATP	Adenosine Triphosphate
BrdU	Bromodeoxyuridine or 5-bromo-2'deoxyuridine
BTK	Bruton's Tyrosine Kinase
CaMKII	Calcium/Calmodulin-Dependent Protein Kinase II
cAMP	Cyclic Adeonsine Monophosphate
CBX	Carbenoxolone
CD4	Cluster of Differentiation 4
Cdx2	Caudal Type Homeobox 2
cGMP-PK	Cyclic Guanidine Monophosphate
c-myc	Myc Proto-Oncogene, BHLH Transcription Factor
CIL	Contact Inhibition of Locomotion
CNS	Central Nervous System
CREB	Cyclic Adenosine Monophosphate Responsive Element Binding Protein
Cx43	Connexin 43
Cys/C	Cysteine
DEA NONOate	Diethylamine NONOate
DMEM	Dulbecco's Modified/Eagle's Medium
EDL	Extensor Digitorum Longus
Edt^{+}	Ethidium
ERK	Extracellular Signal Regulated Kinase
eGFP	Enhanced Green Fluorescent Protein
EGFR	Epidermal Growth Factor Receptor
EMT	Epithelium-to-Mesenchymal Transition
ER	Endoplasmic Reticulum
ERAD	ER-Accelerated Degradation
ETV3-5	ETS Variant 3-5
FGF	Fibroblast Growth Factor
FGFR1	Fibroblast Growth Factor Receptor 1
Fgr	FGR Proto-Oncogene, Src Family Tyrosine Kinase
FOXD3	Forkhead Box D3
GATA2/3	GATA Binding Protein Type 2/3
GLT25D1	collagen β(1-O) galactosyltransferase
Gly0	Unglycosyalted Pannexin 1
Gly1	High Mannose Species of Pannexin 1
Gly2	Complex Glycosylated Species of Pannexin 1
GNSO	S-nitrogluthione
Grhl2/3	Grainyhead-like protein 2/3
Hand2	Heart and Neural Crest Derivates Expressed 2

HBP1	Hight Mobility Group Box Transcription Factor 1
HCC	Hepatocellular Carcinoma
HEK293T	Human Embryonic Kidney Cells
HIF1	Hypoxia Inducible Factor 1
HIV	Human Immunodeficiency Virus
IGFR1	Insulin Growth Factor Receptor 1
IL-6	Interleukin 6
INRG	The International Neuroblastoma Risk Group
Insm1	Insulinoma-Associated Protein 1
INSR	Insulin Receptor
INSS	The International Neuroblastoma Staging System
IP3	Inositol (1,4,5) Triphosphate
JAK/STAT	Janus Kinase/Signal Transducer and Activator of Transcription
JAK2	Janus Kinase 2
JNK	C-Jun NH2-Terminal Kinases
JUNB	Proto-Oncogene, Activator Protein 1 Transcription Factor Subunit
KCNQ1	potassium voltage-gated channel superfamily Q member 1
kDA	KiloDalton
Let-7	MicoRNA Let-7
Lin28B	Lin-28 Homolog B
LOH	Loss of Heterozygosity
Λ-PP	Lambda Protein Phosphatase
LXRs	Liver X Receptors
M	Mesoderm
MASH-1	Achaete-Scute Family BHLH Transcription Factor 1
MG132	Triterpene, peptide-aldehyde proteasomal inhibitor
MGAT1	α-1,3-mannosyl-glycoprotein 2-β-acetylglucosaminyltransferase
MGAT4B	α-1,3-mannosyl-glycoprotein 4-β-acetylglucosaminyltransferase
MM	Multiple Myeloma
MMPs	Matrix Metalloproteinases
Msx1	Msh Homeobox 1-Like Protein
MYCN	Proto-Oncogene, BHLH Transcription Factor
Myc-N255A	PANX1 with C-terminal myc-ddk tag; Asparagine→Alanine at 255
Myc-PANX1	C-terminal myc-ddk tagged PANX1
Myc-Y10F	PANX1 with C-terminal myc-ddk tag; Tyrosine→Phenylalanine at 10
N	Notochord
NC	Neural Crest
NB	Neuroblastoma
NEGF-2	Neurite Growth Promoting Factor 2
NF	Neurofilament
NMDA	N-Methl-D-Aspartate
NO	Nitric Oxide
Notch	Notch Protein Pathway
NPM-ALK	Nucleophosmin 1-anaplastic lymphoma kinase
P2X	Purinergic Receptor 2 like 1-7
P2Y	Ionotropic Receptor 2 like 1, 2, 4, 6, 11, 12, 13, 14
$PANX1^{1-89}$	PANX1 truncation of 89 amino acids

$PANX1^{1-99}$	PANX1 truncation of 99 amino acids
$PANX1^{1-181}$	PANX1 truncation of 181 amino acids
PANX1/Panx1	Pannexin 1
PANX2/Panx2	Pannexin 2
PANX3/Panx3	Pannexin 3
Pax3	Paired Box 3
PBN	Probenecid
PDGFR	platelet derived growth factor receptor
Phox2A/B	Paired Like Homeobox 2A/2B
PI3K	Phosphoinositide 3-Kinase
PKA	Protein Kinase A
PKC	Protein Kinase C
PKG	Protein Kinase G
PLCγ	Phosphoinositide phospholipase C
PMNT	Phenylethanolamine N-methyltransferase
Poly-HEMA	Poly(2-hydroxyethyl) methacrylate
PRDM1	PR Domain Zinc Finger Protein 1
PTMs	Post-Translational Modifications
RAS/MAPK	RAS Guanosine triphosphatases/Mitogen-Activated Protein Kinase
RNA	Ribonucleic Acid
RyR1	Ryanodine Receptor Type 1
SCG10	Superior Cervical Ganglion-10 Protein
Snail2	SNAIL Family Zinc Finger 2
Ser/S	Serine
SERCA	Sarcoplasmic and Endoplasmic Reticulum Calcium ATPases
Shh/BMP	Sonic HedgeHog Protein/Bone Morphogenetic Protein
shCTL	Short-Hairpin Scrambled Sequence
shPANX1	Short-Hairpin PANX1 Sequence
SNP	Sodium Nitroprusside
Sox1, 4, 9, 10	SR-Box Type 1, 4, 9, 10
Src	Proto-Oncogene, Non-Receptor Tyrosine Kinase
Stage MS/4S	Special low-risk stage of NB; spontaneous regression
STAT3	Signal Transducer and Activator of Transcription Type 3
TERT	Telomerase Reverse Transcriptase
TH	Tyrosine Hydroxylase
Thr/T	Threonine
TNFα	Tissue Necrosis Factor alpha
TRAP2a	Encodes PSMD2 (S6S Subunit, non ATPases 2
TRPC5	transient receptor potential 5
TWIST1	TWIST Basic Helix-Loop-Helix Transcription Factor 1
TYK2	Tyrosine Kinase 2
Tyr/Y	Tryosine
UGGT1	UDP-Glucose glycoprotein glycosyltransferase
VEGF	Vascualr Endothelial Growth Factor
Wnt	Wingless Signalling Pathway
ZAP70	Zeta Chain of T-Cell Receptor Associated Protein
Zic1/2	Zinc Finger Protein 1/2

1.0 Introduction

1.1 Development of the Neural Crest and Neural Crest Stem Cell Differentiation

In vertebrate embryogenesis, the neural crest (NC) forms and gives rise to a diverse group of cell types such as peripheral neurons[1], enteric ganglia[2], melanocytes[3], Schwann cells[4], sympathetic nervous system[5], adrenal medulla[6], cartilage[7], bone[7], tendons[8], connective tissues[9], endocrine[10] and adipose tissues[11]. NC development is a complex pathway that arises in early embryogenesis involving multipotent neural stem cell precursors that control formation of these diverse cell groups. The NC is formed through distinct stages. After gastrulation resulting in three germ layers being formed, specification and development of the neural tube occurs early in the first trimester of fetal development through the process of neurulation[12]. Neurulation results in the formation of neural folds occurring between sections of the neural ectoderm and epithelial ectoderm[12]. Overtime, this neural tube closes resulting in the completion of the first stage of NC development which occurs approximately 28 days post-fertilization[12]. Closure of the neural tube is a complex process that is regulated by cellular events and molecular control of the Wnt/planar cell polarity pathway, Shh/BMP signalling, and the activity of several transcription factors such as Grhl2/3, Pax3, Cdx2 and Zic2[13]. This is summarized in Figure #1 below.

After the neural tube has closed, NC stem cells are released form the neural tube. Once released, these cells undergo epithelium-to-mesenchymal transition (EMT), enabling progenitor cells to differentiate into the many tissue types described above[13]. During EMT, NC cells separate from the neuroepithelium and the ectoderm through a global switch from cadherin-1 (E) to cadherin-2 (N) usage, as well as expression of weaker cadherins (6, 7, and 11) resulting in contact inhibition of locomotion (CIL)[14]. CIL is a process that relies on cell-

to-cell contact signalling. Indeed, the loss of cadherin-1 results in the repolarization of protrusion via loss of cellular contacts[14]. The process of CIL and cadherin switch is stimulated by an upregulation of a series of transcription factors (ZIC1, PAX3, TPAP2a, Notch, and PRDM1) which further aid the EMT and NC induction[14]. The expression of these transcription factors push cells to initiate the process of CIL through cadherin switch, and activation of metalloproteinases[15]. Matrix metalloproteinases (MMPs) and, a disintegrin and metalloproteinases (ADAMs) allow for the remodelling of the extracellular matrix, and regulate NC migration[15]. Importantly, ZIC1, PAX3, and Msx1 allow for the expression and activation of Snail2, FOXD3, TWIST1, and Sox9[16,17]. These transcription factors aide in NC speciation by downregulating the expression of cellular adhesion proteins and activation of cadherin-N[18,19]. The process described above is termed delamination of NC cells, which accounts for the second stage of neural crest differentiation into the sympathoadrenal lineage.

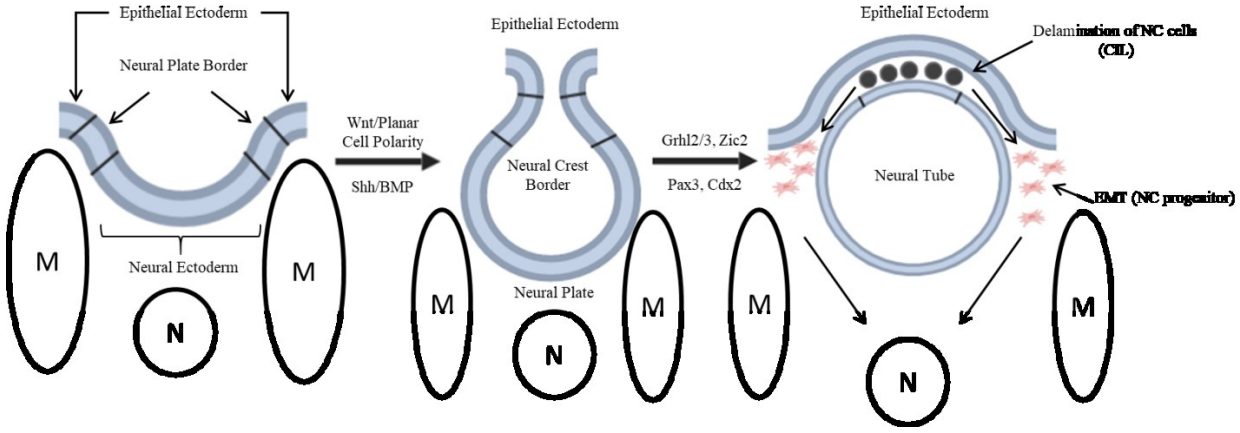

Figure 1: The Process of Neurulation: termed as the fourth germ layer, formation of the neural tube through neurulation occurs early in embryogenesis. During embryogenesis, the neural ectoderm/neural plate boarder are bud towards the notochord (N), which can be found between each mesoderm (M). Through various cellular pathways such as Wnt, and Shh/BMP signalling, the invagination of the neural crest increases in depth forming the neural plate. Eventually, the neural tube closes with expression of transcription factors Grhl2/3, Zic2, Pax3, Cdx2. Eventually, delamination from the neural tube promotes NC stem cells through a process of EMT. During EMT, the NC progenitor migrate distally from the neural tube, where sympathoadrenal lineage can be speciated from the neural crest precursor. Image created with BioRender, modified from[20].

The final stage of NC differentiation is the NC speciation into the sympathoadrenal lineage. After the loss of adhesion, NC cells then activate BMP, Wnt, and FGF signalling pathways to differentiate mesenchymal stem cells into a late phase mesenchymal[21–24]. Importantly, these cells express a cumbersome number of pro-survival and pluripotency factors such as SOX10, FOXD3, C-myc and MYCN[19,25,26]. These factors allow for NC cells to evade apoptosis and remain in a proliferative state. Pluripotent late phase mesenchymal cells can differentiate into the numerous tissues that arise from the NC. Sympathoadrenal precursor cells are produced through the differentiation of the NC cell through expression of several transcription factors, such as Phox2B[27,28], Ascl1[29], Insm1[30], Hand2[31], MYCN[32], Gata2/3[31,33,34] and AP-2β[35], which drive early the differentiation processes. Phox2B and Sox proteins appear to be the master regulators for this process. Expression of Phox2B maintains MASH-1 which is directly involved in the synthesis of catecholamines and is maintained by GATA2/3[28,34]. MASH-1 expression activates Phox2a which is also expressed in late phase differentiation and is closely regulated to Phox2B[36]. Subsequently, Sox transcription factors, in particular SoxC/E proteins 10, 4, 11, are also expressed in late phase differentiation[25,37,38].

The sympathoadrenal differentiation of the NC crest results in the formation of sympathetic neurons or chromaffin cells, sharing similar characteristics. Such similarities include expression of catecholamine synthesizing enzymes, such as tyrosine hydroxylase and dopamine-β-hydroxylase[39]. The main difference between the formation of the sympathetic neuron and chromaffin cells, is that chromaffin cells express phenylethanolamine N-methyltransferase (PMNT), which induces adrenaline synthesis[40]. Sympathetic neurons by contrast express neurofilament and SCG10, which stimulates neurite outgrowth, and is

regulated by Phox2B overexpression and inactivation of MASH-1[39,41]. This process is summarized in the Figure #2 below.

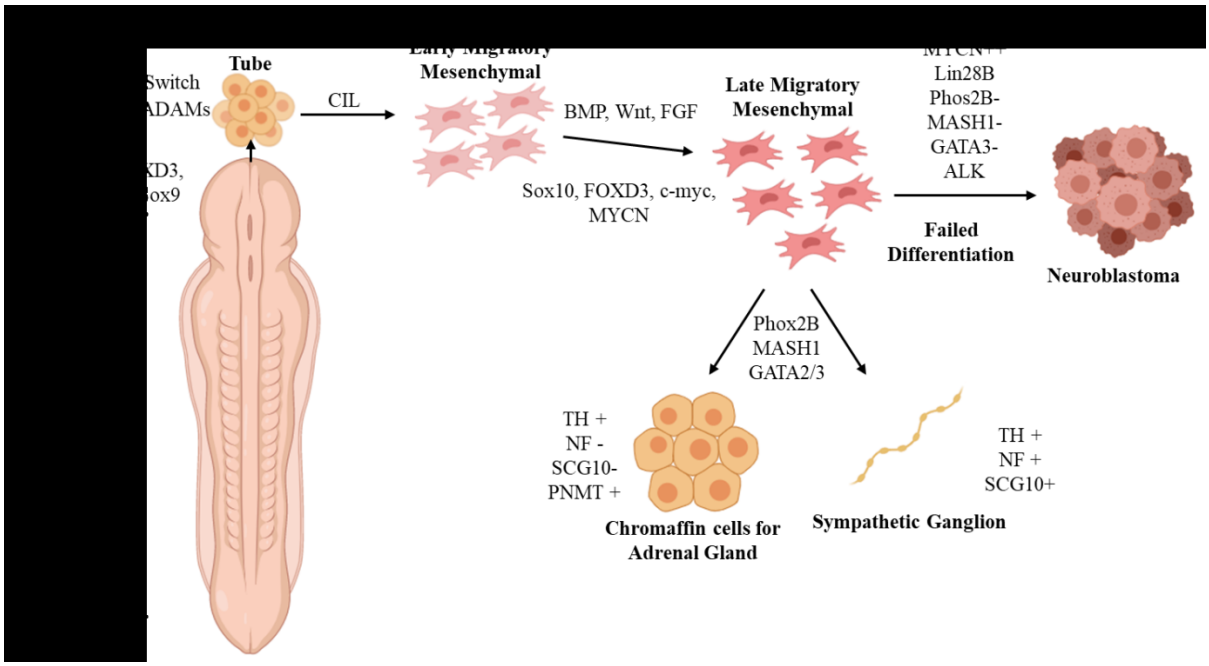

Figure 2: The Sympathoadrenal Lineage of the NC Progenitor Cell and Failed Differentiation Leads to NB: the neural tube release NC cells that undergo EMT transition, through delamination of the NC. This process requires, cadherin switch, activation of MMPs and ADAMs, and activation of transcription factors Snail2, FOXD3, TWIST1, and Sox9. The resultant contact inhibition of locomotion (CIL) produces cells that migrate dorsally and then laterally around the neural tube. Once migration occurs, BMP, Wnt, and FGF activate neural stemness and proliferation. Furthermore, activation of pro-survival genes such as Sox10, FOXD3, c-Myc, and MYCN promotes survival and proliferation. Eventually, sympathoadrenal speciation occurs through overexpression of Phox2B, MASH1 and GATA2/3 help promote differentiation into chromaffin and/or sympathetic ganglion. These endpoint cells share similarities that are derived from the same neural stem cell. For example, both cells express tyrosine hydrolyse (TH), but sympathetic ganglia express neurofilament (NF) and SCG10. Chromaffin cells do not express NF and SCG10, but expresses PMNT, and other enzymes required for catecholamine synthesis. However, due to unknown circumstances, culminating genetic, proteomic, and biochemical changes affecting the activation of stemness factors there is failure of differentiation into the sympathoadrenal lineage. Over-expression of pro-survival and pro-proliferative promotes formation NB tumour. Indeed, several genes have been shown to be dysfunctional in NB specimens. By example, MYCN, ALK, Lin28B, MASH1, GATA3, Phox28B, chromosomal aberrations, and DNA ploidy have all be implemented in the NB malignant phenotype. Image created with BioRender.

1.2 Neuroblastoma Overview

Neuroblastoma (NB) is the most common extracranial solid tumour in childhood[42]. NB originates from the failed differentiation of the NC precursor cell derived from the sympathoadrenal lineage of the NC. Clinically, 90% of patients diagnosed with NB are <10 years of age with a median age of 18 months[43]. NB tumours arise anywhere in the sympathetic nervous system as a result of their sympathoadrenal origin with approximately >50% occurring in the adrenal medulla[44]. NB is an aggressive form of cancer with a metastasis rate of ~50% at diagnosis. Metastasis are frequently present in regional lymph nodes, bone/bone marrow, skin, and liver[45,46].

1.3 Genetic and Prognostic Indicators of Neuroblastoma

To acquire the NB phenotype many genetic factors that encompass genetic mutations, protein expression, and chromosomal instability have been shown to occur.

1.3.1 MYCN Amplification, a current prognostic marker in Neuroblastoma

The MYCN proto-oncogene serves as a regulator for fundamental cellular processes including differentiation, proliferation, and survival[47,48]. In healthy patients MYCN expression is restricted to the forebrain, hindbrain, and kidneys[49]. In NB, *MYCN* amplification has been associated with a poor outcome and is detected in approximately 20% of all NB cases[50,51]. *MYCN* amplification has since been the most frequently used prognostic indicator for NB patients[50]. Interestingly, MYCN amplification is associated with high-risk patients, whereas, in Stage MS/4S patients, which display spontaneous regression, a MYCN non-amplified state is observed[52]. In high-risk NB with *MYCN* amplification, expression of MYCN target genes is enhanced[53]. Downstream targets of MYCN include expression of pro-neural genes *ASCL1*

(MASH1/HASH1), and stem cell lineage-determining factors, *Phox2B* and *Hand2,* which both have been implicated in NB progression[53,54]. Furthermore, MYCN amplification in NB has been linked to the failed differentiation of NB precursor cells, as a result of supressed neural differentiation markers, nerve growth factor, and estrogen[55]. MYCN also aides in the maintenance of NC cells, however, induced *MYCN* amplification has been shown to result in the NB phenotype[56].

1.3.2 Lin28B, the inhibitor of miRNA family Let-7, associated to poor NB prognosis

During normal development the RNA binding protein Lin28B regulates the expression of the miRNA family called let-7. Let-7 is a tumour suppressor miRNA, which is induced in embryogenesis and during brain development and is frequently downregulated in various cancers[57]. Lin2B serves as an inhibitor for let-7 biogenesis[58]. In NB, Lin28B has been shown to be genetically unstable and overexpressed, as a result of single nucleotide polymorphisms found in the *Lin28B* gene[58,59]. Lin28B is frequently overexpressed in NB tumour specimens in association with MYCN amplification[58,59]. Interestingly, one study has indicated that overexpression of Lin28B in the sympathoadrenal cell lineage induces the development of NB associated with low let-7 expression and high MYCN implication[58]. An additional study indicated that NB tumours with Lin28b overexpression have fewer genomic events to those with MYCN and ALK overexpression, suggesting it as an oncogenic driver[59]. In most cases, Lin28B overexpression is associated with a gain in chromosome 3, which has been attributed to a poor outcome[59]. Currently, there is a paucity of therapeutic strategies targeting the Lin28B-let-7 interaction, however targeting this pathway should focus on increasing Let-7 expression or reducing Lin28B inhibitory activity.

1.3.3 Gain-of-Function Mutations of ALK in NB

The *ALK* gene corresponds to the anaplastic lymphoma kinase (ALK) receptor and is altered in NB with a gain-of-function mutation in 14% of high-risk NB patients[60–62]. ALK functions as a tyrosine kinase, which has been described as an oncoprotein when complexed to Nucleophosmin 1 (NPM-ALK) in lymphoma cells[63,64]. In NB, a single-base pair missense mutation occurs in the regulatory regions of the kinase domain (R1275, F1174, F1245) of ALK disrupting its auto-inhibitory function[62]. ALK signals through multiple downstream pathways that stimulates transcription of ETV3-5[65], MYCN[66,67], VEGF[68], HIF1[69], c-myc[70], STAT3[71], cyclin-D[72], JUNB[65,73], and HBP1[74], and regulates a host of cellular processes including survival[75], proliferation[76], cell cycle[77,78], and metastasis[66]. Importantly, ALK has been shown to function through neurite growth promoting factor-2, NEGF-2, or Midkine, which are important for the regulation sympathoadrenal lineage proliferation during development[76]. Furthermore, ALK is implicated in JAK/STAT, RAS/MAPK, PI3K, and PLCγ pathways, all which are key contributors to sympathoadrenal lineage formation and are commonly dysregulated in NB development[79–83].

1.3.4 Loss of sympathoadrenal differentiation markers in NB

Sympathoadrenal speciation of the NC progenitor cell is a complex differentiation process that requires an abundant array of genes that encompass NC induction, NC border speciation, NC speciation, and sympathoadrenal speciation. In NB some of these corresponding genes have been associated to the failed differentiation of NC stem cells during the formation of the NB phenotype. Of note, some of these modifications include a germline loss-of-function mutation in *Phox2B* which is reported in both familial and high-risk NB tumour specimens[84,85]. *Phox2B* is a regulator of sympathoadrenal differentiation from the late mesenchymal cell stage, in part as a result of BMP signalling which activates *Phox2A* and

Phox2B expression[86,87]. *Phox2B* has been identified to have missense mutations in conserved regions as well as frameshift mutations that result in protein truncation and reduced protein function[88]. Furthermore, other factors that have been reported to be misregulated in NB include *HAND2* and *GATA3* enzymes which regulate transcription of norepinephrine synthesis[89]. High expression of GATA3 and HAND2 appear to be associated with proliferation and self-renewal, and their increased activity in NB forces cells into acquiring sympathoadrenal characteristics[33]. *GATA3* appears to be linked with expression of *Phox2B* and *Mash1* transcripts which control stem cell fate promoting sympathoadrenal speciation[34]. Furthermore, *GATA3* down-regulation in NB appears to increase cyclin D1 expression promoting a persistent proliferative state[90]. In addition, early NC cell induction genes, such as BMP[87], STAT3[91], Wnt[23], and Notch/Delta[92], have all been implicated in NB in which their dysregulation leads to downregulation of their respective signalling pathways maintaining a proliferative state by inhibiting NC differentiation. Lastly, *TWIST1* has been known to initiate delamination of the EMT late phase mesenchymal cells. In NB however, *TWIST1* transcribes into an inhibitor of apoptosis promoting cell survival and is commonly upregulated to MYCN amplified NB specimen[23,93,94].

1.3.5 Chromosomal Instability

Chromosomal instability in NB has been heavily analyzed and incorporated into the current NB (International Neuroblastoma Staging System (INSS) and International Neuroblastoma Risk Group (INRG)) classification systems. Studies have demonstrated that chromosomal aberrations and DNA ploidy/index[95,96] can contribute to NB malignancy. The genetic events show allelic loss on chromosomes 1p, 11q, 14q, 4p, 7q, 2q, 3p, and 19q[97–105]. This genetic loss-of-heterozygosity (LOH) corresponds to a poor outcome in many studies. By example, chromosomal aberrations such as LOH 1p36 (23%), 11q23 (34%), and unb11q were

features found in high-risk NB tumour specimens associated with MYCN oncogene amplification[106]. Furthermore, there have been allelic gains on chromosomes 2p, 17q, 18q, 1q, 7q, and 5q which have been implicated in growth control[60,105,107–109]. Notably, chromosome 2p contains MYCN which when amplified is strongly associated to clinical aggressiveness, advanced stages diseases, and treatment failure[45]. Furthermore, gain of 17q is strongly associated to MYCN amplification in high-risk NB[110]. High risk NB also displays genomic rearrangement at 5p15.33, controlling expression of *TERT* (telomerase reverse transcriptase), leading to increased TERT expression, downstream DNA methylation, and further chromosomal changes[111]. Chromosome 5p has also been shown to undergo chromothripsis which downregulates expression of stem cell differentiation factors[112]. Furthermore, more aggressive NB tumours display increased total copy number variances in Stage 4/M diseases but significantly reduced in Stage MS/4S NB specimens[113]. Altogether, these findings suggest that chromosome instability is a key feature of NB that may drive tumourigenesis.

1.4 Pannexin Family of Proteins Overview

Pannexins are large pore and metabolite channels which were discovered in the early 2000s through their sequence homology to the invertebrate gap junction forming proteins called innexins[114]. Since their discovery in the early 2000s, the Pannexin family has increased to three family members: Pannexin 1 (426aa) (PANX1 in human; Panx1 in rodents), Pannexin 2 (677aa) (PANX2 in human; Panx2 in rodents), Pannexin 3 (392aa) (PANX3 in human; Panx3 in rodents)[114,115]. Originally, it was proposed that Pannexins serve similar features to that of connexins, the large superfamily of vertebrate gap junctions, however in mammalian cells pannexins do not form gap junctions but rather single membrane channels[116]. Upon comparing pannexins and connexins there is no sequence homology, however, they do share

similar structural topology. Pannexins and connexins contain four α-helical transmembrane domains, with two extracellular loops, and one intracellular loop[117]. The N- and C-terminal tails both extend from the plasma membrane and are exposed intracellularly[117]. This can be visualized in Figure #3. Noticeably, there are some differences between the structure of the various pannexins. Visually, PANX2 contains a larger C-terminal domain which may constitute addition regulatory functions that differ from the pannexin family[118].

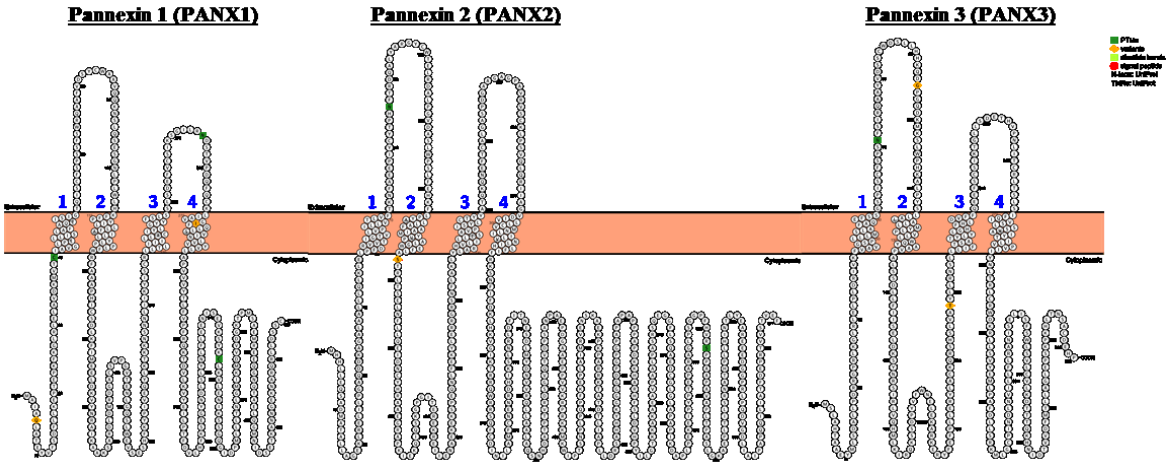

Figure 3: Topology of the Pannexin Family of Membrane Channels: Prepared using Protter, a software program that can map out the 2-D membrane topology of respective proteins. The Pannexin family of membrane channel proteins is composed of three species: Pannexin 1 (PANX1), Pannexin 2 (PANX2), Pannexin 3 (PANX3). Each family member contains four transmembrane domains, similar to that of their innexin (invertebrate) and connexin (vertebrate) gap junctional proteins counterparts. As noted, PANX2 contains a longer C-terminal tail, than both PANX1 and PANX3, which may give rise to alternative regulatory mechanisms.

Each member of the pannexin family has a distinct expression profile. PANX1 has the most diverse expression profile. In specific, PANX1 has expressed in: the sensory systems of the inner ear[119–121], eye[122], taste buds[123], olfactory epithelium[124]; the brain, specifically in the regions of cerebellum, cortex, neocortex, hippocampus, amydgala, substantia nigra, neurons, and glial cells [125–127]; the cardiovascular system, specifically pertaining to erythrocytes[128], arteries[129], arterioles[129], cardiac myocytes[130], heart[129]; and in tissues corresponding to exocrine

glands[131]; as well as in the prostate[132], liver[133], adrenal gland[134], lung epithelial[135], skin[136,137], skeletal muscle[138], and colon[139]. As a result, PANX1 expression is largely ubiquitous throughout the human body. PANX2 has been shown to have a more restricted distribution, being expressed primarily in the central nervous system (CNS). As such, PANX2 can be found in the cerebral cortex[140], cerebellum[140], astrocytes[140], hippocampus[140], retina[141], and gastrointestinal tract[141]. PANX3, also with a more restricted distribution to that of PANX1, is primarily expressed in skin[137], osteoblasts[142], cartilage[142], skeletal muscle[138], cochlea[143], and duodenum of the small intestine[144].

Based on their abundant expression profile in tissue, pannexins have been linked to a wide variety of physiological responses in the human body. PANX1 has been implicated in blood pressure regulation[145], taste response[146,147], glucose uptake[148,149], airway defence[135,150], keratinocyte differentiation[137], skeletal muscle myogenesis[138], ischemic cell death[151], epileptic seizure[152,153], immune response[154–159], apoptotic cell clearance[157,160], tumourigenesis and tumour metastasis[161–163], morphine withdrawal responses[164], stroke[151,165,166], inflammatory bowel disease[139,167,168], and neuropathic pain induction[169]. PANX2 has been implicated in neuronal differentiation[170] and development[141], and in ischemia/brain injury responses[166,171]. Lastly, PANX3 has been shown to be involved in bone[142], skeletal muscle[138]and skin development[137]. The remainder of this thesis will primarily focus on PANX1.

PANX1 and PANX3 forms hexameric protein channels through the oligomerization of six subunits[172,173], while PANX2 forms an eight-octameric protein channel[117]. The hexameric PANX1 are termed pannexons. Pannexins, similar to the connexon family of channel proteins, have been shown to intermix by forming homologous and heterologous protein channels[174]. PANX1 and PANX2 have been shown to intermix, which can be regulated by N-linked

glycosylation[133,175]. However, PANX3 has not been shown to intermix with either PANX1 or PANX2 and form only homologous pannexon channels[176]. Intermixing of Panx1 and Panx2 has been associated to reduced channel activity when expressed *Xenopus* oocytes, however, endogenous expression of Panx1/Panx2 heteromeric channels increased instability over time as compared to their homomeric counterparts[175]. However, further understanding of this interaction is essential to elucidate possible differences in their interactome when homomeric versus heteromeric channels are formed.

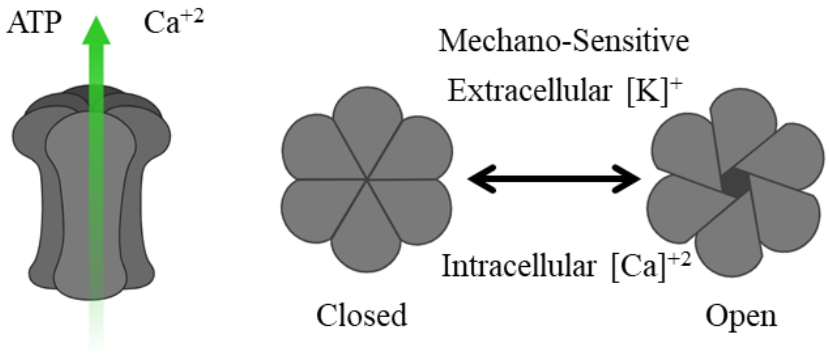

Figure 4: Pannexins form homologous/heterologous protein channels that regulate ATP and calcium in the cell: PANX1 has been shown to serve as a calcium leak channel in the ER and an ATP release channel at the cell surface. PANX1 channel activity has been shown to be regulated by mechanical stimulation/membrane stretch, elevated extracellular potassium concentration of 10mM, and elevated intracellular calcium concentration which serve to activate/open PANX1 channels. PANX1 when in a hexameric formation is called a pannexon, which can form homologous (all PANX1) or heterologous species (PANX1 channel intermixing with PANX2), but the later has not been identified in mammalian cells.

Pannexin channels allow the passage of molecules of up to 1 kDa[177]. Typically, pannexins have shown to mediate adenosine triphosphate (ATP) release at the plasma membrane and serve as a calcium leak channel in the endoplasmic reticulum (ER)[128,178,179]. Biologically, ATP release constitutes a signalling molecule that has been shown to have direct interaction with other membrane bound proteins. By example, PANX1 channels can be activated by ionotropic P2X and metabotropic P2Y receptors through ATP-induced ATP

release, which can be inhibited by a negative feedback loop through increased extracellular ATP concentrations[178,180,181]. Calcium release also serves as a secondary messenger signalling molecule. Organelles such as the endoplasmic reticulum and/or sarcoplasmic reticulum contain a high intra-organelle calcium concentration through sarcoplasmic and endoplasmic reticulum calcium ATPases (SERCA) family calcium pumps[179]. To balance the influx of calcium from SERCA pumps, calcium leak channels are in place to allow for a steady state to be maintained[179]. PANX1 channels were first documented to serve as a calcium leak channel in the ER by Abeele et al., 2006[179]. Since then, it has been documented that increased intracellular calcium concentration can activate PANX1 channels, however, the exact mechanism of activation by calcium has not yet been indentified[134,178,182,183].

Pannexin channels have also been demonstrated to be mechano-sensitive by Bao et al. 2004, in a heterologous expression system with *xenopus oocytes*[184]. Recently, it has been demonstrated in human breast cancer that mechano-sensitivity of PANX1 channels contributed to the metastatic potential of breast cancer as they pass through the vasculature[162]. Bhalla-Gehi et al., 2010 proposed that the mechanism for this might be through interaction of the C-terminal of PANX1 with F-actin, thus tethering it to the cellular cytoskeleton to induce channel activation[185]. Indeed, PANX1 channels have been demonstrated as well to be activated by membrane stretch[128,183]. This was demonstrated in erythrocytes exposed to a hypotonic solution which caused cell swelling leading to ATP release via PANX1[128].

PANX1 channels have also been shown to be activated by high concentrations (10mM) of extracellular potassium[156]. This discovery was established under voltage clamp conditions and was shown not to be as a result of membrane depolarization, leading to the discovery that potassium may interact with the first extracellular loop of PANX1[156,186].

PANX1 has also been shown to be activated by increased intracellular calcium, particularly when coupled with metabotropic receptors Gαq-containing heterotrimeric G proteins[178]. In particular, P2Y receptors, P2Y1 and P2Y2, when co-expressed with PANX1 showed increased ATP release as a result of PANX1 activation[178]. In this setting, the addition of a calcium ionophore caused a dose-dependent channel activation of PANX1, leading to elevated ATP release. PANX1-mediated release of ATP causes activation of P2Y receptors, leading to activation of inositol (1,4,5) triphosphate (IP_3)[178] and protein kinase C. The resultant effect of these signalling cascades were activation of calmodulin, calmodulin-dependent kinases, increasing CREB expression, and gene expression regulation. In addition, PAR1/3-mediated ATP release was dependent on PANX1 activation as it was abrogated by either BAPTA, a calcium chelator, or through direct inhibition of PANX1 by carbenoxolone[187]. Lastly, PANX1 activation by intracellular calcium is a topic of interest in HIV infection. Interestingly, HIV binding of CD4 and CXCR4/CCR5 induces the opening of PANX1 channels releasing ATP[188]. In this setting, the release of ATP attenuates P2X1, P2X7, and P2Y1 activity resulting in influx of calcium[188,189]. Increased intracellular calcium further activates PANX1 channels and facilitates calcium dependent signalling[188,189].

Taken together, PANX1 channel activation is mechano-sensitive, responsive to high extracellular potassium, and high intracellular calcium, and allows for the passage of ATP which can contribute to activation of other plasma membrane receptors such as the metabotropic and ionotropic P2Y and P2X receptors.

1.5 Pannexin 1 Inhibition via Pharmacological Channel Blockers

Some compounds have been shown to interact with pannexin resulting in the inhibition of channel activity. Of these, two compounds are commonly used. Firstly, PANX1 channels

can be attenuated by carbenoxolone (CBX)[190]. CBX is a disodium salt of the hemisuccinate derivate of 18-β-glycyrrhetinic acid, derived from licorice root, and has previously been used to inhibit gap junction channels[191]. The use of CBX for pannexin research followed identification of its interaction with PANX1 first extracellular loop, through chimeric interactions[154]. This study further identified that aa W74 of PANX1 actively drives the inhibitory action of CBX, while aa 67-86 also appears to play an important role in CBX-mediated inhibition[154]. CBX is current approved for clinical treatment in Great Britain for use in gastric and esophageal ulcers[191]. CBX however, is a global gap-junction inhibitor, thus its usage can interfere with the channel activity of gap junctional proteins, not just pannexins[125]. However, it has been shown that only CBX concentrations exceeding 50uM are associated with inhibition of connexions[192]. As a result, all studies utilizing CBX for the specific inhibition of pannexin channels use concentrations of 50uM or less.

Another commonly used inhibitor of pannexin channel activity is probenecid (PBN). Initially described for the inhibition of pannexin channels by Silvermann et al., 2008, PBN is used as a well-established treatment for gout, a severe form of arthritis, by affecting uric acid excretion in the kidney[193]. Importantly, unlike CBX, PBN does not appear to affect connexin channels[155,193]. However, the exact mode of inhibition of PBN on PANX1 has not been elucidated.

The use of peptide-based drugs has also constituted another method to inhibit PANX1 channels. ^{10}Panx (WRQAAFVDSY) was derived as a Panx1-mimetic peptide that has been shown to inhibit PANX1 channel activity[152,164,194,195]. However, there has been some reports suggesting non-selective connexin inhibition[195]. More recently, several new PANX1 specific inhibitors have been examined, including the food dye Brilliant Blue FC[196–198]. This dye is a

well-known inhibitor of purinergic receptors P2X7, and has now been shown to inhibit PANX1 channels[196–198]. Furthermore, the broad spectrum antibiotic trovafloxacin, has been established as a PANX1 channel inhibitor. This study indicated that trovafloxacin inhibited PANX1 channel function during apoptosis which resulted in dysregulation of apoptotic body production[199]. Thus, elucidating a role for PANX1 controlled apoptotic body formation during apoptosis[199]. The use of trovafloxacin has since shown promise as a neuroprotection agent after traumatic brain injury acting through PANX1 channels[200].

To date, PANX1 channel inhibition has largely been studied using CBX, PBN, and ^{10}Panx, however, as more research is accumulated more PANX1 specific inhibitors are being established.

1.6 Pannexin 1 Regulation via Post-Translational Modifications

It has been well demonstrated that post-translational modifications (PTMs) affect protein conformation, stability, localization, and function. Similarly, pannexins are regulated by a vast array of PTMs, which have been reported to impact PANX1 intracellular trafficking and channel function. These PTMs can be found summarized in Table 2.

Table 1: PANX1/Panx1 is extensively regulated by post-translational modifications: PANX1 has been demonstrated to be modulated by PTMs which affect PANX1 channel function through modulation of ATP release and trafficking in the cell**.**

Post-Translational Modification	Target Site on PANX1	Effect on PANX1
N-linked Glycosylation	(H) N255 (predicted) (M) N254	Impacts trafficking to the plasma membrane and PANX1/PANX2 intermixing
Tyr- Phosphorylation	Y308, Y198, Y10, Y150	Proposed to impact channel function; Y10 yet to be assessed

Ser/Thr – Phosphorylation	S206, S385, S425, S189, S182	Proposed to impact channel function
S-nitrosylation	C40, C346, C426	Channel function, removal of sites makes channel function null
Ubiquitination	K201, K203, K204, K212, K307, K343, K381, K406	Wide array of functions; suggested to have a role in degradation
Caspase Cleavage	D376	Constitutively active protein channel (C-terminal may be auto-inhibitory)

1.6.1 Glycosylation of Panx1 Regulates Trafficking and Function

Glycosylation is the process by which sugar moieties are added through N-linked or O-linked modifications. N-linked glycosylation attaches sugar moieties on asparagine (Asn, N) aa residues[201]. After which further branching occurs by a series of membrane-associated glycosyltransferases in the ER[202]. Glycosylation serves primarily in protein stability[203]. Failure of protein folding causes their exportation to the cytoplasm where E3 ligases can mediate protein degradation through the ER-accelerated degradation (ERAD) pathway[203]. In the ER, various enzymes are required for the process of transferring glycan subunits, resulting in branching glycans that are then trimmed to form mature species[203].

Pannexins have been reported to be glycoproteins that undergo N-linked glycosylation. This modification was hypothesized to account for their molecular weight changes seen after treatment with N-linked glycosidases, and was later confirmed for Panx1 using site-directed mutagenesis of N254 (2nd extracellular loop), which targeted Panx1's glycosylation site[204]. By

sequence homology to murine Panx1, human PANX1 has been predicted to be glycosylated at N255[204]. Additionally, other Asn have been predicted to undergo in N-linked glycosylation, such as N338 and N394, but these have not been confirmed to be involved in trafficking and channel activity[205].

N-linked glycosylation impacts PANX1 molecular weight banding pattern. PANX1 is detectable by Western blot as three molecular weight bands, which constitute three N-linked glycosylated species: the unglycosylated core termed Gly0 (41kDa), the high mannose species termed Gly1 (44kDa), and the complex glycosylated species termed Gly2 (48kDa)[204]. The glycosylation status of PANX1 impacts its channel subcellular localization[204]. The Gly0 species is predominantly localized to the ER, Gly1 localizes in the Golgi apparatus, and Gly2 localizes at the cell surface[204]. However, glycosylation may not serve as the only PTM affecting cell surface localization, as N254Q mutants appear not only to have mediated dye uptake but also have reduced trafficking towards the cell surface[172]. Furthermore, glycosylation is also implicated in PANX1/PANX2 channel intermixing[175,204].

While not confirmed for Panx2, studies have demonstrated that both Panx1 and Panx3 are regulated via a Sar1-mediated COPII-dependent manner which is a classical ER-Golgi secretory pathway[185], independent of clatharin, adaptor protein AP2, and caveolin 1/2[206]. Throughout this process from ER to PM, Panx1 is further glycosylated to form the Gly1 and Gly2 species.

1.6.2 PANX1 is Modified by Phosphorylation by a Multitude of Kinases Affecting its Channel Activity

PANX1 has multiple serine, threonine, and tyrosine amino acids that may serve as residues for phosphorylation events (summarized in Table 2). Tyrosine phosphorylation in particular has been demonstrated with the Src family of non-receptor tyrosine kinases. This was first reported in excitotoxicity events which showed that phosphorylation of PANX1 at Tyr308 by Src complexed with NMDA receptors[207]. When formed, this complex contributed to cell death through membrane blebbing, calcium dysregulation, and mitochondrial dysfunction[207]. By disrupting this complex using an interfering peptide (TAT-Panx$_{308}$), it was found to be neuroprotective *in vivo*[207]. Phosphorylation of Tyr198, located on the intracellular loop affects channel activity[208]. Initially phosphorylation of Y198 by Src was first characterized in relation to tissue necrosis factor (TNF-α)-induced ATP release affecting leukocyte adhesion and emigration through the venous wall during acute systemic inflammation[209]. Most recently, PANX1 has been shown to mediated ATP release in vascular smooth muscle cells, through α1-adrenergic receptor vasoconstriction, mediating blood pressure homeostasis[145,210]. Phosphorylation at Tyr198 via Src was shown to be directly involved in this process[208]. Specific-phospho-Y198 targeting antibodies indicated that Tyr^{198} is expressed primarily in the endothelial wall[208]. While the mechanism underlying Src phosphorylation of PANX1 has not been completely elucidated, these data indicate that PANX1 can be post-translationally modified by phosphorylation which affects its channel activity.

Additionally, PANX1 contains of 6 serine (Ser) and 1 threonine (Thr) residues at the C-terminal which may be target for kinases that affect PANX1 function and activity[211]. There have been few studies thus far that demonstrate that this phenomenon occurs, however one study indicates that PANX1 is phosphorylated during skeletal muscle contraction. During

muscle contraction several Ser and Thr kinases are activated, calcium/calmodulin-dependent protein kinase II (CaMKII), protein kinase A (PKA), and protein kinase C (PKC) suggesting that they interact with PANX1 during contraction[211,212]. It was further shown using phospho-serine and phospho-threonine antibodies that both unglycosylated and glycosylated PANX1 species undergo phosphorylation with enhanced expression after electrical stimulation of soleus and extensor digitorum longus (EDL) muscles[211]. Furthermore, electrically stimulated muscles showed induced ethidium (Etd^+) uptake that was inhibited by the application of ^{10}panx1[211]. This Etd^+ uptake was proposed to be mediated by PANX1 coupling to P2Y receptors[178,211]. In a separate study, nitric oxide was shown to inhibit PANX1 through the cGMP-protein kinase G (cGMP-PKG) dependent pathway. This study indicated that PANX1 contains a consensus PKG phosphorylation site (^{202}KKNSSHLIM^{210}) which when mutated at the Ser206 residue prevented PKG phosphorylation[213]. Once mutated the nitric oxide donor, sodium nitroprusside (SNP), could no longer inhibit PANX1 currents[213]. This supports the notion that serine phosphorylation at Ser206 by PKG modulates PANX1 channel activity[213]. Taken together, these studies support a role for the modulation of Panx1 channel activity by serine/threonine phosphorylation.

Other kinases such as C-Jun NH2-terminal kinases (JNK) have been shown to play a role in modulating Panx1 channel activity[214]. It was shown in previous studies by Kilic and colleagues, that Panx1 contributes to ATP release in liver cells undergoing lipoapoptosis when induced by saturated free fatty acids[215]. In this study, JNK regulated Panx1 channel activity, whose ATP release stimulated migration of human monocytes involved in chronic liver injury caused by saturated free fatty acids, ischemia/reperfusion, acetaminophen, and hepatocellular

carcinoma[214]. The JNK-mediated phosphorylation site on PANX1 however, has yet to be assessed.

1.5.3 PANX1 is modified by caspase cleavage leading to a constitutively active protein channel

The release of ATP by PANX1 channels results in a location signal that can recruit macrophages to clear apoptotic cells[157,160,177,216]. It has been demonstrated that the C-terminus of PANX1 channels has an inhibitory role for PANX1 channels[160]. During the intrinsic apoptosis pathway, caspase 3/7 mediated cleavage of Panx1 leads to truncation of the C-terminus of Panx1 at ^{376}DVVD^{379}, which causes Panx1 to be constitutively active. Indeed, the C-terminal of PANX1 serves a channel auto-inhibitory mechanism as electron microscopy demonstrates channel closure when present[173]. Complete caspase-mediated removal of the C-terminal tail of Panx1 resulted in an increase of Panx1 channel activity with high conductance and open probability[173]. The resultant efflux of ATP has been shown to activate immune system clearance[157,160,173].

1.5.4 S-nitrosylation inhibits PANX1 channel function

The PTM involving s-nitrosylation is a reversible modification in which nitric oxide (NO) is covalently bound to reactive cysteine thiols via an S-nitrosothiol bond. NO is generated by many cell types through NO synthases from the oxidation of arginine. The addition of NO to proteins have been contributed to several membrane channels such as Cx43[217], potassium voltage-gated channel superfamily Q member 1 (KCNQ1)[218], transient

receptor potential (TRPC5)[219], ryanodine receptor type 1 (RyR1)[220], and NMDA receptors[221]. Interestingly, membrane bound proteins that contain cysteines are frequently targeted for s-nitrosylation. Not only is PANX1 highly expressed in NO rich tissues, it also contains two cysteines (Cys40, Cys346) which are s-nitrosylated[222]. Treatment with cells with independent NO donors such as S-nitrsogluthione (GSNO) and diethylamine NONOate (DEA NONOate), resulted in the inhibition of channel function[222]. Site-directed mutagenesis of Cys40 and Cys346 prevented s-nitrosylation by GNSO and resulted in ATP release of Panx1 channels, suggesting that s-nitrosylation regulates Panx1 channel activity[222]. Under ischemic conditions, Panx1 channels have demonstrated to be active[151,166] and NO expression acts as a secondary messenger/protein-modifying molecule, suggesting that nitrosylation of Cys40 and Cys346 may act as a negative regulatory mechanism of Panx1 channels in the vasculature[223]. Taken together, the cysteine residues 40 and 346 of Panx1 may be affected by s-nitrosylation and/or oxidation regulating channel function.

1.7 Pannexin 1 as a Driver for Tumourigenesis

Membrane channel proteins have been implicated in many aspects of tumourigenesis, including proliferation, cell survival, gene regulation, transcription, apoptosis, invasion, metastasis, and angiogenesis. Thus, understanding how the various protein channels function in this capacity and in specific tumour types and subtypes could constitute novel therapeutic options for cancer patients. Panx1 has been demonstrated to have a role in driving tumourigenesis in glioma[224], breast[162], melanoma[161,163], hepatocellular carcinoma[225], colon[226], multiple myeloma[227], leukemia[228], prostate[179], gallbladder[229], and rhabdomyosarcoma[230] which can be summarized below in Table 2.

Table 2: PANX1/Panx1 is Implicated in a Wide-Variety of Human Cancers

Cancer Type	PANX1 Expression	Effect on Tumourigenesis
Rhabdomyosarcoma	Low PANX1 expression	PANX1 re-introduction into RMS cell lines alleviates RMS malignant properties through non-canonical channel functions
Neuroblastoma	Panx1/Panx2 expressed	Panx1 and Panx2 expressed in Murine NB N2a cell line; treatment with PBN reduced N2a proliferation
Melanoma	High Panx1 expression	Decrease Panx1 expression stimulates melanocytes differentiation
Breast	PANX1 expression; $PANX1^{1-89}$ truncation observed	$PANX1^{1-89}$ truncation in breast cancer associated with both increased metastatic potential and PANX1 channel activity when co-expressed with WT PANX1
Testicular	High Panx1 expression	Panx1 expression correlates with ERK1/2; treatment with PBN reduces malignant properties
Colon	Panx1 expression	Interacts with LXR, caspase-1, P_2X_7 through PANX1 associated ATP release
Leukemia	Panx1 expression	Expression has shown to induce channel activity after caspase-3 clavage
Gallbladder	Decreased expression in gallbladder adenocarcinoma;	Not determined
Hepatocellular carcinoma	Low in non-metastatic cancer High in metastatic cancer	PANX1 may regulate metastatic process through channel associated function
Glioma	Panx1 expression	Panx1 serves as a tumour suppressor; ATP release associated to activation of P_2X_7

Multiple Myeloma	High Panx1 expression	Panx1 expression high across MM cell lines; effect not examined
Prostate	Panx1 expression is high in prostate cancer cell lines	Impacts intraluminal calcium levels; regulating calcium signalling

Panx1 was first described to have tumour-suppressive effects in C6 glioma cells[224]. Future studies indicated that endogenous expression of PANX1 in human gliomas resulted in regulation of intercellular biochemical interactions which are vital for glioma formation[231]. In particular, Panx1 channels serve as ATP release channels that stimulate P_2X_7 receptors, upregulating actinomyosin function which has been shown to drive stability of tumour 3-D structure[231,232]. Furthermore, knockdown of PANX1 in human U87-MG glioma cells reduces cell proliferation[224], suggesting that PANX1 is vital in the regulation of glioma progression.

Additional cancers such as hepatocellular carcinoma (HCC), a frequent form of liver cancer, was shown to have a 4-fold increase in PANX1 expression in a highly metastatic HCC cell line, Hca-F[225]. This study compared expression to that found in a stable, low-metastatic, HCC cell line Hca-P, suggesting that PANX1 may be vital for cancer aggressiveness and metastasis[225]. An upregulation of PANX1 gene expression can also be seen in human multiple myeloma (MM)[227]. PANX1 is also expressed in prostate cancer[179], and over-expression of PANX1 reduced intraluminal calcium, suggesting that PANX1 regulates calcium levels in prostate cancer[179]. PANX1 has also been found to be downregulated in gallbladder adenocarcinomas, while being expressed in normal human gallbladder epithelium[229].

To further establish a role for PANX1 in tumourigenesis, PANX1 was examined in colon cancer. Liver X receptors (LXRs) have been shown to induce caspase-1 dependent proptosis through activation of NLRP3 and subsequent activation of P_2X_7 receptors through ATP stimulation[226]. This study correlated that activation of P_2X_7 receptor to ATP release through PANX1 channels[226]. LXRβ, which is found in the cytoplasm, was shown to mediate ATP release through PANX1 channels, which was inhibited by treatment with an LXR antagonist, T0901317[226]. In leukemia, PANX1 expression was found to be upregulated as compared to control T-cells[228]. Interestingly, treatment of these cells with pro-apoptotic chemotherapeutic drugs, such as topoisomerase II-kinase and proteasome inhibitors, activated the proteolytic cleavage of Panx1 by caspase-3[228]. Thus, Panx1 channels are activated after treatment with various chemotherapeutic agents[228].

In human breast cancer, there is neither an upregulation nor downregulation of PANX1. Instead, a gain-of-function mutation of PANX1 forms an 89 aa peptide ($PANX1^{1-89}$) in breast cancer tissue[162]. While expression of $PANX1^{1-89}$ itself has no channel activity, co-expression of this peptide leads to enhanced endogenous PANX1 channel activity[162]. The resultant increase in ATP release and purinergic signalling promotes breast cancer cell survival and metastatic spread[162]. Through intravenous tail-vein injections, expression of $PANX1^{1-89}$ was shown to enhance breast cancer metastasis to the lungs[162]. This suggests that both changes in PANX1 expression as well as mutations in PANX1 may contribute to cancer tumourigenesis or metastatic potential.

Panx1 has also been studied in melanoma. As compared to normal melanocytes, heightened expression of Panx1 was found in aggressive melanoma cell lines B16-F0, B16-F10, and B16-BL6[161]. Furthermore, reducing Panx1 expression in these cell lines through an

siRNA targeting knockdown approach resulted in an increase in normal melanocyte characteristics including increased melanin production, decreased cell migration, and increased cellular projections[161]. Furthermore, reduced tumour progression, tumour size, and metastatic potential was observed in an *in vitro* tumour growth assay[161]. In addition, treatment of melanoma cells with PANX1 channel inhibitors, PBN and CBX, resulted in decreased cell proliferation and increased melanin production, which resulted in reduced tumour proliferation and metastasis in chicken embryo xenografts[163]. In this setting, it was suggested that PANX1 may play a role in Wnt/β-catenin signalling as reduced Panx1 expression paralleled a reduction in β-catenin expression[163]. Panx1 channel inhibitors have also been used to show reduced cell proliferation of N2a cells, a murine NB cell line, which expresses Panx1[233]. Recently, these PANX1 channel inhibitors have also been demonstrated to reduce migration and invasion in I-10 testicular cancer cells[234]. In testicular cancer, increased Panx1 expression and channel activity was correlated to expression p-ERK1/2[234]. As a result, targeting PANX1 channel activity may constitute novel therapeutic strategies in cases of NB, melanoma, breast, and testicular cancers.

Our lab has recently demonstrated that PANX1 inhibits rhabdomyosarcoma progression through a mechanism independent of it canonical channel function[230]. We showed that re-introduction of PANX1 into rhabdomyosarcoma cell lines Rh18 and Rh30, which have low PANX1 levels, resulted in a significant decrease in their malignant properties *in vitro* and *in vivo*[230]. While all prior studies, including those related to tumourigenesis, have indicated that PANX1's effect is mediated through its channel function, often related to ATP release, this was the first study to demonstrate a channel independent function for PANX1. In this setting, PANX1 tumours suppressive effect was mediated by PANX1 downstream signalling

independent of its channel function, as PANX1 channel null mutants had a similar effect as compared to wild-type PANX1[230].

Taken together, many studies have established a clear role for PANX1 in tumourigenesis related to its expression level and channel activity. Furthermore, we have shown that PANX1 also affects cancer progression through novel non-canonical channel functions that have yet to be fully elucidated. Thus, PANX1's role in tumourigenesis is complex and only recently beginning to be uncovered.

1.8 Project Rationale

Panx1 has been shown to be expressed in the murine neuroblastoma cell line N2a, and the use of PBN resulted in a decrease in N2a cell proliferation. Furthermore, melanoma (a cancer derived from a similar NC cell progenitor) expresses PANX1 in which inhibition of its channel function via CBX and PBN reduces its tumourigenic profile in mice[163]. As summarized below in Figure 5, our lab has demonstrated that PANX1 was present in human NB tumour specimens, where its increased expression correlated with more undifferentiated tumours, as well as being present in seven neuroblastoma cell lines derived from high-risk patients. Interestingly, PANX1 channels were active in all patient-derived neuroblastoma cell lines as demonstrated by dye uptake assay and could be inhibited by either CBX or PBN. Furthermore, the use of the PANX1 channel blockers, CBX or PBN, resulted in decreased NB cell proliferation and cell viability, and increased apoptosis. In *in vitro* tumour growth assays, PANX1 channel inhibition decreased tumour formation and, in some cases, induced regression. In pre-clinical xenograph mouse models, blockage of PANX1 channels decreased tumour growth and significantly increased mean survival. Taken together, this suggests

PANX1 channel inhibition constitutes a novel therapeutic target for neuroblastoma patients. (Unpublished data; M-E St-Pierre, S. H. Holland et al.).

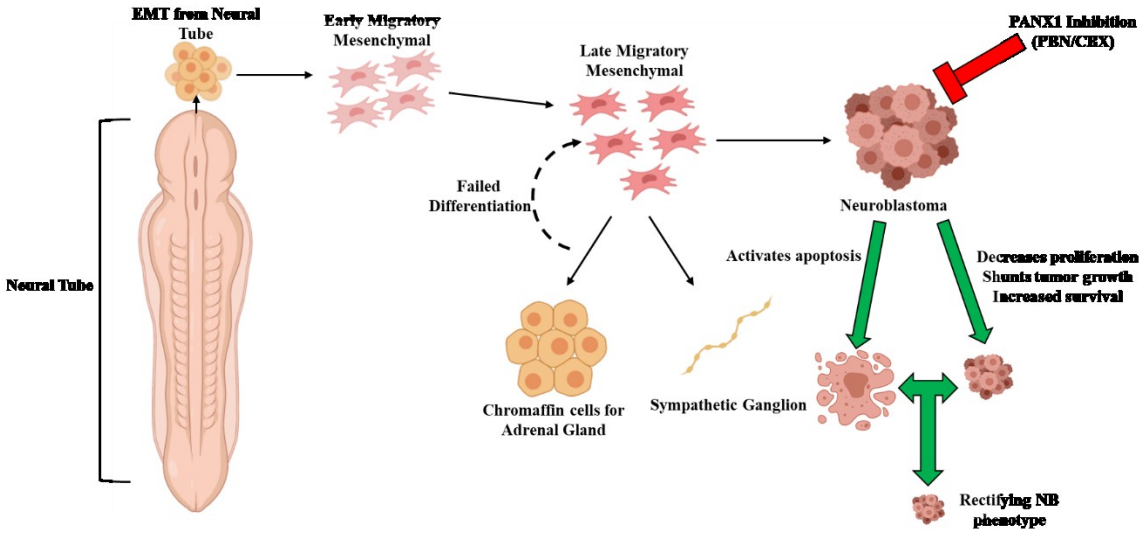

Figure 5: PANX1 inhibition with F.D.A approved pharmacological inhibitors constitutes a novel therapeutic approach for NB: Normally as described above, neural tube cells release neural crest progenitor cells which undergo differentiation into chromaffin cells and sympathetic ganglion. In NB, this differentiation process fails. Our lab has shown that NB expresses active PANX1 channels and that treatment of NB *in vitro* decreases NB cell proliferation and, induces apoptosis. Treatment with CBX and PBN furthermore reduced NB tumour growth and in some cases initiated their regression *in vitro* and reduced tumour growth and increased survival *in vivo* (unpublished data; M-E. St-Pierre, S.H Holland et al.)

From this study, we speculated that PANX1 may be regulated differently in NB as compared to healthy tissues. Consistent with this, a higher molecular weight (~50 kDa) PANX1 immunoreactive band was detected in NB tumour specimens and NB cell lines but absent in neuronal controls as shown in Figure 6.

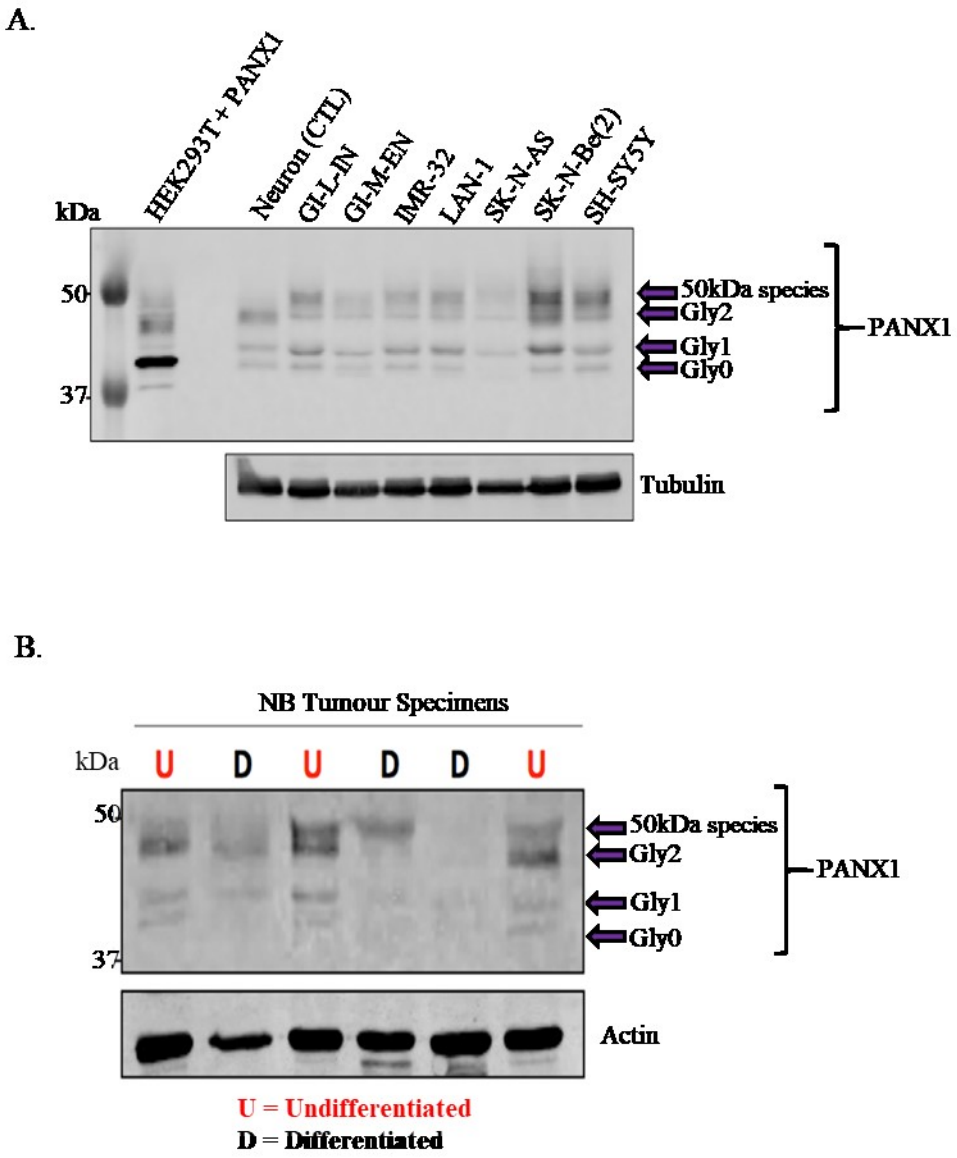

Figure 6: A higher molecular weight PANX1 immunoreactive species is detected in high-risk patient derived cell lines and NB tumour specimen: A) PANX1 protein levels in seven high-risk patient derived NB cell lines indicated expression of 4 PANX1 species (Gly0, Gly1, Gly2, 50 kDa). This 50 kDa species remained undetected in control human neuronal lysates. Protein expression was analyzed via Western blot using PANX1 targeting antibodies (1:000) and a loading control of tubulin (1:2000) (N=3). B) PANX1 protein levels in six NB tumour specimens. Less differentiated tumours denoted as undifferentiated (U) as compared to more differentiated (D) tumours. A similar four PANX1 immunoreactive bands are noted. Protein expression was analyzed via Western blot using PANX1 targeting antibodies (1:000) and a loading control of tubulin (1:2000) (N=1) - (Unpublished data; M-E St-Pierre, S. H. Holland et al.).

1.8 Hypothesis

Post-translational modifications and/or mutations in Pannexin 1 (PANX1) contribute to the malignant phenotype of neuroblastoma.

1.9 Research Aims

1) Characterize the PANX1 species expressed in neuroblastoma.
2) Assess whether PANX1 post-translational modifications in neuroblastoma affect its localization and channel function, and promote a malignant phenotype.
3) Assess whether mutations of PANX1 in neuroblastoma affect its channel function.

2.0 Materials and Methods

2.1 Cell Culture

HEK293T and ad293 (a gift from Dr. Dale Laird laboratory at Western University, London, ON, Canada) cells were cultured in 10cm plates using complete medium (DMEM high glucose (HyClone, #SH30022.01), 10% Fetal Bovine Serum (Sigma-Aldrich, #F1051-500,), 1% glutamine (Fisher, #SH3003401), 1% penicillin/streptavidin (Fisher #SV30010). Neuroblastoma cell lines (a kind gift from Dr. Bob Korneluk's laboratory at Children's Hospital of Eastern Ontario, Ottawa, ON)) GI-M-EN, GI-L-IN, IMR-32, LAN-1, SK-N-AS, SK-N-Be(2) and SH-SY5Y were maintained in 10cm plates using DMEM high glucose complete medium. Lastly, 293TN (System Bioscience #LV900A-1) cells were maintained using DMEM high glucose complete medium supplemented with 1% sodium pyruvate (Gibco #11360070). Doxycycline-inducible control (scramble sequence) and PANX1-knockdown (shPANX1) NB cells (TRIPZ Inducible Lentiviral shRNA kit (#RHS5087-EG24145, Dharmacon, Chicago, IL)) were maintained in complete DMEM high glucose medium. PANX1 knockdown was induced by treating cells with 2ug/mL doxycycline (#D9891, Sigma-Aldrich, Oakville, ON). All cell cultures were maintained at 37^0C and 5% CO_2.

2.2 Plasmids and Transfections

PANX1-myc/ddk vector (Origene, #RC204474) was obtained to express PANX1. This construct was also utilized for site-directed mutagenesis to produce the myc-Y10F, myc-N255A and $PANX1^{1-99}$ constructs. For other experiments, Cuo-PANX1-GFP vector was produced as described in[230]. For the dephosphorylation experiments, a Cx43 expression plasmid (a gift from Dr. Dale Laird laboratory at Western University, London, ON, Canada)

was used. For transfection control, an eGFP-pCDNA3.1 plasmid was used (a gift from Dr. Richard Beliveau laboratory at Ste-Justine Hospital, Montreal, QC, Canada).

Cells were transfected using Lipofectamine 2000 (#52887, Life Technologies, Carlsbad, CA) as per the manufacturer's protocol. Unless otherwise stated, all cell experiments were performed 48hrs post-transfection.

2.3 Site Directed Mutagenesis

Using the Quikchange site-directed mutagenesis kit (Agilent Technologies, #200518), PANX1 tagged with myc-ddk (tagging at C-terminal tail of Panx1), described as myc-PANX1, was mutated to produce the Y10F (myc-Y10F), N255A (myc-N255A) and $PANX1^{1-99}$ mutants. Using the Quikchange Primer Design, specific primers were designed. For myc-Y10F the following primers were used Fwd 5'-CCGAGAACACGAACTCCGTGGCCAGGTG-3' and Rev 5'- CACCTGGCCACGGAGTTCGTGTTCTCGG-3'. For myc-N255A the following primer was utilized Fwd 5'- GCATCAAATCAGGGATCCTGAGAGCCGACAGCACCGT-3' and Rev 5'-ACGGTGCTGTCGGCTCTCAGGATCCCTGATTTGATGC -3'. For $PANX1^{1-99}$ the following primers were used Fwd 5'-TGCAGAGCGAGTCTTGAAACCTCCCACTGT-3' and Rev 5'-ACAGTGGGAGGTTTCAAGACTCGCTCTGCAG-3'. Each primer set was diluted to 50µM using PCR grade H_2O.

The control PCR reaction was prepared by combining 10X reaction buffer, 10ng of pWhitescript 4.5kB control plasmid (5ng/µL), 125ng of oligonucleotide primer #1 and #2 (34-mer (100ng/µL), 1uL of dNTP mix, 39.5µL of PCR grade H_2O to a final volume of 50µL and 1 µL of *PfuTurbo* DNA polymerase (2.5 U/µL) was added for the reaction. To produce the

PANX1 mutants, 10x Reaction Buffer, 30ng of myc-ddk tagged PANX1 backbone, 125ng of respective primers, 1 µL of dNTP mix and PCR Grade H_2O to a final volume of 50µL and 1µL of *PfuTurbo* DNA polymerase (2.5 U/µL) was added for the reaction. The PCR reaction was then placed in a thermocycler (which one) and set for the following cycle: initial denaturation 95^0C for 30 seconds, and 12 cycles of denaturation at 95^0C for 30 seconds, annealing at 55ºC for 1 minute, extension at 68ºC for 6.1 minutes (1min per kb).

After the reaction was completed, the reaction was placed on ice for 2 minutes. 1 µL of *Dpn I* (10 U/µL) was added to each amplification reaction and incubated at 37ºC for 1 hour to digest the parental strand. Bacterial transformations were performed with XL1-Blue super-competent (Agilent Technologies #200236) cells followed by amplification under antibiotic (kanamycin) selection and mini-prep (QIAGEN #27106) DNA extraction. Mutants were verified by sequencing at the Toronto SickKids Center for Applied Genomics.

2.4 Cell Lysis and Western blotting

Cell lysates were obtained as previously described[136,230,235] using 2X IP lysis buffer (1% Triton X-100 (Fisher #AC327371000), 150mM NaCl (Fisher #BP358), 10mM Tris-base, 1mM EDTA (Sigma #E5134), 1mM EGTA (Sigma #E3889), 0.5% NP-40 (Fluka #74385), pH 7.4) which was supplemented with PhoSTOP phosphatase inhibitor (Roche #04906837001) and cOmplete ULTRA protease tablets ((Roche #04693159001) unless otherwise stated). Protein concentrations were determined by microBCA (Pierce #23227). Samples were separated by SDS-PAGE (100V for 15 minutes then at 120V for 115-125minutes) and then transferred to PVDF membrane (BioRad #10026933. After the transfer, PVDF membranes were blocked in Odyssey Blocking Buffer (Li-Cor #LIC927-40003) for 1 hour at room temperature. Membranes were then incubated with desired primary and

secondary antibodies (see section 2.15) and scanned using the Odyssey CLx Imaging System (Li-Cor). Immunoblots were quantified using ImageStudio software.

2.5 Deglycosylation Assays

To assess which PANX1 species are glycosylated in NB, a protein deglycosylation kit (New England Biolabs #P6044S) was used as per the company's protocol. Cell lysates (100ug) from HEK293T, SH-SY5Y, SK-N-Be(2) cells transfected with PANX1 (untagged) were used. As per company protocol, control reaction (without (-) glycosidases) was prepared using dH_2O instead of the deglycosylation enzymes mix. Lysates were then analyzed via Western blot.

To assess the glycosylation status of PANX1, lysates from HEK293T cells transfected with myc-PANX1 were treated with N- and O-linked glycanases from a deglycosylation enzyme kit and extender kit (Prozyme #GK80110 & #GK80115). As per the company's protocol, lysates were incubated with N-Glycanase, O-Glycanase, Sialidase A, β(1,4) Galactosidase, or β-N-Acetylglucosaminidase. The negative control (without (-) the respective enzyme) was prepared using dH_2O to substitute each glycosidase. 50µg of treated cell lysates were then examined by Western blot.

To assess glycosylation status of myc-Y10F and myc-N255A, HEK293T cells were transfected with each respective DNA construct, as well as with myc-PANX1, and incubated with PNGaseF (New England Biolabs #P0704S) as per company's protocol. 50µg of treated cell lysates were then examined by Western blot.

2.6 Dephosphorylation Assay

A lambda protein phosphatase (λ-PP) kit was used to assess phosphorylation status of PANX1 as described in[207], using a λ-PP kit (New England Biolabs #P0753S). To summarize,

HEK293T cells transfected with PANX1 (untagged), SH-SY5Y and SK-N-Be(2) lysates were incubated with as per kit instructions. Lysates prepared in the absence of phosphatase inhibitors were incubated at 60ºC for 1hr with λ-PP. Lysate from HEK293T over-expressing Cx43 was used as a positive control. Samples were then examined via Western blot.

2.7 Immunofluorescence

HEK293T cells were plated on coverslips (Fisher #12-545-80) coated with 100µg/mL of rat-tail collagen (Corning #354236) and then transfected with myc-PANX1, myc-Y10F or myc-N255A constructs. After 48hrs, HEK293T cells were fixed using 3.7% paraformaldehyde for 20 minutes at room temperature. Cells were blocked/permeabilized in 2% Bovine Serum Albumin (Sigma-Aldrich #A7906) and 0.1% Triton X-100 in PBS for 45 minutes at room temperature. Cells were washed three times with PBS and then incubated with anti-Myc (1:100, Cell Signalling #2276S) at room temperature for 1hr. Cells were again washed three times with PBS and incubated with anti-rabbit 488 (1:500, Life Technologies, catalog number) at room temperature for 1hr. Finally, cells were washed three times with PBS, then with dH_2O, and mounted with Fluromount-DAPI (SouthernBiotech #0100-20). High resolution images were acquired by confocal microscopy (Olympus Fluoview FV-1000 Laser Confocal Microscope) using a 100X objective lens with oil. High resolutions images were acquired sequentially with the microscope setting kept constant.

2.8 Cell Surface Biotinylation Assay

1.0×10^6 HEK293T cells were seeded in duplicate for cell surface biotinylation in 10cm plates and then transfected with either myc-PANX1, myc-Y10F or myc-N255A in duplicate. Forty-eight hours post-transfection, cells were washed with chilled PBS (containing

phosphatase and protease inhibitors). One set of cells (+) was incubated with biotin (0.5mg/mL biotin (EZ-Link^{TM} NHS-Biotin (ThermoFisher #20217)) in PBS containing phosphatase and protease inhibitors) for 20 minutes at 4^0C, while the other set (-) was incubated with PBS (containing phosphatase and protease inhibitors). To quench the biotin, cells were washed with 100mM Glycine (Fisher #BP-3815) (dissolved in PBS) and incubated for 15 minutes at 4^0C. After this reaction, cells were washed with PBS (containing phosphatase and protease inhibitors) and then lysed with 500µL of 2x IP Lysis Buffer. Total protein concentration of each sample was assessed by a BCA assay.

Lysates (1 mg) were incubated with 50µL of Neutravidin^{TM} agarose beads (Pierce #29200), and placed on a rotary platform overnight. Beads were then pelleted at 2000 RPM for 5 minutes at 4^0C. The supernatant was collected for analysis. The pellet was washed 3 times with 2x IP lysis buffer and then with PBS. After the final wash the supernatant was discarded, and the pellet was combined with 50µL of 2x sample loading buffer and heated at 100ºC for 5 minutes. For the input and supernatant samples, 50µg were submitted for Western blotting analysis using anti-PANX1. For a biotin internalization control, anti-GAPDH was used. For a pulldown efficiency control, anti-EGFR was used. All antibodies were dissolved in Odyssey Blocking Buffer.

2.9 Dye Uptake Assay

Dye uptake was performed as described in[156]. Ad293 cells were used for this assay has they have increased adherence compared to HEK293T cells. $5.0x10^4$ cells were plated in duplicate in 35mm plates, which were then transfected with either eGFP, myc-PANX1, myc-Y10F, or myc-N255A. To assess the effect of the PANX1$^{1-99}$, cells were co-transfected with either pcDNA3.1 and myc-PANX1, pcDNA3.1 and PANX1$^{1-99}$, myc-PANX1 and PANX1^{1-}

[99]; compare to pcDNA3.1 alone. A 50uM high potassium solution (60mM NaCl, 50mM KCl (Sigma #P-9333), 1.4mM $CaCl_2$ (Alfa Aesar #89866), 1.0mM $MgCl_2$ (Sigma #M2670), 10mM HEPES (Sigma #H3375), pH 7.4), and a 5uM low potassium solution (145mM NaCl, 5mM KCl, 1.4mM $CaCl_2$, 1.0mM $MgCl_2$, 10mM HEPES , pH 7.4). Cells were pre-exposed to their respective conditions (high or low potassium) for 10 minutes at 37°C. Then cells incubated in high or low potassium solutions containing 2 mg/mL sulfurhodamine B dye (Molecular Probes #31307) for 30 minutes at 37°C in the absence or presence of PBN (1 mM;Invitrogen #P36400) or CX (100 uM; Sigma-Aldrich #C4790). Cells were washed carefully and then examined using a fluorescent microscope (Life Technologies – EVOS FL Auto). Ten randomized pictures were taken with phase (exposure setting 2mS; 0.0 gain) and TxRed (exposure setting 85mS; 0.0 gain) of each condition and quantified using the ImageJ software. Cells were lysed and subjected to Western blot analysis to normalize for protein expression. Channel activity is reported as dye uptake incidence by dividing the proportion of cells that showed dye uptake in high potassium solution to the proportion of cells that showed dye uptake in low potassium solution for each condition.

2.10 Cell Proliferation Assay

Cells (2.0×10^5-4.0×10^5 cells per well) were plated in a 6 well plates containing collagen-coated coverslips and transfected with eGFP, myc-PANX1, myc-Y10F, or myc-N255A. After 24hrs, the medium was replaced with starvation medium (DMEM High Glucose + 1% FBS + 1% Glutamine + 1% Pen/strep). SK-N-Be(2), GI-L-IN, IMR-32 and GI-M-EN cells were then incubated with a 1:100 solution of BrdU Labelling Reagent (ThermoFisher #000103) in complete medium for three hours, while LAN-1 cells were incubated for fours

hours, and SH-SY5Y and SK-N-AS cells for six hours. The difference in labelling time was due to the different growth rates among the NB cell lines.

Cells were then fixed in 3.7% paraformaldehyde for 20 minutes at RT and processed for BrdU labeling. Following blocking and permeabilization, the cells were incubated with 2N HCl (Fisher #HX0603-3) for 30 minutes at room temperature. Cells were washed with PBS and then incubated with a BrdU antibody (1:50) diluted in blocking buffer (what is it?) for 1 hour at room temperature. Cells were washed with PBS and incubated with an Alexa-Fluor mouse-594 (1:500) secondary antibody for 1 hour at room temperature. Cells were washed in PBS and incubated with anti-myc (1:100) diluted in blocking buffer for 1 hour at room temperature. Cells were washed with PBS and then incubated with rabbit 488 (1:500) diluted in blocking buffer for 1 hour at room temperature. Coverslips were washed and mounted with Fluoromount G-DAPI.

Images were taken using a fluorescent microscope (EVOS FL Auto- Life Technologies) using a 20x objective lens. Ten randomized images were obtained of each coverslip. ImageJ was then used to count BrdU and transfected positive cells. Data are presented as the mean of percentage of BrdU-Postive and transfection positive cells +/- the standard deviation

2.11 Anoikis Assay

Anoikis resistance was assessed as described in[236] with modification. Untransfected cells or cells (2.0×10^6 cells) transfected with myc-PANX1, myc-Y10F, myc-N255A, or eGFP, were plated on 6 well plates pre-coated with concentration 1.2% Poly(2-hydroxyethyl) methacrylate dissolved in 95% ethanol (Sigma #P3932) (Poly-HEMA) Cells were collected at

0hr, 1hr, 3hrs, 5hrs and 8hrs following plating on Poly-HEMA. The number of total, live, and dead cells was counted (Countess,Invitrogen)). The remaining cell suspension was pelleted, lysed, and stored at -80C. Data are presented as the live cell count number calculated each time point +/- standard deviation.

2.12 Mutation Scans for PANX1$^{1-99}$ and Intron Mutation

Genomic DNA was isolated from GI-M-EN, GI-L-IN, IMR-32, LAN-1, SK-N-AS, SK-N-Be(2) and SH-SY5Y using a QIAamp DNA Mini Kit (QIAGEN #51304) and DNA concentration was measured using a nanodrop (ND-100 Spectrophotometer). Primers were developed to allow for amplification of regions upstream and downstream of suspected mutant site obtained through isolation of genomic DNA from NB cell lines. For the splice mutation Fwd 5'-GCCTGTAAGAAGCGTATGCT-3' Rev 5'-TAGACTCCCGTAGCCTCTGC-3' primers were used. For PANX1$^{1-99}$ Fwd 5'-TCCACGCTTGCCTCTTGAAT-3' Rev 5'-ACAGCACTGGTTGGCTACAA-3' primers were used. For the PCR reactions, 150pg of genomic DNA was combined with 2x Master Mix (Fisher #PRM7502), 1µM primer mix and nuclease free water to a solution volume of 20µL. PCR reaction was ran as followed using a thermocycler (BioRad – T100 Thermo Cycler): initial denaturation 95^{o}C for 2 minutes, denaturation 95^{o}C for 30 seconds, annealing temperature 58^{0}C for 30 seconds, extension 72^{o}C for 1 minute and 20 seconds, 45 cycles and a final extension at 72^{0}C for 5 minutes. Samples were analyzed on a 1% agarose gel using PANX1-CuO-GFP as a positive control for amplification. For PANX$^{1-99}$ a PCR purification (QIAGEN #28104) step was performed to isolated amplified DNA for sequencing. For the splice mutation, gel extraction (QIAGEN #28704) was performed to isolated amplified DNA for sequencing. Sequencing was performed at TCAG Toronto SickKids Center of Applied Genomics using 100ng of DNA per sample.

GI-M-EN, GI-L-IN, IMR-32, LAN-1, SK-N-AS, SK-N-Be(2) and SH-SY5Y cell lysates have also been analyzed by Western blot using an antibody against the N-terminal domain of PANX1.

2.13 Characterization of PANX1$^{1-99}$ mutant

SK-N-Be(2), SH-SY5Y, and HEK293T cells were transfected with PANX1$^{1-99}$. Fourty-eight hours post-transfection, cells were treated with 10μM of MG132 (Sigma #M8699) or DMSO (vehicle control) for 8hrs. Cell were then lysed and analyzed by Western blot using a PANX1 antibody recognizing its N-terminal domain.

2.14 Antibodies

For Western blot analysis, all primary antibodies were diluted in the Odyssey blocking buffer containing sodium azide. PANX1 (Sigma-HPA016930) recognizes the C-terminal of PANX1 and was used for Western blot and immunofluorescence analysis unless otherwise stated; PANX1 (Cell Signalling-D9M1C-#91137) recognizes the N-terminal of PANX1 and was used for Western blot and immunofluorescence analysis unless otherwise stated; anti-connexin-43 (Sigma #C6219) was used as a positive control for dephosphorylation; anti-EGFR (A-10) (Santa Cruz #sc-373746) was used as a pulldown control for the cell surface biotinylation assay; anti-Myc (rabbit) (71D10) (Cell Signalling #2276S) and anti-Myc (mouse) (9B11) (Cell Signalling #2278S) were used intermittently throughout my experiments; anti-GAPDH (Advanced Immunology #2RGM2) was used as a loading control for Western analysis and biotin internalization control for the cell surface biotinylation assay; anti-BrdU (ZBU30) (Fisher #03-3900) was used to assess cell proliferation; and anti-GFP was from Santa Cruz (#sc-9996). Secondary antibodies anti-rabbit 488 (Invitrogen #A11017, #A11009) and

anti-mouse 594 (Life Technologies #A11012) were used for immunofluorescence studies, while anti-rabbit 680 (Invitrogen #A21109)) and anti-mouse (Molecular Probes #A11045) were used for Western blot analysis.

2.15 Statistics

Statistical significance was determined using unpaired, two tailed Student's *t*-tests and analysis of variance (ANOVA) followed by post-Bonferroni test. Results with $P < 0.05$ were considered significant (*P value < 0.05; **P value < 0.01; ***P value < 0.001).

3.0 Results

3.1 The ~50 kDa band detected by anti-PANX1 antibodies in NB corresponds to PANX1

Preliminary data from our laboratory revealed that PANX1 and PANX2 is expressed in NB tumour specimens and high-risk patient-derived cell lines (unpublished; St-Pierre et al., 2019). Interestingly, while PANX1 was also detected in control neurons by Western blotting, its banding pattern was strikingly different as a band at around ~50 kDa was found in all cell lines, but not in neurons. In neurons, PANX1 is detected in its classic form as three molecular weight species, representing Gly0, Gly1 and Gly2. However, expression of PANX1 in NB cell lysates and tumour specimens revealed an additional higher molecular weight species, at ~50 kDa (Figure 6A and 6B). Henceforth, to examine whether the ~50 kDa species detected in NB is PANX1-specific, PANX1 expression was knocked down using doxycycline-inducible PANX1 shRNAs in NB cells. As seen in Figure 7A, treatment with 2ug/mL doxycycline over a course of 4 days resulted in an increase in RFP expression in both the scrambled shRNA (shCTL) and shPANX1 expressing cell lines. PANX1 levels were decreased after treatment with 2 ug/mL doxycycline over the course of four days in GI-M-EN (Figure 7B). Total PANX1 levels were decreased significantly by 63±7.77% compared to the cells expressing shCTL (Figure 7C). As the levels of the ~50 kDa species also decreased by 55±4.32 % (Figure 7C), this indicated that the ~50 kDa band corresponds to a PANX1 species.

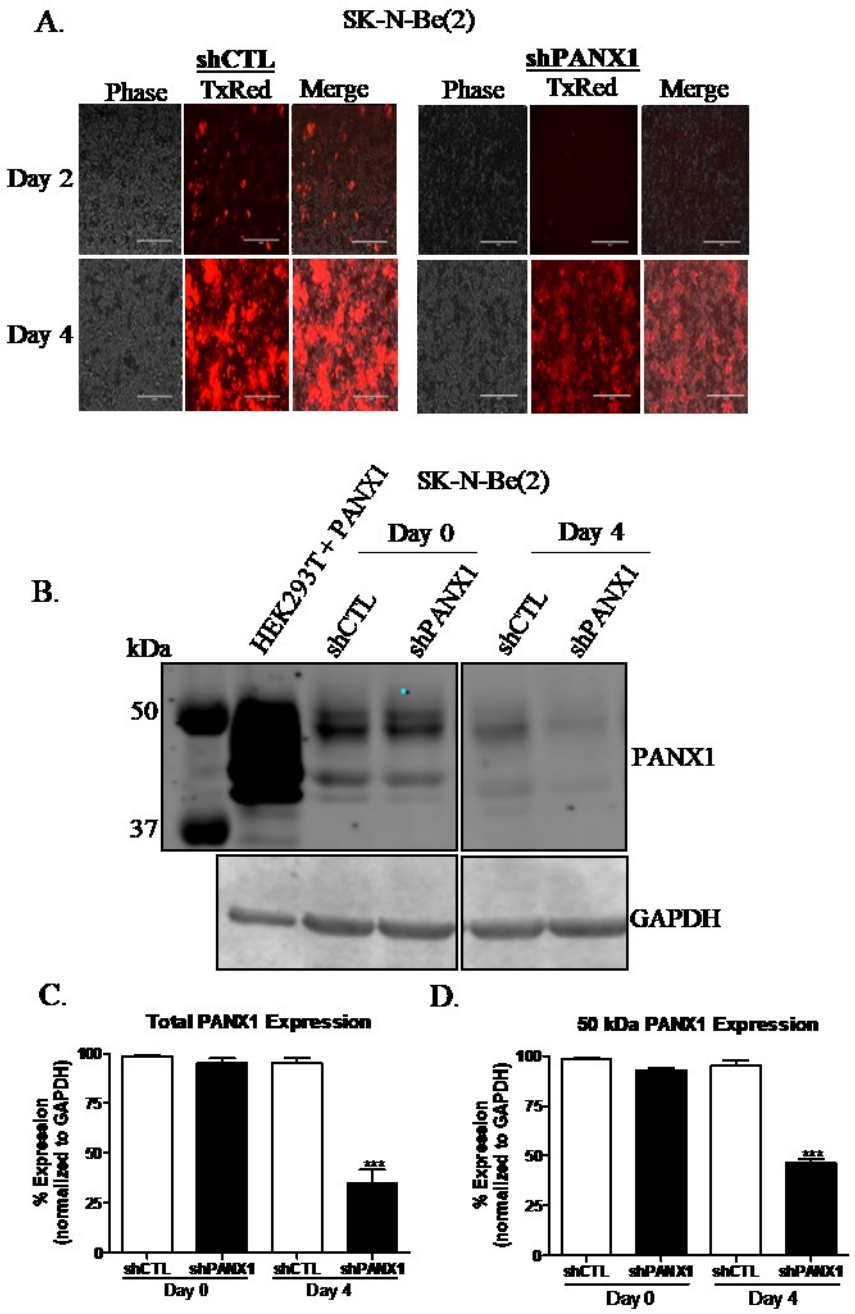

Figure 7: ~50 kDa PANX1 species detected in NB is PANX1-specific: A) The doxycycline-inducible knockdown system contains a RFP protein downstream of the shCTL and shPANX1 sequences. Treatment with 2 µg/mL doxycycline induced RFP expression in both shCTL and shPANX1 transfected cells. B) PANX1 levels were measured by Western blot using a PANX1 antibody that targets the C-terminal of PANX1. While there was no change over the time course with shCTL, shPANX1 showed a reduction in PANX1 protein levels. C) Densitometry demonstrated that while the total PANX1 protein levels in shCTL expressing SK-N-Be(2) cells remained unchanged, shPANX1 expressing SK-N-Be(2) cells displayed a 62% reduction in total PANX1 protein (N=3; P-value >0.001=***). D) Similarly, densitometry demonstrated a 52% reduction in total PANX1 protein in SK-N-Be(2) cells expressing shPANX1, while levels remained unchanged in control shCTL cells (N=3; P-value >0.001=***).

3.2 The ~50 kDa PANX1 species is modified by glycosylation

To assess whether the ~50 kDa PANX1 species is modified by glycosylation, NB cell lysates were treated with a combination of O- and N-linked glycosidases. Since PANX1 is a known glycoprotein and murine Panx1 has been confirmed to be modified by N-linked glycosylation, we used HEK293T (devoid of pannexins) expressing ectopic mouse Panx1 as a positive control. As seen in Figure 8A, when lysates from HEK293T expressing Panx1 were treated with O- and N-linked glycosidases, PANX1 was reduced to one lower molecular weight species. Similar results were obtained using SK-N-Be(2) and SH-SY5Y cell lysates (Figure 8A). These results indicate that the ~50 kDa PANX1 species is glycosylated.

In order to assess whether the higher molecular weight of this PANX1 species is due to phosphorylation, lysates from HEK293T cells expressing PANX1 were treated with λ-PP and submitted to western blot analysis. As a positive control, lysates from HEK293T cells expressing Cx43 were used[237]. While Cx43 displayed two higher molecular weight phospho-species, these were not detected after treatment with λ-PP (Figure 8B). No apparent banding pattern change was observed for PANX1 expressed in HEK293T cells (Figure 8C). Similar results were obtained using SK-N-Be(2) and SH-SY5Y, which express PANX1 endogenously (Figue 8C). This results suggest that phosphorylation of PANX1 does not mediate a molecular banding pattern shift in NB.

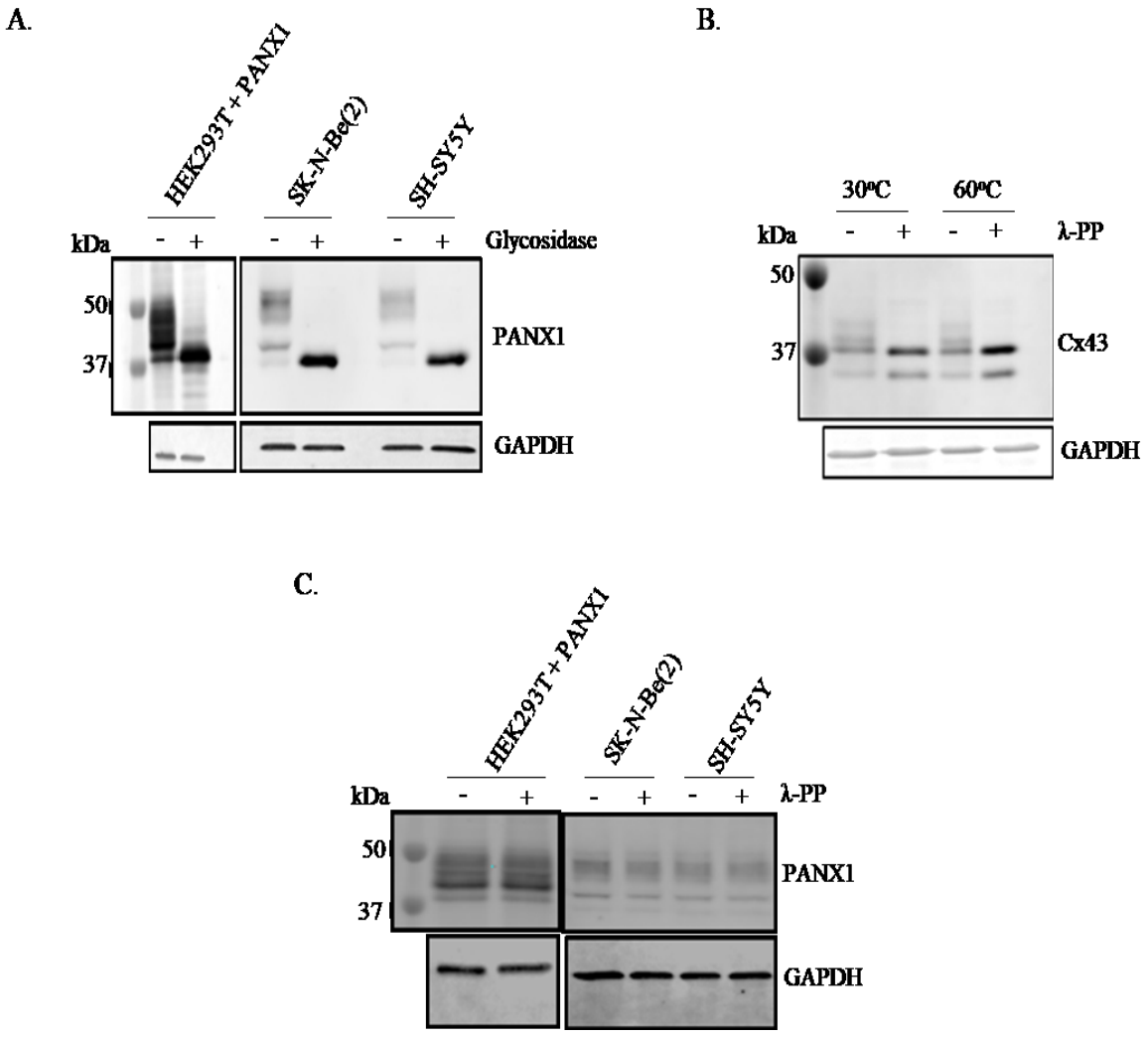

Figure 8: Glycosylation impacts the molecular weight banding pattern of PANX1 species in NB. A) PANX1-expressing HEK293T and NB (SK-N-Be(2) and SH-SY-5Y) cell lysates were treated with a mixture of N- and O-linked glycanases. As shown by western blotting, following treatment with glycanases, all PANX1 species migrated to one lower molecular weight species (Gly0). The ~ 50 kDa PANX1 species expressed in NB also migrated further following treatment with glycanases indicating that this species is glycosylated. (B) As expected, treatment of Cx43-expressing HEK293T cell lysates with lambda phosphatase (λ-PP) resulted in a shift of molecular weight species. (C) However, no change in PANX1 banding pattern was observed when lysates from HEK293T cells ectopically expressing PANX1, or NB cells were treated with λ-PP.

3.3 Computational analysis reveals sites of PANX1 PTMs

In silico analysis of the PANX1 sequence revealed many candidate PTM sites that could potentially modulate PANX1 localization and modulate channel activity. As seen in Figure 9A, PhosphoSite Plus (www.phosphosite.org) PTM sites were identified which included sites of glycosylation, phosphorylation, acetylation, s-nitrosylation, ubiquitination, and caspase cleavage which have been identified by mass spectroscopy screens or through individual published manuscripts. The current understanding of the PANX1 lifecycle suggests that Panx1 is modified by N-linked glycosylation at N254 which alters channel function and localization. It has been predicted but not confirmed through sequence homology between Panx1 and PANX1 that PANX1 is modified by N-linked glycosylation at N255. Since the ~50 kDa PANX1 species detected in NB phenotype is glycosylated, understanding the role of PANX1 glycosylation in NB is imperative. Interestingly, mass spectroscopy analysis of NB phosphorylated proteins revealed that PANX1 is phosphorylated at $Y10^{238}$. This modification is intriguing as there are few reported modifications that occur at the N-terminal domain of PANX1 and this modification was identified in the patient-derived NB cell line SK-N-Be(2).

Assessing NB tumour specimens using the Catalogue of Somatic Mutations in Cancer (COSMIC), cBioPortal for Cancer Genomics, Integrative Onco Genomics (Intogen), and International Cancer Genome Consortium (ICGC) revealed two PANX1 mutations, which are predicted to form truncated peptides. A missense mutation detected at c.295G>T translates into a 99 aa PANX1 peptides. This mutation is located near the end of the second exon of *PANX1*. Interestingly, a patient who expressed this mutant was listed as a 2yr old female with stage 4 NB which is currently in remission (COSMIC). The second mutation is a splicing mutation that occurs at the 4^{th} exon splice acceptor site at c.546-2A>T. Computational analysis

of this sequence predicts the formation of a 181 aa truncated peptide. Each of these peptides lack the predicted glycosylation site and lack additional predicted sites of PTM such as caspase cleavage, Ser/Thr/Tyr predicted phosphorylation, S-nitrosylation sites attached to the C-terminal, etc.

A.

Site of Interest	Type (PTM or Tumor Specimen	Modification	Mutant Created
Y10	PTM	Phosphorylation	Myc-Y10F
N255	PTM	Glycosylation	Myc-N255A
G99stop	Tumor Specimen	Truncated Peptide	$PANX1^{1-99}$

B.

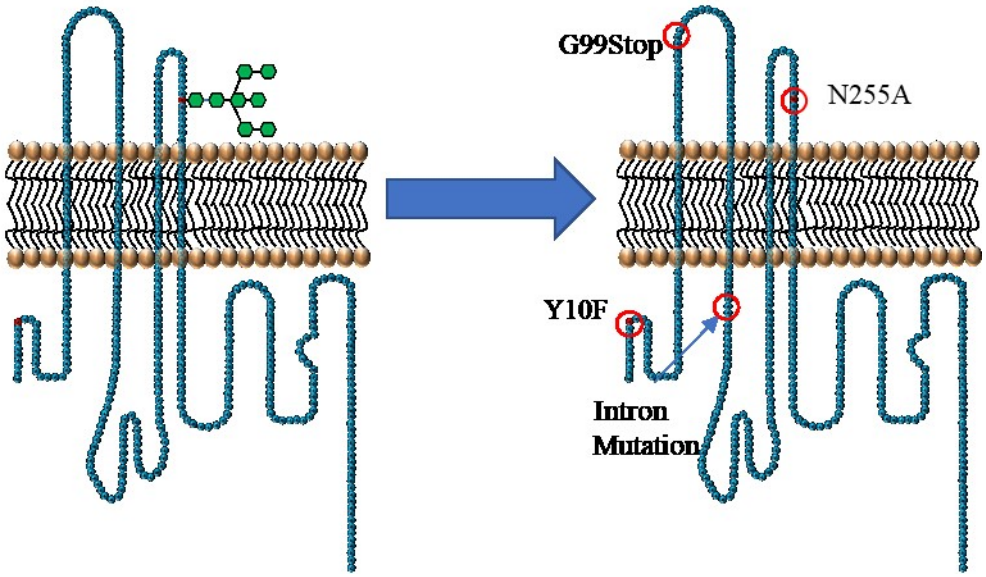

Figure 9: Four potential sites of modification appear in NB. A) Computational mutants revealed three potential alterations (2 PTMS and 1 mutation) to PANX1 that will be of focus for my Master's Thesis. The first one is a phosphorylation site of PANX1 at Y10 that was identified in the NB cell line SK-N-Be(2)[238]. The second one is the predicted glycosylation site of PANX1, N255. The third one is predicted to be an early missense mutation detected in NB tumour specimens (COSMIC) that would generate a truncated peptide of 99 aa: $PANX1^{1-99}$. B) A topology map displays the location of these PTMS and mutation. Figure modified from[133].

3.4 Characterization of myc-Y10F and myc-N255A expression and localization prolife

In order to assess the role of PANX1 phosphorylation on Y10 and glycosylation on N255 (Figure 9B), two PANX1 mutants were generated: Y10F and N255A, respectively. It is important to note that to differentiate between endogenous PANX1 expression in the NB cell lines, PANX1 mutants have been engineered to express a myc-ddk tag at their C-terminus. These two mutants were first expressed in HEK293T cells as these cells are devoid of pannexin expression. As expected, western blot analysis of myc-PANX1 revealed a classic Gly0, Gly1, and Gly2 banding pattern where Gly2 was the most prominent band (Figure 10A). Myc-Y10F in HEK293T was detected as only two species detected at the same molecular weight than Gly0 and Gly1 (Figure 10A). Myc-N255A was detected as a single band, likely corresponding to Gly0 (Figure 10A). These results suggest an intracellular localization of myc-Y10F and N255A PANX1 mutants. To further characterize these PANX1 mutants, immunofluorescence microscopy was thus performed to examine their localization pattern *in vitro*. As shown in Figure 10B, myc-PANX1 was detected at the plasma membrane, as well as in intracellular compartment when expressed in HEK293T cells. However, the myc-Y10F PANX1 mutant predominantly displayed intracellular localization. On the other hand, the myc-N255A mutant could be detected at the cell surface but seemed to show more intracellular localization.

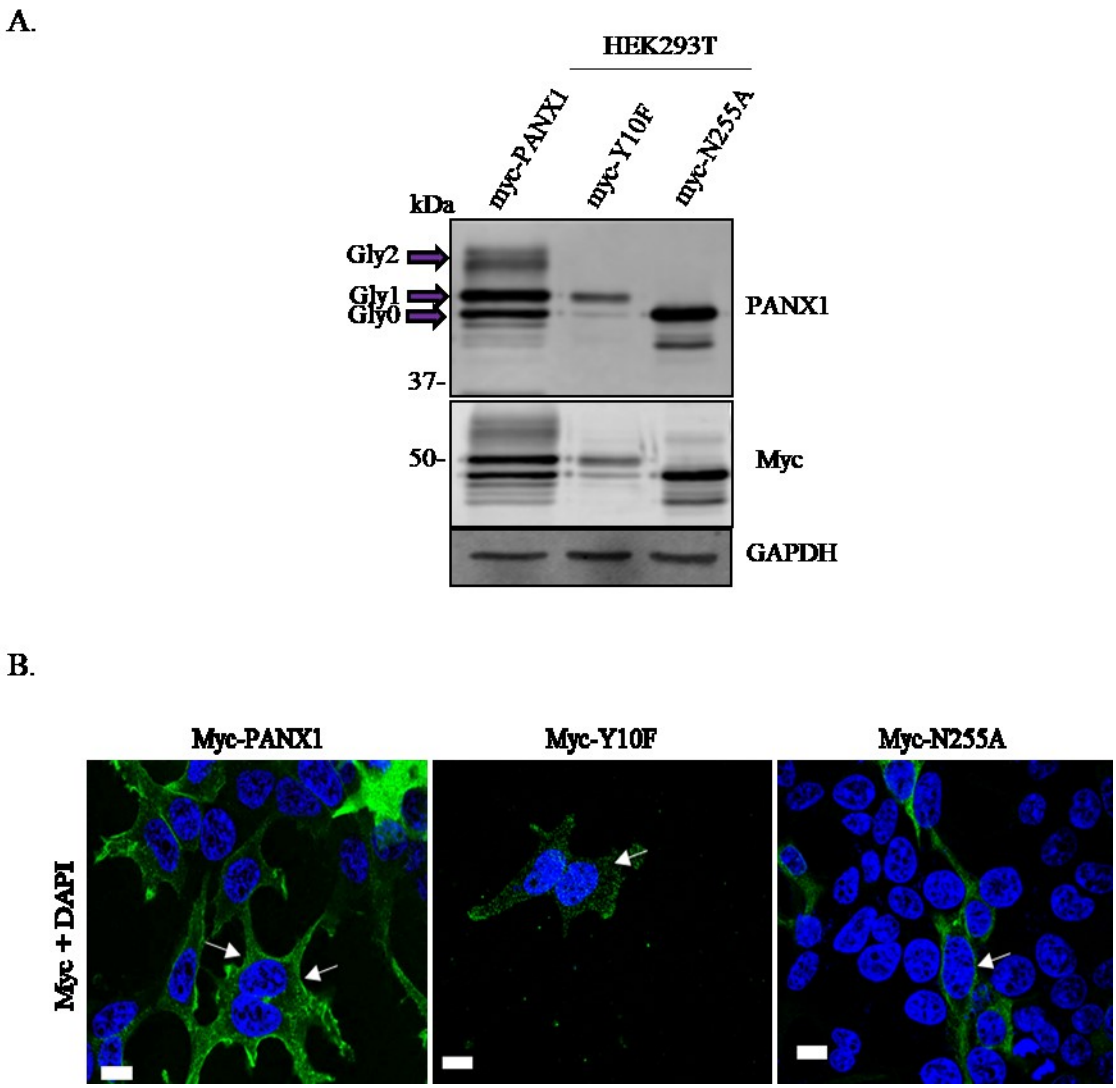

Figure 10: Expression and localization pattern of myc-Y10F and myc-N255A PANX1 mutants. A) Myc-PANX1 is detected as three main molecular weight species, likely Gly0, Gly1, and Gly2, myc-Y10 was detected as two lower molecular weight species, while the N255A mutant was detected as only one species (N=3). B) HEK293T cells were transfected with either myc-PANX1, myc-Y10F, or myc-N255A and were visualized using anti-myc (green; white arrows). While myc-PANX1 was mainly detected at the cell surface but could also be seen in intracellular compartments, the Y10F and N255A seem to display less plasma membrane localization and more intracellular staining. Blue = nuclei; bars = 10 μM.

3.6 Limited localization of the myc-N255A mutant at the cell surface.

In order to quantify the amount of the PANX1 mutants compared to wild-type PANX1, cell surface biotinylation assays were performed using Ad293 cells after ectopic expression of myc-PANX1, myc-N255A, or myc-Y10F. As shown in Figure 11A and 12A, myc-PANX1 was detected at the cell surface. While myc-N255A could also be detected at the cell surface, there was a reduction in the proportion detected at the plasma membrane compared to that of myc-PANX1 (Figure 11B and C). While there was also a reduction in the proportion of the Y10F detected at the cell surface (Figure 12B and C), it was not statistically significant when compared to myc-PANX1.

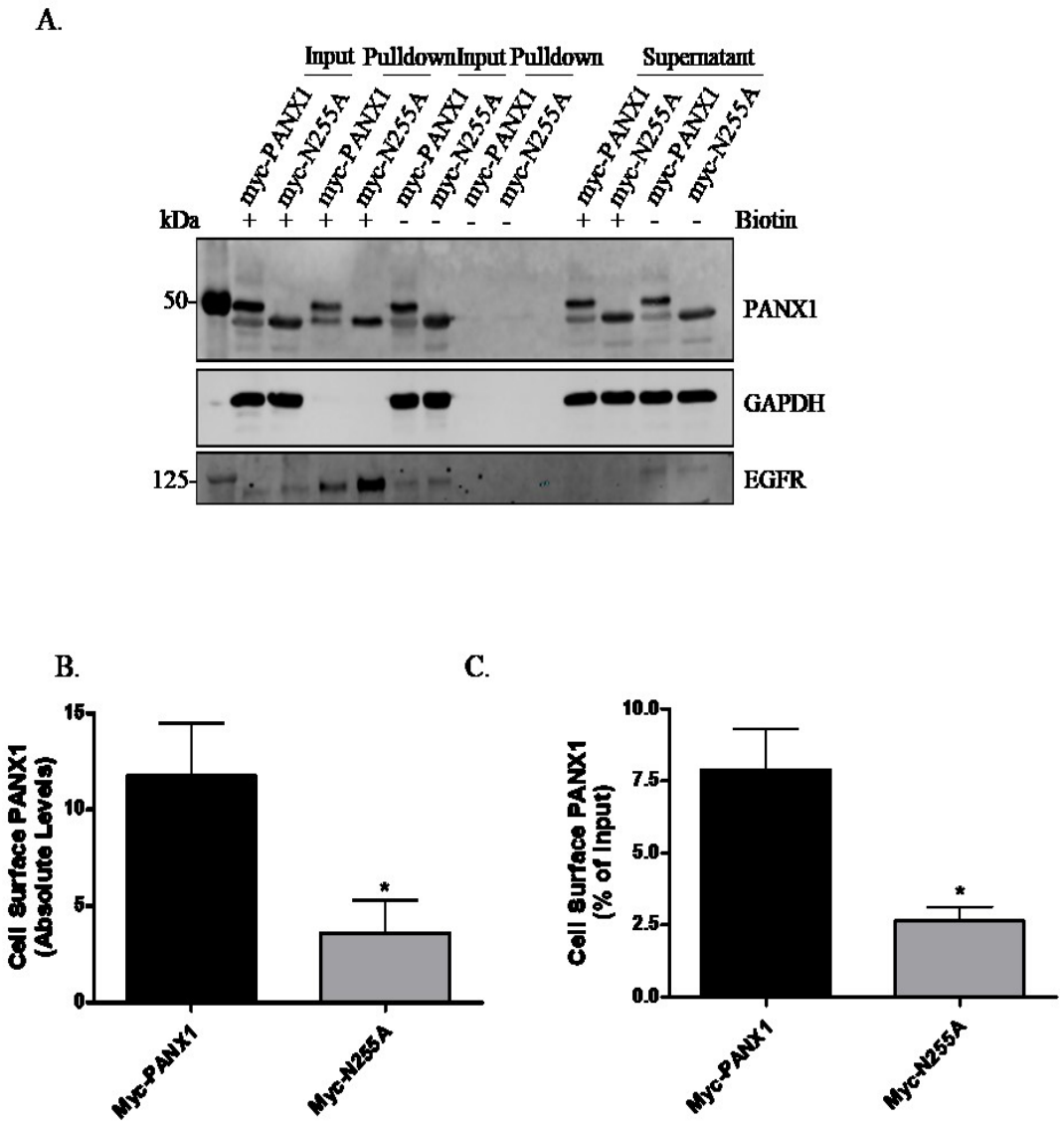

Figure 11: Limited localization of the myc-N255A mutant at the cell surface. A) Ad293 cells expressing ectopic myc-N255A or myc-PANX1 were submitted to cell surface biotinylation assays followed by western blot analysis. GAPDH was used as negative control (intracellular protein), while EGFR was used as a plasma membrane protein positive control. B) Absolute PANX1 levels at the cell surface and C) relative PANX1 levels at the cell surface were calculated (N=4; P-value <0.05 = *)

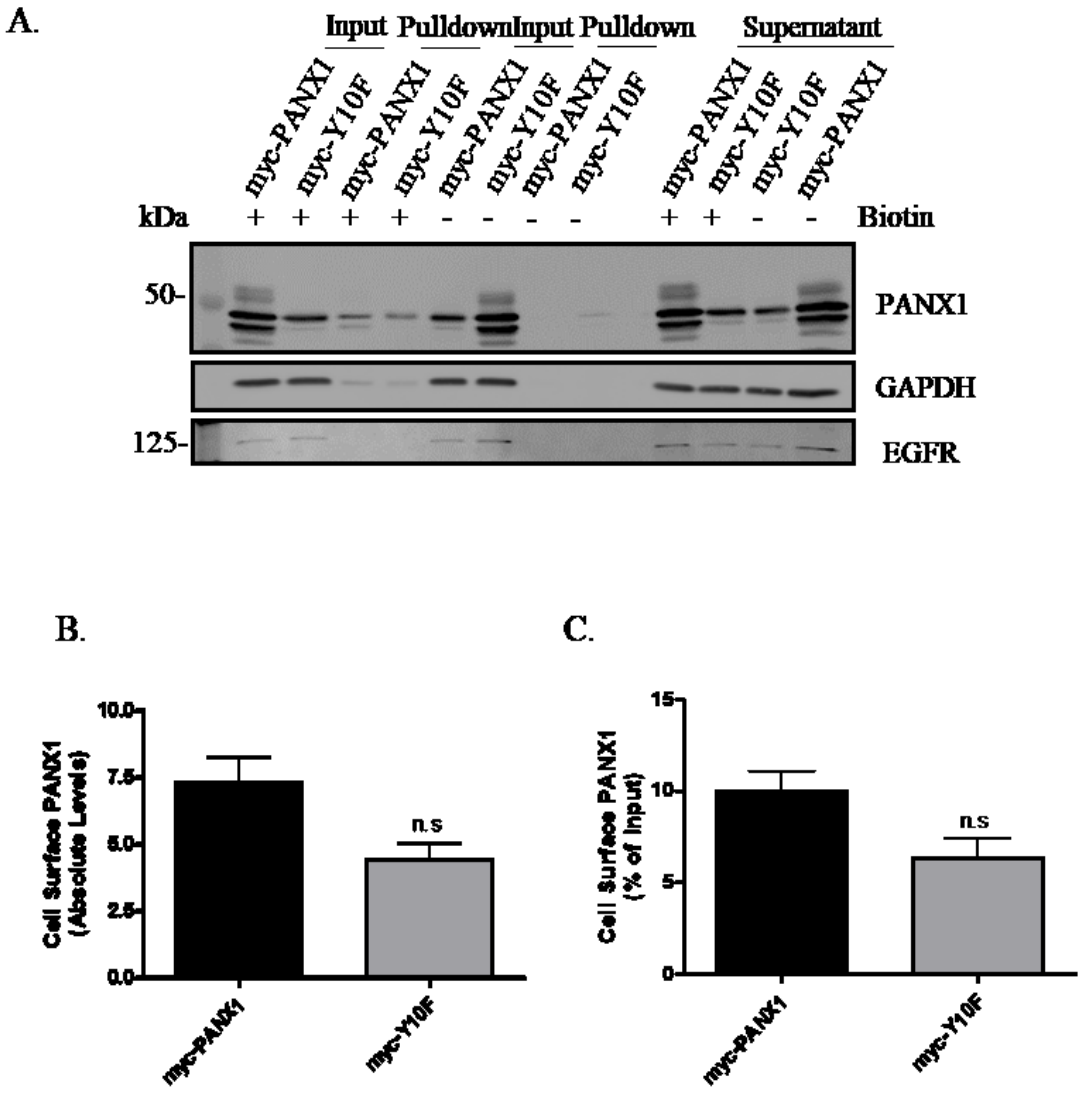

Figure 12: Localization of the Y10F mutant at the cell surface is similar to that of PANX1. A) Ad293 cells expressing ectopic myc-Y10F or myc-PANX1 were submitted to cell surface biotinylation assays followed by western blot analysis. GAPDH was used as negative control (intracellular protein), while EGFR was used as a plasma membrane protein positive control. B) Absolute PANX1 levels at the cell surface and C) relative PANX1 levels at the cell surface were calculated (N=4; n.s. = non significant).

3.7 Myc-Y10F PANX1 mutant is glycosylated, but not myc-N255A.

In order to determine whether N255 is the sole glycosylation site of PANX1, lysates of myc-N255A-expressing HEK293T cell lysates were treated with various N- and O-linked glycanases and compared to that of myc-PANX1. Lysates of HEK293T cells expressing the Y10F mutant were also similarly treated to characterization its glycosylation status.

To confirm that myc-PANX1 is glycosylated solely by N-linked glycans, myc-PANX1 HEK293T cell lysates were treated with O-glycanase, sialidase A, N-glycanase, β(1,4) Galactosidase, or β-N-Acetylglucosaminidase. Following treatment with N-Glycanase, which cleaves all N-linked complex hybrid and/or high mannose oligosaccharides, the Gly2 and Gly1 species of myc-PANX1 were no longer detected (Figure 13A). O-linked glycanases such as Sialidase A, O-Glycanase, β(1,4) Galactosidase, and β-N-Acetylglucosaminidase did not affect the banding pattern of myc-PANX1. This data confirms previous reports that PANX1 is solely N-linked glycosylated[133,235,239–241]. Based on this, the glycosylation status of myc-Y10F and myc-N255A was assessed using the global N-linked glycanase enzyme called PNGaseF. As expected, treatment with PNGaseF caused all glycosylation species of myc-PANX1 to migrate to Gly0 (Figure 13B). The myc-Y10F PANX1 mutant also migrated as Gly0 following deglycosylation treatment, suggesting that the Y10F mutant is glycosylated with high mannose species. On the other hand, there was no change in the banding pattern of the myc-N255A mutant after treatment with PNGaseF, suggesting that the sole glycosylation site of human PANX1 is N255.

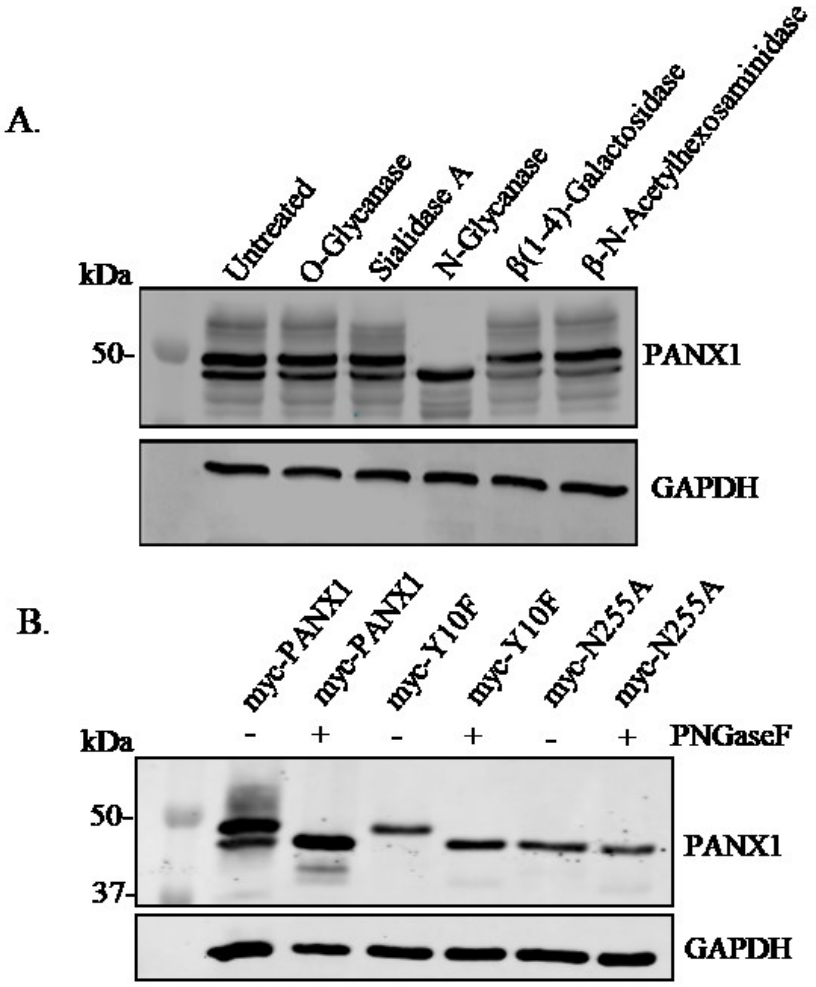

Figure 13: Myc-Y10F PANX1 mutant is glycosylated, but not myc-N255A.

A) PANX1 is N-linked glycosylated as treatment with O-linked glycanases did not cause any shift in its banding pattern. However, treatment with an N-Glycanase caused all glycosylated species to migrate to Gly0 (N=3). B) As predicted glycosylation site of PANX1, N255 is confirmed to be the location of glycosylation as treatment with PNGase F (N-linked glycanase) did not affect the apparent molecular weight of the myc-N255A PANX1 mutant. Furthermore, following treatment with PNGaseF, the myc-Y10F mutant is detected as a Gly0 species suggesting that it is glycosylated. Figure needs to be fixed: it is not 'B' for the last two enzyme names but beta.

3.8 The myc-Y10F shows reduced channel activity

To assess the channel function of the myc-Y10F and myc-N255A mutants, PANX1 channels were activated by high potassium concentration using Ad293 cells. As expected, myc-PANX1 showed a significant increase in dye uptake when stimulated with high potassium (50 mM), but not when a low concentration (5 mM) was used (Figure 14A). The increase in dye uptake was significantly inhibited by the PANX1 channel blockers CBX and PBN (Figure 14A) indicating that the dye uptake measured was PANX1 specific. This assay was then used to examine the channel activity of the myc-N255A and Y10F mutants. Expression of myc-N255A resulted in a decrease in channel activity (approximately 42%) when compared to that of myc-PANX1. However, this effect was not statistically significant. Similar to myc-PANX1, the channel activity of the N255A mutant was inhibited by CBX and PBN. On the other hand, expression of myc-Y10F completely abolished PANX1 channel activity (Figure 14B).

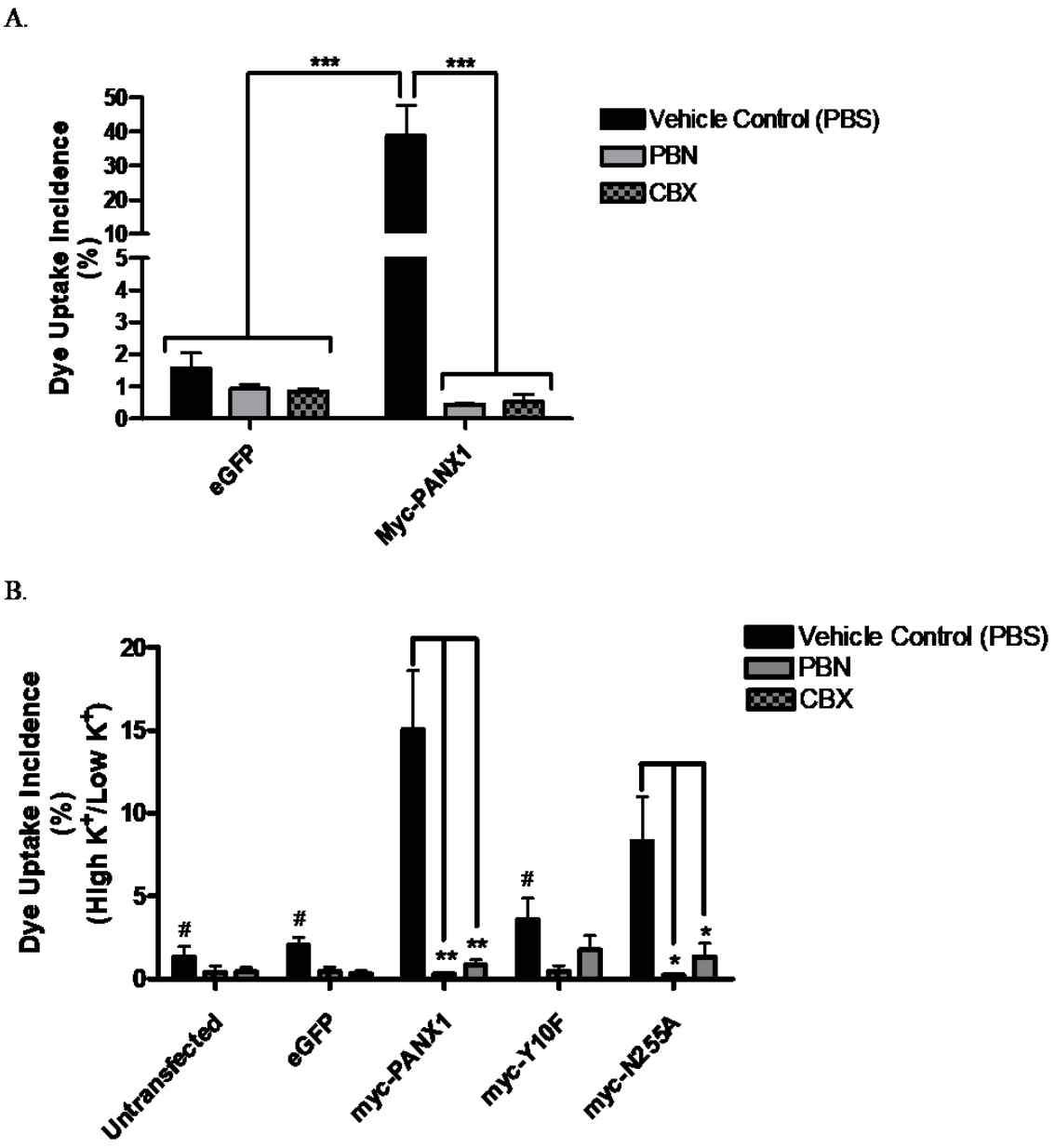

Figure 14: The myc-Y10F PANX1 mutant shows reduced channel activity, A) Ad293 cells ectopically expressing myc-PANX1 or eGFP were submitted to a dye uptake assay in high potassium or low potassium conditions in the presence or absence of CBX (100 uM), PBN (1 mM), or the saline vehicle control. Dye uptake incidences in high potassium and low potassium conditions were quantified (N=3; *** P=<0.001). B) Myc-Y10F and myc-N255A were assessed for channel activity in the same conditions as described in (A). Myc-Y10F, but not the N255A mutant, shows a significant reduction of channel activity when compared to that of myc-PANX1 (N=3; # P=<0.05 comparison to myc-PANX1 control, ** P= <0.01 comparison of myc-PANX1 and inhibitors, * P =<0.05 comparison to myc-N255A control).

3.9 Expression of myc-Y10F and myc-N255A PANX1 mutants decreased NB cell proliferation *in vitro*

To assess the effect that phosphorylation and glycosylation of PANX1 has on NB cell proliferation, 5-bromo-2'-deoxyuridine (BrdU) incorporation assay was performed in all 7 patient-derived NB cell lines (Figure 15A and B) in which myc-PANX1 and myc-tagged mutant expressing cells were detected using anti-myc (green). BrdU-positive cells were counted in myc-expressing cells only. As shown in Figure 15B, in most NB cell lines expression of myc-PANX1 had no effect on cell proliferation when compared to wild-type cells or control transfected cells (eGFP). Expression of myc-Y10F and N255A PANX1 mutants significantly reduced the proliferation of all 7 NB cell lines when compared to their wild-type counterpart or cells expressing eGFP. The effect of the Y10F mutant on cell proliferation was more pronounced than that of myc-N255A.

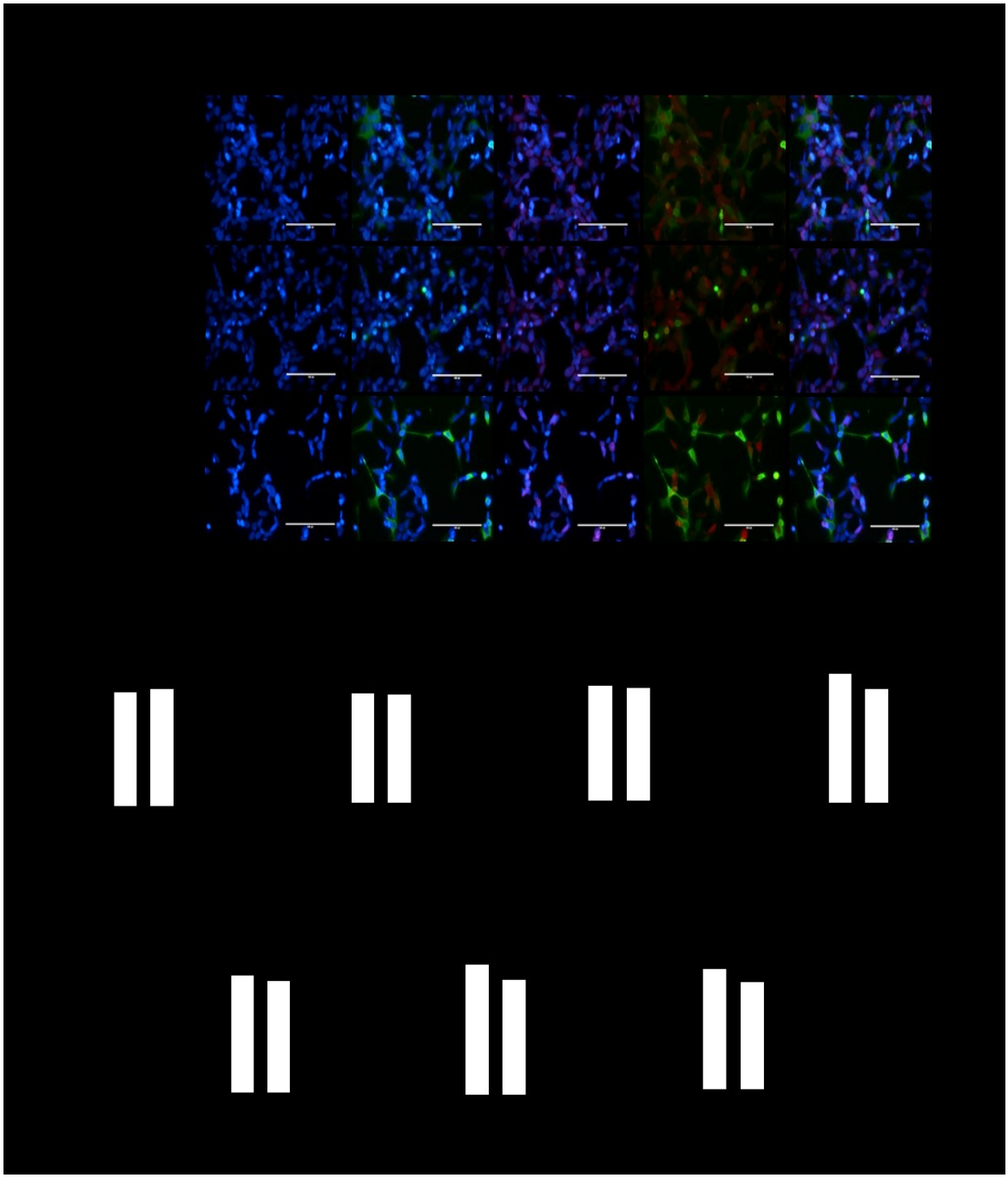

Figure 15: Expression of myc-Y10F and myc-N255A reduces NB cell proliferation in all seven high-risk patient-derived cell lines. A) SK-N-Be(2) cells were transfected with myc-PANX1, myc-Y10F, or myc0N255A. These cells, together with wild-type cells and cells expressing eGFP were subjected to a BrdU incorporation assays. Myc was labeled in green, while BrdU was detected in red. Bars = 100μM; Blue = nuclei. B) BrdU-positive cells were counted. In cells expressing myc-PANX1 or the myc-tagged mutants, BrduU-positive cells were counted only in transfected cells (myc). Data are expressed as the % of BrdU-positve cells (* indicates P value <0.05; *** indicates P value is <0.001).

3.10 Expression of myc-Y10F and myc-N255A PANX1 mutants reduces the metastasis potential of NB *in vitro*

NB is one of the most highly metastatic tumours in childhood with metastases in bones, bone marrow, lymph nodes, skin, and liver[50]. In order to assess metastatic potential *in vitro*, cells were kept in suspension over a period of 8 hours and viable cells were then counted. Again, our seven NB cell lines were used here, as well as HEK293T cells. As shown in Figure 16, viability of HEK293T cells decreased over the 8-hour period, while the viability of the 7 malignant NB cell lines was unaffected or even slightly increased. In all cases, expression of the myc-N255A and myc-Y10F mutants significantly decreased the viability of cells kept in suspension for 8 hours, suggesting a reduction of metastatic potential of NB cells.

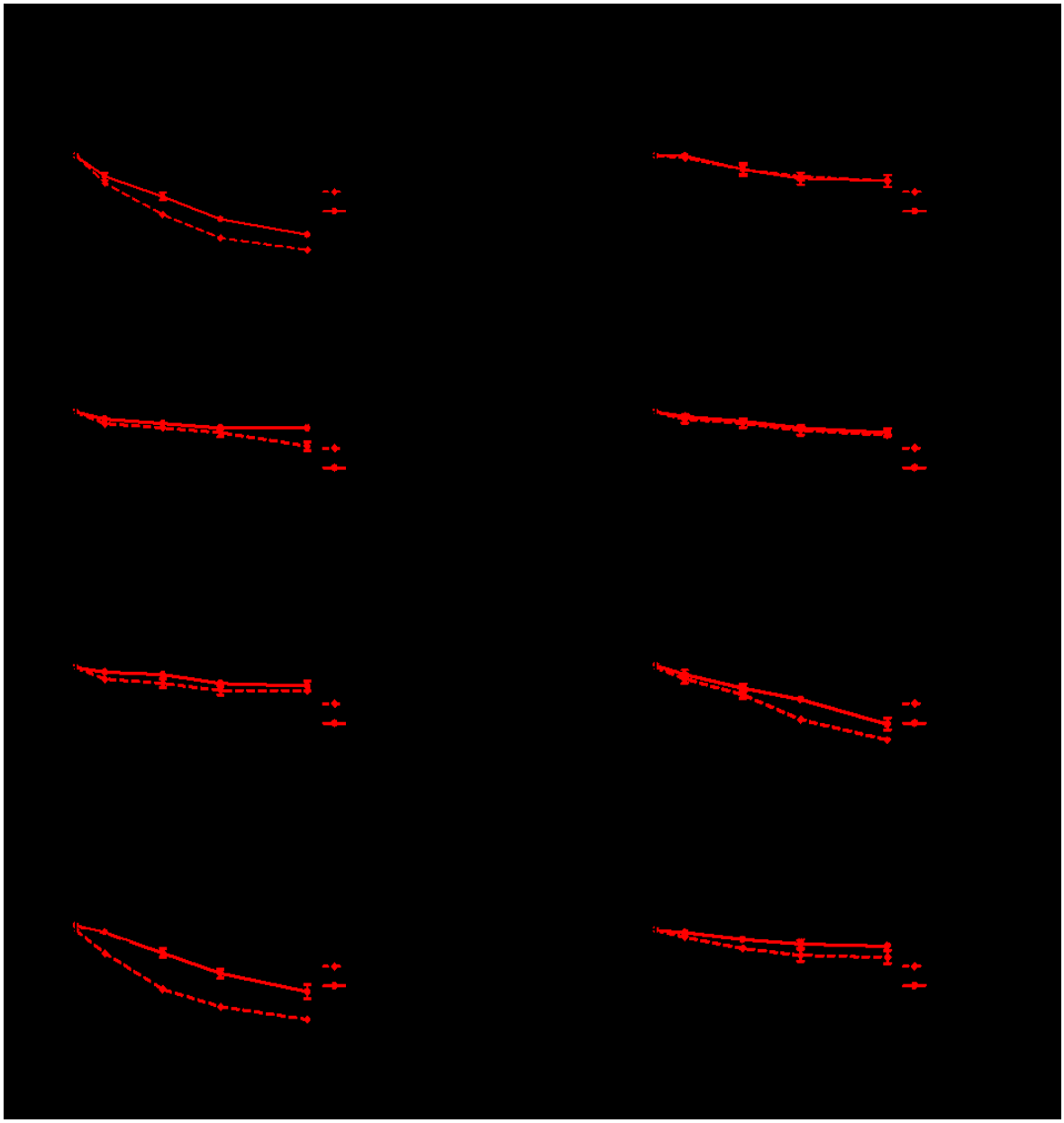

Figure 16: Expression of myc-Y10F and myc-N255A PANX1 mutants reduces NB metastatic potential *in vitro* A) HEK293T and our seven-patient derived NB cell were kept in suspension over a period of 8 hours and the number of live cells was then counted. Cells were ectopically expressing myc-PANX1, myc-Y10F, or myc-N255A and compared to cells expressing eGFP or their wild-type counterparts. In all cell lines, expression of the Y10F and N255A mutants significantly reduced cell viability when kept in suspension. Data are expressed as number of live cells (* indicates P value <0.05;** indicates P value <0.005, *** indicates P value is <0.001).

3.11 Characterization of PANX1$^{1-99}$ truncated peptide expression

One PANX1 mutation that has been found in NB specimens is a missense mutation at c.295G>T predicted to generate a 99 aa peptide of ~10 kDa. In order to examine if any of our patient-derived NB tumour cell lines express this mutation, primers were produced to flank upstream and downstream of the mutation site and genomic DNA was amplified by PCR. PCR products were purified and sent for sequencing using the TCAG Center for Applied Genomics (Toronto SickKids). However, this PANX1 mutation was not found in our NB cell lines.

Since PANX1$^{1-99}$ was not expressed in any of our NB cell lines, site-directed mutagenesis was performed to engineer the PANX1$^{1-99}$ construct. In order to start assessing the effect of this mutation, PANX1$^{1-99}$ was transiently transfected into HEK293T, SK-N-Be(2), and SH-SY5Y. Its expression was then examined by western blotting using a commercially available PANX1 antibody recognizing a portion of N-terminal domain (98% homology to the PANX1$^{1-99}$). As shown in Figure 17A, PANX$^{1-99}$ was successfully expressed at ~10 kDa after 48hrs post-transfection. As data from our lab suggests that PANX1 can be degraded by the proteasome, we next assessed the effect of proteasomal degradation on the levels of PANX$^{1-99}$. PANX$^{1-99}$ levels increased after treatment with the proteasomal inhibitor MG132, suggesting that its levels are regulated by proteasomal degradation (Figure 17B).

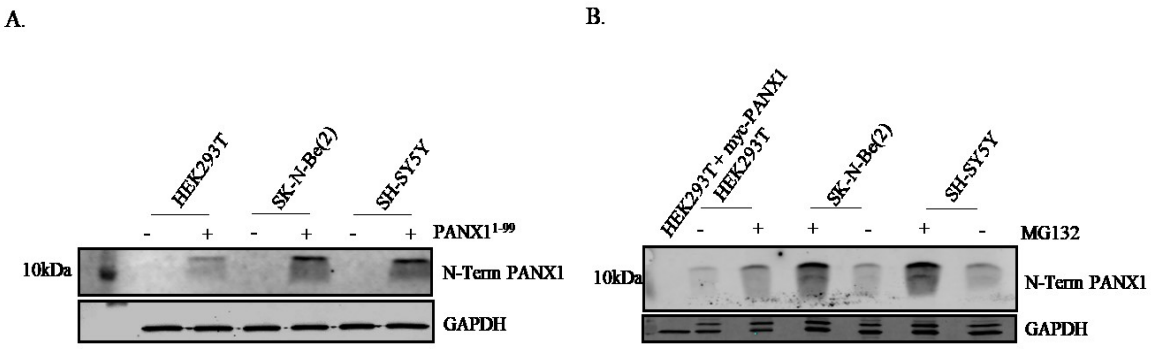

Figure 17: Characterization of PANX1$^{1-99}$ truncated peptide expression. A) PANX1$^{1-99}$ is detected as a ~10 kDa species in HEK293T, SK-N-Be(2), and SH-SY5Y cell lines using an anti-PANX1 antibody recognizing an epitope at the N-terminal domain of PANX1 (N=3). B) Inhibition of proteasomal degradation by MG132 treatment increased PANX1$^{1-99}$ levels (N=3).

3.12 Co-expression of PANX$^{1-99}$ with PANX1 causes reduced channel activity

To assess the channel activity of PANX1$^{1-99}$, a high potassium (50 mM) induced dye uptake assay was performed as described earlier. Interestingly, a smaller truncated peptide PANX1$^{1-89}$ resulted in a significant increase in PANX1 channel activity when co-expressed with PANX1^{162}. In order to determine whether the PANX1$^{1-99}$ peptide has a similar effect, Ad293 cells expressing PANX1$^{1-99}$ and/or myc-PANX1 were incubated in high (50 mM) and low (5 mM) potassium solutions and assessed for dye uptake. As shown in Figure 18, expression of myc-PANX1 resulted in a significant increase in dye uptake. The dye uptake of cells expressing PANX1$^{1-99}$ however was similar to those expressing a control vector. While these results suggest that PANX1$^{1-99}$ does not form active channels at the cell surface, when co-expressed with myc-PANX1, PANX$^{1-99}$ significantly decreased PANX1 channel activity.

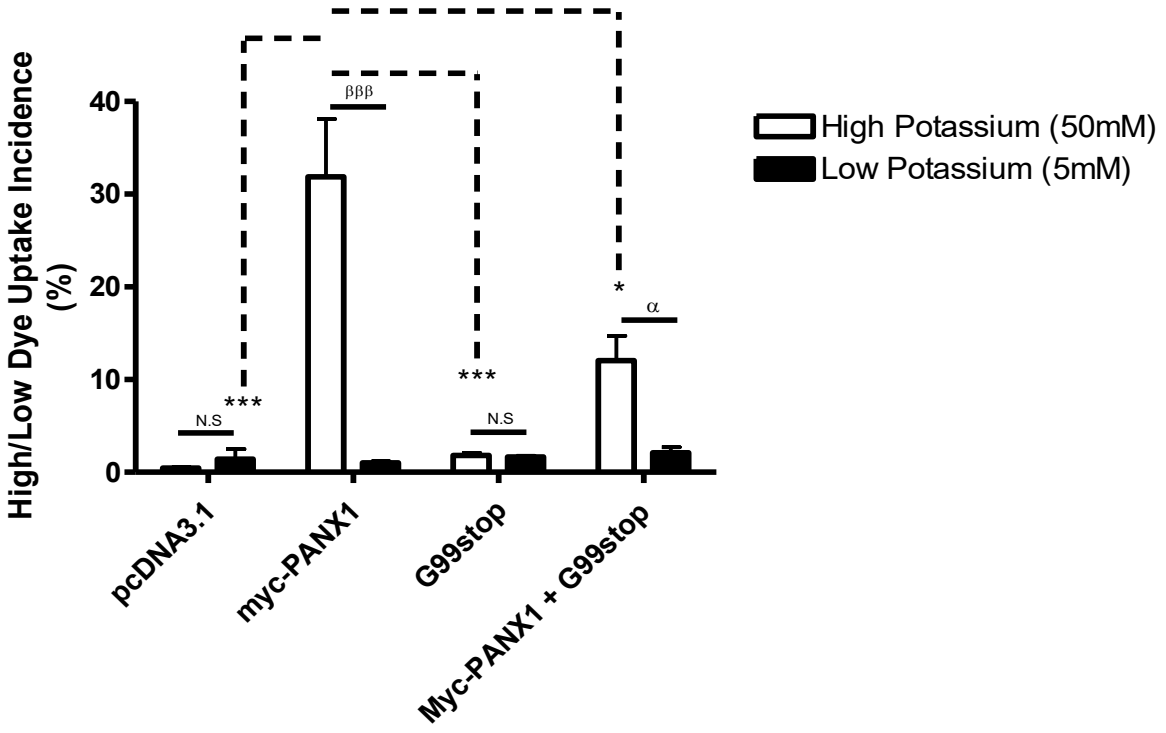

Figure 18: Co-expression of PANX1$^{1-99}$ with myc-PANX1 results in reduced channel activity in ad293 cells. A) Ad293 cells were co-transfected with myc-PANX1 + pcDNA3.1, PANX1$^{1-99}$ + pcDNA3.1, pcDNA3.1, or myc-PANX1 + PANX1$^{1-99}$ and submitted to dye uptake assays in high or low potassium conditions. Data are expressed as dye uptake incidence (N=3; *** P=<0.001 comparison to myc-PANX1 (high potassium); α P=<0.05 comparison to myc-PANX1 + PANX1$^{1-99}$; βββ P=<0.001 to myc-PANX1 in both high and low potassium conditions).

4.0 Discussion

Previous work from our laboratory investigated the role of PANX1 channels in NB. We have shown that PANX1 is expressed in our seven NB tumour specimens and patient-derived NB cell lines and that inhibiting PANX1 channel function using the clinically-approved drugs, PBN and CBX, inhibits NB progression *in vitro* and *in vivo* (unpublished data; St-Pierre, Holland, *et al.*). Interestingly, we observed that while PANX1 was also detected in control neurons by western blotting, its banding pattern was strikingly different as a band at around ~50 kDa was found in all NB cell lines, but not in neurons (shown in Figure 6A and B of the introduction). These data suggested that PANX1 may be differentially modified by post-translational modifications (PTMs) in NB. To investigate whether this ~50 kDa species is PANX1 specific, a doxycycline-inducible shRNA system was used to knockdown PANX1 expression. ShRNA targeting PANX1 successfully reduced the known Gly0, Gly1, and Gly2 forms of PANX1 as well as the ~50 kDa species indicating that the ~50 kDa species also corresponds to PANX1. Using deglycosylation enzymes, we have shown here that this ~50 kDa PANX1 species is glycosylated. Interestingly, PANX1 has been identified as a potential biomarker for traumatic brain injury and concussion patients[171]. PANX1 is significantly increased in blood serum after brain impact has occurred and its levels strongly and negatively correlated with the Glasgow Coma Scale (designed in 1974, provides a practical method for assessment of impairment in level of consciousness in response to certain stimuli)[171]. Thus, it would be of great interest to fully characterize the ~50 kDa PANX1 species, examine its role in NB, and determine whether it could constitute a novel prognostic indicator for NB patients.

Murine Panx1 is glycosylated at N254[175,204,235,241,242] and based on sequence homology, human PANX1 is predicted to be glycosylated at N255. Interestingly, Y10 phosphorylated

PANX1 peptides were isolated in a mass spectroscopy screen performed in NB by Palacios-Moreno et al., 2015[238]. After examination of PANX1/Panx1 sequence in various species, Y10 appears to be highly conserved. In order to examine the role of these PTMs in regulating PANX1 expression, channel activity, and function in NB, the myc-tagged N255A and Y10F were engineered. Myc-N255A was detected as one PANX1 species by western blotting, Gly0, while myc-Y10F was detected as two PANX1 species, Gly0 and Gly1. Gly0 represents an unglycosylated PANX1 species found in the ER, Gly1 represents a high-mannose PANX1 species that can be found in the ER and Golgi apparatus, Gly2 is a complex glycosylated species thought to be localized to the plasma membrane[136,185]. Based on this, one can suspect that the levels of the N255A and Y10F mutants at the cell surface may be minimal as both lack the Gly2 species. Immunofluorescence microscopy and cell surface biotinylation assays indicate that the levels of N255A mutant at the cell surface is reduced compared to that of wild-type PANX1. While immunolocalization data suggest that the Y10F mutant is mainly localized in intracellular compartments, the cell surface biotinylation experiments did not show a statistically significant difference when compared to that of PANX1. The profile of the Y10F mutant by western blot and immunofluorescence studies strongly suggest that its localization at the cell surface is highly reduced. These experiments were done 48 hours post-transfection. However, since it was noticed that the expression of the Y10F construct induced cell death at this time point, cell surface biotinylation assays were performed 24 hours post-transfection to prevent entry of biotin into the dying cells. At this time point, Y10F localization at the cell surface was reduced but not statistically significantly. All together, these results suggest that glycosylation at N255 and phosphorylation at Y10 regulate PANX1 cell surface localization.

The present study confirmed that presence of N-linked glycosylation of PANX1 after treatment with N-Glycanase and PNGaseF. N255 appears to be the sole glycosylation site of PANX1, as this mutant is detected as only one species that does not migrate further following treatment with N-linked glycan PNGaseF. On the other hand, the myc-Y10F is glycosylated as our western blot analysis revealed that while it is detected as two bands (Gly0 and Gly1) it migrated further into one single band following treatment with PNGaseF. Based on what is known about mouse Panx1, these results would suggest that the myc-Y10F mutant is glycosylated to the high mannose species (Gly1). This finding may suggest that phosphorylation on Y10 is part of the process leading to the PANX1 complex glycosylated species Gly2 and localization at the cell surface. Panx1 trafficking to the cell surface has been shown to be regulated by N-linked glycosylation and a Sar1-mediated COPII dependent manner[185]. Furthermore, Panx1 interacts with actin microfilaments through its C-terminus regulating Panx1 cell surface localization[185].

Furthermore, we have shown that myc-Y10F and myc-N255A mutants have reduced channel activity when compared to that of myc-PANX1. This reduction in channel activity of the myc-N255A mutant may be due to its decreased localization at the plasma membrane, as evidenced by our cell surface biotinylation assay. Mutation of the Y10 site abolished PANX1 channel activity as the channel activity of the myc-Y10F mutant was not further diminished in the presence of CBX or PBN. These results may suggest that Y10 phosphorylation is essential for PANX1 channel activity. In the conditions in which dye uptake was assessed (24 hours post transfection), there was a slight reduction in myc-Y10F at the cell surface when compared to myc-PANX1 but this was not statistically significant. Phosphorylation on Y10 may thus directly regulate PANX1 channel function. However, based on the banding pattern seen by

western blotting 48 hours post transfection, we cannot exclude an effect on localization at the cell surface. Since unpublished data from our laboratory revealed that inhibition of PANX1 channels inhibits NB progression *in vitro* and *in vivo*, the effect of expressing the myc-N255A and myc-Y10F on NB cell proliferation was examined. We found that expression of myc-Y10F and myc-255A, in NB results in reduced cell proliferation in all seven patient-derived NB cell lines. We have also found that expression of myc-N255A and more so myc-Y10F reduced the viability of NB cell when kept in suspension, suggesting is a reduction in metastatic potential. Thus, further exploration into the role of these PTMs in NB and the identification of the molecular mechanisms involved in the glycosylation and/or phosphorylation of PANX1 may open potential therapeutic avenues.

Interestingly, computational analysis of PANX1 interactors using PathwayNet (www.pathwaynet.princeton.edu) identified several potential glycosylating enzymes that may modulate PANX1 glycosylation. Some of these include α-1,3-mannosyl-glycoprotein 2-β-acetylglucosaminyltransferase (MGAT1), α-1,3-mannosyl-glycoprotein 4-β-acetylglucosaminyltransferase (MGAT4B), collagen β(1-O) galactosyltransferase (GLT25D1), and UDP-Glucose glycoprotein glycosyltransferase 1 (UGGT1). MGAT1 and MGAT4B serve as mannosyl transferases that could glycosylate PANX1 into the Gly1 high mannose species. GLT25D1 and UGGT1 on the other hand may function in the generation of the Gly2 complex glycosylated species. GLT25D1 encodes for an α1-2 glucosyltransferase enzyme[243,244]. UGGT1 serves as endoplasmic reticulum quality control and adds additional glucose moieties to N-linked glycoproteins, promoting solubility from the ER[245,246]. Notably, UGGT1 serves as trafficking correction from the ER[246]. In terms of assessing phosphorylation at Y10, several computational databases are available to examine for candidate kinases.

Indeed, NetPhos 3.1 revealed that Y10 may be phosphorylated by Src, Insulin Receptor (INSR), and Epidermal Growth Factor Receptor (EGFR). KinasePhos2 revealed additional potential kinases such as the Src family tyrosine kinase, Fgr; anaplastic lymphoma kinase (ALK), platelet derived growth factor receptor (PDGFR), Bruton's tyrosine kinase (BTK), proto-oncogene (Ret), insulin growth factor receptor 1 (IGF1R), Ephrin receptor (EPH), Janus kinase 2 (JAK2), tyrosine kinase 2 (TYK2), proto-oncogene, (Fes), Zeta chain of T-cell receptor associated protein (ZAP70), fibroblast growth factor receptor 1 (FGFR1) and proto oncogene (Lyn). Interestingly, it has been previously reported that Src phosphorylates PANX1 at tyrosine 198 (Y198) at the plasma membrane regulating its channel activity[208,209]. Src has also been linked to Panx1 phosphorylation at Y308, which was required for Panx1 channel activation during excitotoxicity[207]. In NB, Src family kinases have been shown to be highly expressed compared to control CNS tissues[247,248]. Furthermore, recent therapeutic advancements showed that inhibiting Src family kinase activity using SI 34 and bosutinib reduces NB tumour growth rate, suggesting that Src activity may modulate the NB malignant phenotype[249,250]. JAK2 on the other hand activates STAT3 activity, which is increased in NB tumours[251]. In NB, JAK/STAT3 signalling activates interleukin-6 (IL-6) which aids in the ability of NB cells to migrate and invade bone marrow as metastases[252,253]. Treatment with sorafenib, which inhibits JAK2 activity, reduced NB growth and activated apoptotic pathways[254]. ALK has been implicated in NB pathogenesis through the acquisition of point mutations located in its kinase activity domain. ALK gain-of-function mutations result in increase activity, which may contribute to PANX1 phosphorylation in the NB phenotype[59,76,81]. As Y10 of PANX1 has shown to be phosphorylated in NB, and the present study shows that preventing its phosphorylation by site-directed mutagenesis reduces NB

proliferation and metastatic spread, targeting this phosphorylation site may have therapeutic potential for patients with NB.

While PANX1 can be modified by PTMs, analysis using the COSMIC database revealed two PANX1 mutation sites. The first site is a splicing mutation before the 4th and largest exon produced a 181 aa peptide (PANX1$^{1-181}$) and the second is a missense mutation in the 2nd exon producing a 99 aa peptide (PANX1$^{1-99}$). In order to study the role of PANX1$^{1-99}$ in NB, a PANX1$^{1-99}$ construct was generated using site-directed mutagenesis. PANX1$^{1-99}$ was detected as a ~10 kDa protein and its levels were increased following treatment with the proteasome inhibitor MG132. While PANX1 is thought to be degraded mainly via the lysosomal pathway[206], our data suggest that PANX1$^{1-99}$ can be degraded by the proteasome. Interestingly, a missense mutation producing PANX1$^{1-89}$ is expressed in highly metastatic breast cancer cells and increased channel activity when co-expressed with PANX1^{162} promoting breast metastatic spread[162]. As opposed to PANX1$^{1-89}$, our data revealed that, when co-expressed with myc-PANX1, PANX1$^{1-99}$ reduced PANX1 channel activity. One possible explanation for this is that PANX1$^{1-99}$ contains ten additional amino acids, as compared to that of PANX1$^{1-89}$, which correspond to the exact sequence of the PANX1 mimetic peptide channel inhibitor, ^{10}Panx1. As the expression of PANX1$^{1-89}$, reported in Furlow et al, does not contain the ^{10}Panx1 inhibitor sequence, this may explain the lack of inhibitory action of this peptide in their study. Based on our data suggesting that inhibition of PANX1 channel activity inhibits NB malignant properties, expression of PANX1$^{1-99}$ may be beneficial for NB patients. In order to test this possibility, the effect of PANX1$^{1-99}$ on NB progression *in vitro* and *in vivo* would need to be examined.

While the mechanism by which PANX1 channel activity promotes NB progression needs to be further investigated, it likely involves ATP release. PANX1 associated channel activity has been established to promote proliferation, through metabotropic and ionotropic receptors[194,255]. Most notably, extracellular ATP efflux by PANX1 results in the activation of P2Y1, which are coupled to G_q modulating intracellular calcium and cAMP concentrations[211]. As explained above, increases in intracellular calcium can further activate PANX1 channels[178,179]. In lung cancer, increased extracellular ATP activates P2X and P2Y receptors, which induces increased cytosolic calcium concentration[256]. This rise in cytosolic calcium been shown to increase the ratio of anti-apoptotic/pro-apoptotic proteins Bcl-2/Bax, which promote cell survival, and progression into the vasculature[256]. Furthermore, PANX1 activity has been implicated in breast cancer metastasis. As mentioned above, highly metastatic breast cancer cells express a truncated $PANX1^{1-89}$ peptide, which has been shown to increase PANX1 channel activity and promote breast cancer metastasis[162]. In human and murine melanoma, PANX1/Panx1 levels are up-regulated and inhibiting PANX1/Panx1 channels reduce ATP release, triggers melanoma differentiation into a melanocytic phenotype, and reduce tumour growth[161,163].

In conclusion, we have found that the ~50 kDa PANX1 species expressed in NB patient-derived cell lines, but not in neurons, corresponds to a PANX1 glycosylated species. We have further assessed the implications of PANX1 PTMs in regulating its channel function in NB and the potential downstream biological effects. Indeed, our data revealed that glycosylation of PANX1 at N255 and phosphorylation at Y10 regulate PANX1 channel function, as well as the proliferation and metastatic potential of NB cells *in vitro*. These data suggest that preventing glycosylation at N255 and/or phosphorylation at Y10 may have

therapeutic potential. We have also found that the PANX1 mutation leading to the expression of PANX1$^{1-99}$ could potentially be beneficial for NB patients as its co-expression with myc-PANX1, reduced PANX1 channel activity. Based on the importance of PANX1 channel activity in regulating NB malignant properties, future studies should focus on elucidating the PANX1 interactome, the molecular pathways that lead to PANX1 glycosylation on N255 and phosphorylation on Y10, as well as further examine the effects of PANX1$^{1-99}$ on NB tumour growth and metastatic spread *in vivo*.

5.0 References

1. Newbern, J. M. Molecular Control of the Neural Crest and Peripheral Nervous System Development. *Curr. Top. Dev. Biol.* **111**, 201 (2015).

2. Young, H. M. & Newgreen, D. Enteric neural crest-derived cells: Origin, identification, migration, and differentiation. *Anat. Rec.* **262**, 1–15 (2001).

3. Sommer, L. Generation of melanocytes from neural crest cells. *Pigment Cell Melanoma Res.* **24**, 411–421 (2011).

4. Woodhoo, A. & Sommer, L. Development of the Schwann cell lineage: From the neural crest to the myelinated nerve. *Glia* **56**, 1481–1490 (2008).

5. Kasemeier-Kulesa, J. C., Kulesa, P. M. & Lefcort, F. Imaging neural crest cell dynamics during formation of dorsal root ganglia and sympathetic ganglia. *Development* **132**, 235–245 (2005).

6. YAMAMOTO, M., YANAI, R. & ARISHIMA, K. Study of Migration of Neural Crest Cells to Adrenal Medulla by Three-Dimensional Reconstruction. *J. Vet. Med. Sci.* **66**, 635–641 (2004).

7. Hall, B. K. The induction of neural crest-derived cartilage and bone by embryonic epithelia: an analysis of the mode of action of an epithelialmesenchymal interaction. *Development* **64**, (1981).

8. Xu, W. *et al.* Human iPSC-Derived Neural Crest Stem Cells Promote Tendon Repair in a Rat Patellar Tendon Window Defect Model. *Tissue Eng. Part A* **19**, 2439 (2013).

9. Rinon, A. *et al.* Cranial neural crest cells regulate head muscle patterning and

differentiation during vertebrate embryogenesis. *Development* **134**, 3065–3075 (2007).

10. Adams, M. S. & Bronner-Fraser, M. Review: The Role of Neural Crest Cells in the Endocrine System. *Endocr. Pathol.* **20**, 92–100 (2009).

11. Billon, N. *et al.* The generation of adipocytes by the neural crest. *Development* **134**, 2283–2292 (2007).

12. Sadler, T. W. Embryology of neural tube development. *Am. J. Med. Genet. Part C Semin. Med. Genet.* **135C**, 2–8 (2005).

13. Nikolopoulou, E., Galea, G. L., Rolo, A., Greene, N. D. E. & Copp, A. J. Neural tube closure: cellular, molecular and biomechanical mechanisms. *Development* **144**, 552–566 (2017).

14. Scarpa, E. *et al.* Cadherin Switch during EMT in Neural Crest Cells Leads to Contact Inhibition of Locomotion via Repolarization of Forces. *Dev. Cell* **34**, 421 (2015).

15. Alfandari, D. *et al.* Xenopus ADAM 13 is a metalloprotease required for cranial neural crest-cell migration. *Curr. Biol.* **11**, 918–30 (2001).

16. Plouhinec, J.-L. *et al.* Pax3 and Zic1 trigger the early neural crest gene regulatory network by the direct activation of multiple key neural crest specifiers. *Dev. Biol.* **386**, 461–472 (2014).

17. Monsoro-Burq, A.-H., Wang, E. & Harland, R. Msx1 and Pax3 Cooperate to Mediate FGF8 and WNT Signals during Xenopus Neural Crest Induction. *Dev. Cell* **8**, 167–178 (2005).

18. Ikenouchi, J., Matsuda, M., Furuse, M. & Tsukita, S. Regulation of tight junctions during the epithelium-mesenchyme transition: direct repression of the gene expression of claudins/occludin by Snail. *J. Cell Sci.* **116**, 1959–1967 (2003).

19. Taneyhill, L. A., Coles, E. G. & Bronner-Fraser, M. Snail2 directly represses cadherin6B during epithelial-to-mesenchymal transitions of the neural crest. *Development* **134**, 1481–1490 (2007).

20. Sewell, M. J., Chiu, Y. E. & Drolet, B. A. Neural Tube Dysraphism: Review of Cutaneous Markers and Imaging. *Pediatr. Dermatol.* **32**, 161–170 (2015).

21. Goldstein, A. M., Brewer, K. C., Doyle, A. M., Nagy, N. & Roberts, D. J. BMP signaling is necessary for neural crest cell migration and ganglion formation in the enteric nervous system. *Mech. Dev.* **122**, 821–833 (2005).

22. Leung, A. W. *et al.* WNT/β-catenin signaling mediates human neural crest induction via a pre-neural border intermediate. *Development* **143**, 398–410 (2016).

23. Szemes, M., Greenhough, A. & Malik, K. Wnt Signaling Is a Major Determinant of Neuroblastoma Cell Lineages. *Front. Mol. Neurosci.* **12**, 90 (2019).

24. Jaroonwitchawan, T., Muangchan, P. & Noisa, P. Inhibition of FGF signaling accelerates neural crest cell differentiation of human pluripotent stem cells. *Biochem. Biophys. Res. Commun.* **481**, 176–181 (2016).

25. John, N., Cinelli, P., Wegner, M. & Sommer, L. Transforming Growth Factor β-Mediated Sox10 Suppression Controls Mesenchymal Progenitor Generation in Neural Crest Stem Cells. *Stem Cells* **29**, 689–699 (2011).

26. Li, D. *et al.* FOXD3 is a novel tumor suppressor that affects growth, invasion, metastasis and angiogenesis of neuroblastoma. *Oncotarget* **4**, 2021–44 (2013).

27. Pattyn, A., Morin, X., Cremer, H., Goridis, C. & Brunet, J.-F. The homeobox gene Phox2b is essential for the development of autonomic neural crest derivatives. *Nature* **399**, 366–370 (1999).

28. Stanke, M., Stubbusch, J. & Rohrer, H. Interaction of Mash1 and Phox2b in sympathetic neuron development. *Mol. Cell. Neurosci.* **25**, 374–382 (2004).

29. Wylie, L. A., Hardwick, L. J. A., Papkovskaia, T. D., Thiele, C. J. & Philpott, A. Ascl1 phospho-status regulates neuronal differentiation in a Xenopus developmental model of neuroblastoma. *Dis. Model. Mech.* **8**, 429–441 (2015).

30. Lan, M. S. & Breslin, M. B. Structure, expression, and biological function of INSM1 transcription factor in neuroendocrine differentiation. *FASEB J.* **23**, 2024–33 (2009).

31. Lucas, M. E., Müller, F., Rüdiger, R., Henion, P. D. & Rohrer, H. The bHLH transcription factor hand2 is essential for noradrenergic differentiation of sympathetic neurons. *Development* **133**, 4015–24 (2006).

32. Kerosuo, L. *et al.* Enhanced expression of MycN/CIP2A drives neural crest toward a neural stem cell-like fate: Implications for priming of neuroblastoma. *Proc. Natl. Acad. Sci.* **115**, E7351–E7360 (2018).

33. Peng, H. *et al.* Essential role of GATA3 in regulation of differentiation and cell proliferation in SK-N-SH neuroblastoma cells. *Mol. Med. Rep.* **11**, 881–6 (2015).

34. Tsarovina, K. Essential role of Gata transcription factors in sympathetic neuron

development. *Development* **131**, 4775–4786 (2004).

35. Mitchell, P. J., Timmons, P. M., Hebert, J. M., Rigby, P. W. & Tjian, R. Transcription factor AP-2 is expressed in neural crest cell lineages during mouse embryogenesis. *Genes Dev.* **5**, 105–119 (1991).

36. Hirsch, M. R., Tiveron, M. C., Guillemot, F., Brunet, J. F. & Goridis, C. Control of noradrenergic differentiation and Phox2a expression by MASH1 in the central and peripheral nervous system. *Development* **125**, 599–608 (1998).

37. McKeown, S. J., Lee, V. M., Bronner-Fraser, M., Newgreen, D. F. & Farlie, P. G. Sox10 overexpression induces neural crest-like cells from all dorsoventral levels of the neural tube but inhibits differentiation. *Dev. Dyn.* **233**, 430–444 (2005).

38. Potzer, M. R. *et al.* Sequential requirement of Sox4 and Sox11 during development of sympathetic nervous system. *Development* **137**, 775–784 (2010).

39. Vogel, K. S. & Weston, J. A. The sympathoadrenal lineage in avian embryos: I. Adrenal chromaffin cells lose neuronal traits during embryogenesis. *Dev. Biol.* **139**, 1–12 (1990).

40. Evinger, M. J., Ernsberger, P., Regunathan, S. & Reis, D. J. Regulation of phenylethanolamine N-methyltransferase gene expression by imidazoline receptors in adrenal chromaffin cells. *J. Neurochem.* **65**, 988–97 (1995).

41. Morii, H., Shiraishi-Yamaguchi, Y. & Mori, N. SCG10, a microtubule destabilizing factor, stimulates the neurite outgrowth by modulating microtubule dynamics in rat hippocampal primary cultured neurons. *J. Neurobiol.* **66**, 1101–1114 (2006).

42. Monclair, T. *et al.* The International Neuroblastoma Risk Group (INRG) staging system: an INRG Task Force report. *J. Clin. Oncol.* **27**, 298–303 (2009).

43. London, W. B. *et al.* Evidence for an age cutoff greater than 365 days for neuroblastoma risk group stratification in the Children's Oncology Group. *J. Clin. Oncol.* **23**, 6459–65 (2005).

44. Vo, K. T. *et al.* Clinical, Biologic, and Prognostic Differences on the Basis of Primary Tumor Site in Neuroblastoma: A Report From the International Neuroblastoma Risk Group Project. *J. Clin. Oncol.* **32**, 3169–3176 (2014).

45. Campbell, K. *et al.* Association of MYCN Copy Number with Clinical Features, Tumor Biology, and Outcomes in Neuroblastoma: A Report from the Children's Oncology Group. *Cancer* **123**, 4224 (2017).

46. DuBois, S. G. *et al.* Metastatic sites in stage IV and IVS neuroblastoma correlate with age, tumor biology, and survival. *J. Pediatr. Hematol. Oncol.* **21**, 181–9

47. Guglielmi, L. *et al.* MYCN gene expression is required for the onset of the differentiation programme in neuroblastoma cells. *Cell Death Dis.* **5**, e1081 (2014).

48. Kramer, M., Ribeiro, D., Arsenian-Henriksson, M., Deller, T. & Rohrer, H. Proliferation and Survival of Embryonic Sympathetic Neuroblasts by MYCN and Activated ALK Signaling. *J. Neurosci.* **36**, 10425–10439 (2016).

49. Zimmerman, K. A. *et al.* Differential expression of myc family genes during murine development. *Nature* **319**, 780–783 (1986).

50. Matthay, K. K. *et al.* Neuroblastoma. *Nat. Rev. Dis. Prim.* **2**, 16078 (2016).

51. Irwin, M. S. & Park, J. R. Neuroblastoma. *Pediatr. Clin. North Am.* **62**, 225–256 (2015).

52. Taggart, D. R. *et al.* Prognostic value of the stage 4S metastatic pattern and tumor biology in patients with metastatic neuroblastoma diagnosed between birth and 18 months of age. *J. Clin. Oncol.* **29**, 4358–64 (2011).

53. Valentijn, L. J. *et al.* Functional MYCN signature predicts outcome of neuroblastoma irrespective of MYCN amplification. *Proc. Natl. Acad. Sci. U. S. A.* **109**, 19190–5 (2012).

54. Zhang, J. T. *et al.* MycN Is Critical for the Maintenance of Human Embryonic Stem Cell-Derived Neural Crest Stem Cells. *PLoS One* **11**, e0148062 (2016).

55. Dzieran, J. *et al.* MYCN-amplified neuroblastoma maintains an aggressive and undifferentiated phenotype by deregulation of estrogen and NGF signaling. *Proc. Natl. Acad. Sci. U. S. A.* **115**, E1229–E1238 (2018).

56. Olsen, R. R. *et al.* MYCN induces neuroblastoma in primary neural crest cells. *Oncogene* **36**, 5075–5082 (2017).

57. Powers, J. T. *et al.* Multiple mechanisms disrupt the let-7 microRNA family in neuroblastoma. *Nature* **535**, 246–251 (2016).

58. Molenaar, J. J. *et al.* LIN28B induces neuroblastoma and enhances MYCN levels via let-7 suppression. *Nat. Genet.* **44**, 1199–1206 (2012).

59. De Wilde, B. *et al.* The mutational landscape of MYCN, Lin28b and ALK F1174L driven murine neuroblastoma mimics human disease. *Oncotarget* **9**,

8334–8349 (2018).

60. Janoueix-Lerosey, I. *et al.* Molecular analysis of chromosome arm 17q gain in neuroblastoma. *Genes. Chromosomes Cancer* **28**, 276–84 (2000).

61. Janoueix-Lerosey, I. *et al.* Somatic and germline activating mutations of the ALK kinase receptor in neuroblastoma. *Nature* **455**, 967–970 (2008).

62. Bresler, S. C. *et al.* ALK Mutations Confer Differential Oncogenic Activation and Sensitivity to ALK Inhibition Therapy in Neuroblastoma. *Cancer Cell* **26**, 682–694 (2014).

63. Iwahara, T. *et al.* Molecular characterization of ALK, a receptor tyrosine kinase expressed specifically in the nervous system. *Oncogene* **14**, 439–449 (1997).

64. Degoutin, J., Brunet-de Carvalho, N., Cifuentes-Diaz, C. & Vigny, M. ALK (Anaplastic Lymphoma Kinase) expression in DRG neurons and its involvement in neuron-Schwann cells interaction. *Eur. J. Neurosci.* **29**, 275–286 (2009).

65. Van den Eynden, J. *et al.* Phosphoproteome and gene expression profiling of ALK inhibition in neuroblastoma cell lines reveals conserved oncogenic pathways. *Sci. Signal.* **11**, eaar5680 (2018).

66. Hasan, M. K. *et al.* ALK is a MYCN target gene and regulates cell migration and invasion in neuroblastoma. *Sci. Rep.* **3**, 3450 (2013).

67. Zhu, S. *et al.* Activated ALK collaborates with MYCN in neuroblastoma pathogenesis. *Cancer Cell* **21**, 362–73 (2012).

68. Jakovljević, G., Čulić, S., Stepan, J., Bonevski, A. & Seiwerth, S. Vascular endothelial

growth factor in children with neuroblastoma: a retrospective analysis. *J. Exp. Clin. Cancer Res.* **28**, 143 (2009).

69. Påhlman, S. & Mohlin, S. Hypoxia and hypoxia-inducible factors in neuroblastoma. *Cell Tissue Res.* **372**, 269–275 (2018).

70. Zimmerman, M. W. *et al.* MYC Drives a Subset of High-Risk Pediatric Neuroblastomas and Is Activated through Mechanisms Including Enhancer Hijacking and Focal Enhancer Amplification. (2018). doi:10.1158/2159-8290.CD-17-0993

71. Sattu, K. *et al.* Phosphoproteomic analysis of anaplastic lymphoma kinase (ALK) downstream signaling pathways identifies signal transducer and activator of transcription 3 as a functional target of activated ALK in neuroblastoma cells. *FEBS J.* **280**, 5269–5282 (2013).

72. Wood, A. C. *et al.* Dual ALK and CDK4/6 Inhibition Demonstrates Synergy against Neuroblastoma. *Clin. Cancer Res.* **23**, 2856–2868 (2017).

73. Azuhata, T. *et al.* The inhibitor of apoptosis protein survivin is associated with high-risk behavior of neuroblastoma. *J. Pediatr. Surg.* **36**, 1785–1791 (2001).

74. Claeys, S. *et al.* ALK positively regulates MYCN activity through repression of HBP1 expression. *Oncogene* **38**, 2690–2705 (2019).

75. Megison, M. L., Gillory, L. A. & Beierle, E. A. Cell survival signaling in neuroblastoma. *Anticancer. Agents Med. Chem.* **13**, 563–75 (2013).

76. Reiff, T. *et al.* Midkine and Alk signaling in sympathetic neuron proliferation and neuroblastoma predisposition. *Development* **138**, 4699–708 (2011).

77. Miyazaki, M. *et al.* The p53 activator overcomes resistance to ALK inhibitors by regulating p53-target selectivity in ALK-driven neuroblastomas. *Cell Death Discov.* **4**, 56 (2018).

78. Wang, H. Q. *et al.* Combined ALK and MDM2 inhibition increases antitumor activity and overcomes resistance in human ALK mutant neuroblastoma cell lines and xenograft models. *Elife* **6**, (2017).

79. Robbins, H. L. & Hague, A. The PI3K/Akt Pathway in Tumors of Endocrine Tissues. *Front. Endocrinol. (Lausanne).* **6**, 188 (2016).

80. Bai, R. Y., Dieter, P., Peschel, C., Morris, S. W. & Duyster, J. Nucleophosmin-anaplastic lymphoma kinase of large-cell anaplastic lymphoma is a constitutively active tyrosine kinase that utilizes phospholipase C-gamma to mediate its mitogenicity. *Mol. Cell. Biol.* **18**, 6951–61 (1998).

81. Osajima-Hakomori, Y. *et al.* Biological Role of Anaplastic Lymphoma Kinase in Neuroblastoma. *Am. J. Pathol.* **167**, 213–222 (2005).

82. Slupianek, A. *et al.* Role of phosphatidylinositol 3-kinase-Akt pathway in nucleophosmin/anaplastic lymphoma kinase-mediated lymphomagenesis. *Cancer Res.* **61**, 2194–9 (2001).

83. Amin, H. M. *et al.* Selective inhibition of STAT3 induces apoptosis and G1 cell cycle arrest in ALK-positive anaplastic large cell lymphoma. *Oncogene* **23**, 5426–5434 (2004).

84. Mosse, Y. P. *et al.* Germline PHOX2B mutation in hereditary neuroblastoma. *Am. J. Hum. Genet.* **75**, 727–30 (2004).

85. Di Zanni, E. *et al.* Targeting of PHOX2B expression allows the identification of drugs effective in counteracting neuroblastoma cell growth. *Oncotarget* **8**, 72133–72146 (2017).

86. Pei, D. *et al.* Distinct Neuroblastoma-associated Alterations of PHOX2B Impair Sympathetic Neuronal Differentiation in Zebrafish Models. *PLoS Genet.* **9**, e1003533 (2013).

87. Morikawa, Y. *et al.* BMP signaling regulates sympathetic nervous system development through Smad4-dependent and -independent pathways. *Development* **136**, 3575 (2009).

88. Raabe, E. H. *et al.* Prevalence and functional consequence of PHOX2B mutations in neuroblastoma. *Oncogene* **27**, 469–476 (2008).

89. Moriguchi, T. *et al.* Gata3 participates in a complex transcriptional feedback network to regulate sympathoadrenal differentiation. *Development* **133**, 3871–81 (2006).

90. Molenaar, J. J. *et al.* Cyclin D1 is a direct transcriptional target of GATA3 in neuroblastoma tumor cells. *Oncogene* **29**, 2739–2745 (2010).

91. Hadjidaniel, M. D. *et al.* Tumor-associated macrophages promote neuroblastoma via STAT3 phosphorylation and up-regulation of c-MYC. *Oncotarget* **8**, 91516–91529 (2017).

92. Bettinsoli, P., Ferrari-Toninelli, G., Bonini, S. A., Prandelli, C. & Memo, M. Notch ligand Delta-like 1 as a novel molecular target in childhood neuroblastoma. *BMC Cancer* **17**, 352 (2017).

93. Selmi, A. *et al.* TWIST1 is a direct transcriptional target of MYCN and MYC in neuroblastoma. *Cancer Lett.* **357**, 412–418 (2015).

94. Zeid, R. *et al.* Enhancer invasion shapes MYCN-dependent transcriptional amplification in neuroblastoma. *Nat. Genet.* **50**, 515–523 (2018).

95. Muraji, T., Okamoto, E., Fujimoto, J., Suita, S. & Nakagawara, A. Combined determination of N-myc oncogene amplification and DNA ploidy in neuroblastoma. Complementary prognostic indicators. *Cancer* **72**, 2763–8 (1993).

96. Look, A. T., Hayes, F. A., Nitschke, R., McWilliams, N. B. & Green, A. A. Cellular DNA Content as a Predictor of Response to Chemotherapy in Infants with Unresectable Neuroblastoma. *N. Engl. J. Med.* **311**, 231–235 (1984).

97. Guo, C. *et al.* Allelic deletion at 11q23 is common in MYCN single copy neuroblastomas. *Oncogene* **18**, 4948–4957 (1999).

98. Marshall, B., Isidro, G., Martins, A. G. & Boavida, M. G. Loss of heterozygosity at chromosome 9p21 in primary neuroblastomas: evidence for two deleted regions. *Cancer Genet. Cytogenet.* **96**, 134–9 (1997).

99. Weiss, M. J. *et al.* Localization of a hereditary neuroblastoma predisposition gene to 16p12-p13. *Med. Pediatr. Oncol.* **35**, 526–30 (2000).

100. Ejeskär, K., Aburatani, H., Abrahamsson, J., Kogner, P. & Martinsson, T. Loss of heterozygosity of 3p markers in neuroblastoma tumours implicate a tumour-suppressor locus distal to the FHIT gene. *Br. J. Cancer* **77**, 1787–1791 (1998).

101. Fong, C.-T. *et al. Loss of Heterozygosity for Chromosomes 1 or 14 Defines Subsets of*

Advanced Neuroblastomas1. *CANCER RESEARCH* **52**, (1992).

102. Mora, J., Cheung, N. K., Chen, L., Qin, J. & Gerald, W. Loss of heterozygosity at 19q13.3 is associated with locally aggressive neuroblastoma. *Clin. Cancer Res.* **7**, 1358–61 (2001).

103. Caron, H. *et al.* Allelic loss of the short arm of chromosome 4 in neuroblastoma suggests a novel tumour suppressor gene locus. *Hum. Genet.* **97**, 834–7 (1996).

104. Caron, H. *et al.* Allelic loss of chromosome 1p36 in neuroblastoma is of preferential maternal origin and correlates with N–myc amplification. *Nat. Genet.* **4**, 187–190 (1993).

105. Pezzolo, A. *et al.* Presence of 1q gain and absence of 7p gain are new predictors of local or metastatic relapse in localized resectable neuroblastoma. *Neuro. Oncol.* **11**, 192–200 (2009).

106. Attiyeh, E. F. *et al.* Chromosome 1p and 11q Deletions and Outcome in Neuroblastoma. *N. Engl. J. Med.* **353**, 2243–2253 (2005).

107. Jeison, M. *et al.* 2p24 Gain region harboring MYCN gene compared with MYCN amplified and nonamplified neuroblastoma: biological and clinical characteristics. *Am. J. Pathol.* **176**, 2616–25 (2010).

108. Takita, J. *et al.* Allelic imbalance on chromosome 18 in neuroblastoma. *Eur. J. Cancer* **36**, 508–13 (2000).

109. Maris, J. M. *et al.* Region-specific detection of neuroblastoma loss of heterozygosity at multiple loci simultaneously using a SNP-based tag-array platform. *Genome Res.*

15, 1168–76 (2005).

110. O'Neill, S. *et al.* MYCN amplification and 17q in neuroblastoma: evidence for structural association. *Genes. Chromosomes Cancer* **30**, 87–90 (2001).

111. Peifer, M. *et al.* Telomerase activation by genomic rearrangements in high-risk neuroblastoma. *Nature* **526**, 700–4 (2015).

112. Molenaar, J. J. *et al.* Sequencing of neuroblastoma identifies chromothripsis and defects in neuritogenesis genes. *Nature* **483**, 589–593 (2012).

113. Tonini, G. P. Growth, progression and chromosome instability of Neuroblastoma: a new scenario of tumorigenesis? *BMC Cancer* **17**, 20 (2017).

114. Panchina, Y. *et al.* A ubiquitous family of putative gap junction molecules. *Curr. Biol.* **10**, R473–R474 (2000).

115. Panchin, Y. V. Evolution of gap junction proteins--the pannexin alternative. *J. Exp. Biol.* **208**, 1415–9 (2005).

116. Sosinsky, G. E. *et al.* Pannexin channels are not gap junction hemichannels. *Channels* **5**, 193–197 (2011).

117. Ambrosi, C. *et al.* Pannexin1 and Pannexin2 Channels Show Quaternary Similarities to Connexons and Different Oligomerization Numbers from Each Other * □ S Downloaded from. *J. Biol. Chem.* **285**, 24420–24431 (2010).

118. Yen, M. R. & Saier, M. H. Gap junctional proteins of animals: The innexin/pannexin superfamily. *Prog. Biophys. Mol. Biol.* **94**, 5–14 (2007).

119. Zhao, H.-B. Expression and function of pannexins in the inner ear and hearing. *BMC*

Cell Biol. **17 Suppl 1**, 16 (2016).

120. Chen, J., Liang, C., Zong, L., Zhu, Y. & Zhao, H.-B. Knockout of Pannexin-1 Induces Hearing Loss. *Int. J. Mol. Sci.* **19**, (2018).

121. Chen, J., Zhu, Y., Liang, C., Chen, J. & Zhao, H.-B. Pannexin1 channels dominate ATP release in the cochlea ensuring endocochlear potential and auditory receptor potential generation and hearing OPEN. (2015). doi:10.1038/srep10762

122. Kurtenbach, S., Kurtenbach, S. & Zoidl, G. Emerging functions of pannexin 1 in the eye. *Front. Cell. Neurosci.* **8**, 263 (2014).

123. Huang, Y.-J. *et al.* The role of pannexin 1 hemichannels in ATP release and cell-cell communication in mouse taste buds. *Proc. Natl. Acad. Sci. U. S. A.* **104**, 6436–41 (2007).

124. Zhang, H., Chen, Y. & Zhang, C. Patterns of heterogeneous expression of pannexin 1 and pannexin 2 transcripts in the olfactory epithelium and olfactory bulb. *J. Mol. Histol.* **43**, 651–660 (2012).

125. Bruzzone, R., Hormuzdi, S. G., Barbe, M. T., Herb, A. & Monyer, H. Pannexins, a family of gap junction proteins expressed in brain. *Proc. Natl. Acad. Sci. U. S. A.* **100**, 13644 (2003).

126. Zoidl, G. *et al.* Localization of the pannexin1 protein at postsynaptic sites in the cerebral cortex and hippocampus. *Neuroscience* **146**, 9–16 (2007).

127. Weickert, S., Ray, A., Zoidl, G. & Dermietzel, R. Expression of neural connexins and pannexin1 in the hippocampus and inferior olive: a quantitative approach. *Mol. Brain*

Res. **133**, 102–109 (2005).

128. Locovei, S., Bao, L. & Dahl, G. Pannexin 1 in erythrocytes: function without a gap. *Proc. Natl. Acad. Sci. U. S. A.* **103**, 7655–9 (2006).

129. Lohman, A. W., Billaud, M. & Isakson, B. E. Mechanisms of ATP release and signalling in the blood vessel wall. *Cardiovasc. Res.* **95**, 269 (2012).

130. Kienitz, M.-C., Bender, K., Dermietzel, R., Pott, L. & Zoidl, G. Pannexin 1 constitutes the large conductance cation channel of cardiac myocytes. *J. Biol. Chem.* **286**, 290–8 (2011).

131. Li, S. *et al.* Expression and roles of pannexins in ATP release in the pituitary gland. *Endocrinology* **152**, 2342–52 (2011).

132. Alhouayek, M., Sorti, R., Gilthorpe, J. D. & Fowler, C. J. Role of pannexin-1 in the cellular uptake, release and hydrolysis of anandamide by T84 colon cancer cells. *Sci. Rep.* **9**, 7622 (2019).

133. Penuela, S. *et al.* Pannexin 1 and pannexin 3 are glycoproteins that exhibit many distinct characteristics from the connexin family of gap junction proteins. *J. Cell Sci.* **120**, 3772–3783 (2007).

134. Momboisse, F. *et al.* Pannexin 1 channels: new actors in the regulation of catecholamine release from adrenal chromaffin cells. *Front. Cell. Neurosci.* **8**, 270 (2014).

135. Ransford, G. A. *et al.* Pannexin 1 contributes to ATP release in airway epithelia. *Am. J. Respir. Cell Mol. Biol.* **41**, 525–34 (2009).

136. Cowan, K. N., Langlois, S., Penuela, S., Cowan, B. J. & Laird, D. W. Pannexin1 and Pannexin3 Exhibit Distinct Localization Patterns in Human Skin Appendages and are Regulated during Keratinocyte Differentiation and Carcinogenesis. *Cell Commun. Adhes.* **19**, 45–53 (2012).

137. Celetti, S. J. *et al.* Implications of pannexin 1 and pannexin 3 for keratinocyte differentiation. *J. Cell Sci.* **123**, 1363–1372 (2010).

138. Langlois, S. & Cowan, K. N. Regulation of Skeletal Muscle Myoblast Differentiation and Proliferation by Pannexins. in *Advances in experimental medicine and biology* **925**, 57–73 (2017).

139. Diezmos, E. F. *et al.* Expression and localization of pannexin-1 hemichannels in human colon in health and disease. *Neurogastroenterol. Motil.* **25**, e395–e405 (2013).

140. Baranova, A. *et al.* The mammalian pannexin family is homologous to the invertebrate innexin gap junction proteins. *Genomics* **83**, 706–716 (2004).

141. Le Vasseur, M., Lelowski, J., Bechberger, J. F., Sin, W.-C. & Naus, C. C. Pannexin 2 protein expression is not restricted to the CNS. *Front. Cell. Neurosci.* **8**, 392 (2014).

142. Iwamoto, T. *et al.* Pannexin 3 regulates proliferation and differentiation of odontoblasts via its hemichannel activities. *PLoS One* **12**, e0177557 (2017).

143. Wang, X.-H., Streeter, M., Liu, Y.-P. & Zhao, H.-B. Identification and characterization of pannexin expression in the mammalian cochlea. *J. Comp. Neurol.* **512**, 336–346 (2009).

144. Bond, S. R. *et al.* Pannexin 3 is a novel target for Runx2, expressed by osteoblasts and

mature growth plate chondrocytes. *J. Bone Miner. Res.* **26**, 2911–2922 (2011).

145. Nyberg, M. *et al.* Probenecid Inhibits α-Adrenergic Receptor–Mediated Vasoconstriction in the Human Leg Vasculature. *Hypertension* **71**, 151–159 (2018).

146. Medler, K. F. Honing in on the ATP Release Channel in Taste Cells. *Chem. Senses* **40**, 449–51 (2015).

147. Romanov, R. A. *et al.* The ATP permeability of pannexin 1 channels in a heterologous system and in mammalian taste cells is dispensable. *J. Cell Sci.* **125**, 5514–23 (2012).

148. Adamson, S. E. *et al.* Pannexin 1 is required for full activation of insulin-stimulated glucose uptake in adipocytes. *Mol. Metab.* **4**, 610–618 (2015).

149. Tozzi, M. *et al.* The P2X7 receptor and pannexin-1 are involved in glucose-induced autocrine regulation in β-cells. *Sci. Rep.* **8**, 8926 (2018).

150. Ohbuchi, T. *et al.* Possible contribution of pannexin-1 to ATP release in human upper airway epithelia. *Physiol. Rep.* **2**, e00227 (2014).

151. Thompson, R. J., Zhou, N. & MacVicar, B. A. Ischemia opens neuronal gap junction hemichannels. *Science* **312**, 924–7 (2006).

152. Thompson, R. J. *et al.* Activation of Pannexin-1 Hemichannels Augments Aberrant Bursting in the Hippocampus. *Science (80-.).* **322**, 1555–1559 (2008).

153. Aquilino, M. S., Whyte-Fagundes, P., Zoidl, G. & Carlen, P. L. Pannexin-1 channels in epilepsy. *Neurosci. Lett.* **695**, 71–75 (2019).

154. Michalski, K. & Kawate, T. Carbenoxolone inhibits Pannexin1 channels through interactions in the first extracellular loop. *J. Gen. Physiol.* **147**, 165 (2016).

155. Ma, W., Hui, H., Pelegrin, P. & Surprenant, A. Pharmacological Characterization of Pannexin-1 Currents Expressed in Mammalian Cells. *J. Pharmacol. Exp. Ther.* **328**, 409–418 (2009).

156. Silverman, W. R. *et al.* The pannexin 1 channel activates the inflammasome in neurons and astrocytes. *J. Biol. Chem.* **284**, 18143–51 (2009).

157. Elliott, M. R. *et al.* Nucleotides released by apoptotic cells act as a find-me signal to promote phagocytic clearance. *Nature* **461**, 282–286 (2009).

158. Mouasni, S. *et al.* The classical NLRP3 inflammasome controls FADD unconventional secretion through microvesicle shedding. *Cell Death Dis.* **10**, 190 (2019).

159. Bergsbaken, T., Fink, S. L., den Hartigh, A. B., Loomis, W. P. & Cookson, B. T. Coordinated host responses during pyroptosis: caspase-1-dependent lysosome exocytosis and inflammatory cytokine maturation. *J. Immunol.* **187**, 2748–54 (2011).

160. Sandilos, J. K. *et al.* Pannexin 1, an ATP release channel, is activated by caspase cleavage of its pore-associated C-terminal autoinhibitory region. *J. Biol. Chem.* **287**, 11303–11 (2012).

161. Penuela, S. *et al.* Loss of pannexin 1 attenuates melanoma progression by reversion to a melanocytic phenotype. *J. Biol. Chem.* **287**, 29184–93 (2012).

162. Furlow, P. W. *et al.* Mechanosensitive pannexin-1 channels mediate microvascular metastatic cell survival. *Nat. Cell Biol.* **17**, 943 (2015).

163. Freeman, T. *et al.* Inhibition of Pannexin 1 Reduces the Tumorigenic Properties of

Human Melanoma Cells. *Cancers (Basel).* **11**, 102 (2019).

164. Burma, N. E. *et al.* Blocking microglial pannexin-1 channels alleviates morphine withdrawal in rodents. *Nat. Med.* **23**, 355–360 (2017).

165. Good, M. E. *et al.* Endothelial cell Pannexin1 modulates severity of ischemic stroke by regulating cerebral inflammation and myogenic tone. *JCI Insight* **3**, (2018).

166. Bargiotas, P. *et al.* Pannexins in ischemia-induced neurodegeneration. *Proc. Natl. Acad. Sci. U. S. A.* **108**, 20772 (2011).

167. Diezmos, E. F., Bertrand, P. P. & Liu, L. Purinergic Signaling in Gut Inflammation: The Role of Connexins and Pannexins. *Front. Neurosci.* **10**, 311 (2016).

168. Diezmos, E. F. *et al.* Blockade of Pannexin-1 Channels and Purinergic P2X7 Receptors Shows Protective Effects Against Cytokines-Induced Colitis of Human Colonic Mucosa. *Front. Pharmacol.* **9**, 865 (2018).

169. Zhang, Y., Laumet, G., Chen, S.-R., Hittelman, W. N. & Pan, H.-L. Pannexin-1 Up-regulation in the Dorsal Root Ganglion Contributes to Neuropathic Pain Development. *J. Biol. Chem.* **290**, 14647–55 (2015).

170. Swayne, L. A., Sorbara, C. D. & Bennett, S. A. L. Pannexin 2 is expressed by postnatal hippocampal neural progenitors and modulates neuronal commitment. *J. Biol. Chem.* **285**, 24977–86 (2010).

171. Zhou, K. Q., Green, C. R., Bennet, L., Gunn, A. J. & Davidson, J. O. The Role of Connexin and Pannexin Channels in Perinatal Brain Injury and Inflammation. *Front. Physiol.* **10**, 141 (2019).

172. Boassa, D. *et al.* Pannexin1 channels contain a glycosylation site that targets the hexamer to the plasma membrane. *J. Biol. Chem.* **282**, 31733–43 (2007).

173. Chiu, Y.-H. *et al.* A quantized mechanism for activation of pannexin channels. *Nat. Commun.* **8**, 14324 (2017).

174. Laird, D. W. Life cycle of connexins in health and disease. *Biochem. J.* **394**, 527–43 (2006).

175. Sanchez-Pupo, R. E., Johnston, D. & Penuela, S. N-Glycosylation Regulates Pannexin 2 Localization but Is Not Required for Interacting with Pannexin 1. *Int. J. Mol. Sci.* **19**, (2018).

176. Bruzzone, R., Barbe, M. T., Jakob, N. J. & Monyer, H. Pharmacological properties of homomeric and heteromeric pannexin hemichannels expressed in Xenopus oocytes. *J. Neurochem.* **92**, 1033–1043 (2005).

177. Chekeni, F. B. *et al.* Pannexin 1 channels mediate 'find-me' signal release and membrane permeability during apoptosis. *Nature* **467**, 863–7 (2010).

178. Locovei, S., Wang, J. & Dahl, G. Activation of pannexin 1 channels by ATP through P2Y receptors and by cytoplasmic calcium. *FEBS Lett.* **580**, 239–244 (2006).

179. Vanden Abeele, F. *et al.* Functional implications of calcium permeability of the channel formed by pannexin 1. *J. Cell Biol.* **174**, 535–46 (2006).

180. Locovei, S., Scemes, E., Qiu, F., Spray, D. C. & Dahl, G. Pannexin1 is part of the pore forming unit of the P2X(7) receptor death complex. *FEBS Lett.* **581**, 483–8 (2007).

181. Qiu, F. & Dahl, G. A permeant regulating its permeation pore: inhibition of pannexin

1 channels by ATP. *Am. J. Physiol. Cell Physiol.* **296**, C250-5 (2009).

182. Kurtenbach, S. *et al.* Pannexin1 Channel Proteins in the Zebrafish Retina Have Shared and Unique Properties. *PLoS One* **8**, e77722 (2013).

183. Seminario-Vidal, L. *et al.* Thrombin promotes release of ATP from lung epithelial cells through coordinated activation of rho- and Ca2+-dependent signaling pathways. *J. Biol. Chem.* **284**, 20638–48 (2009).

184. Bao, L., Locovei, S. & Dahl, G. Pannexin membrane channels are mechanosensitive conduits for ATP. *FEBS Lett.* **572**, 65–68 (2004).

185. Bhalla-Gehi, R., Penuela, S., Churko, J. M., Shao, Q. & Laird, D. W. Pannexin1 and pannexin3 delivery, cell surface dynamics, and cytoskeletal interactions. *J. Biol. Chem.* **285**, 9147–60 (2010).

186. Jackson, D. G., Wang, J., Keane, R. W., Scemes, E. & Dahl, G. ATP and potassium ions: a deadly combination for astrocytes. *Sci. Rep.* **4**, 4576 (2015).

187. Gödecke, S. *et al.* Thrombin-induced ATP release from human umbilical vein endothelial cells. *Am. J. Physiol. Physiol.* **302**, C915–C923 (2012).

188. Orellana, J. A. *et al.* Pannexin1 hemichannels are critical for HIV infection of human primary CD4+ T lymphocytes. *J. Leukoc. Biol.* **94**, 399–407 (2013).

189. Velasquez, S., Malik, S., Lutz, S. E., Scemes, E. & Eugenin, E. A. Pannexin1 Channels Are Required for Chemokine-Mediated Migration of CD4+ T Lymphocytes: Role in Inflammation and Experimental Autoimmune Encephalomyelitis. *J. Immunol.* **196**, 4338–47 (2016).

190. Davidson, J. S. & Baumgarten, I. M. Glycyrrhetinic acid derivatives: a novel class of inhibitors of gap-junctional intercellular communication. Structure-activity relationships. *J. Pharmacol. Exp. Ther.* **246**, 1104–7 (1988).

191. Pinder, R. M. *et al.* Carbenoxolone. *Drugs* **11**, 245–307 (1976).

192. Sagar, G. D. V. & Larson, D. M. Carbenoxolone inhibits junctional transfer and upregulates connexin43 expression by a protein kinase A-dependent pathway. *J. Cell. Biochem.* **98**, 1543–1551 (2006).

193. Silverman, W., Locovei, S. & Dahl, G. Probenecid, a gout remedy, inhibits pannexin 1 channels. *Am. J. Physiol. Cell Physiol.* **295**, C761-7 (2008).

194. Pelegrin, P. & Surprenant, A. Pannexin-1 mediates large pore formation and interleukin-1beta release by the ATP-gated P2X7 receptor. *EMBO J.* **25**, 5071–82 (2006).

195. Wang, J., Ma, M., Locovei, S., Keane, R. W. & Dahl, G. Modulation of membrane channel currents by gap junction protein mimetic peptides: size matters. *Am. J. Physiol. Physiol.* **293**, C1112–C1119 (2007).

196. Wang, J., Jackson, D. G. & Dahl, G. The food dye FD&C Blue No. 1 is a selective inhibitor of the ATP release channel Panx1. *J. Gen. Physiol.* **141**, 649–56 (2013).

197. Beckel, J. M. *et al.* Pannexin 1 channels mediate the release of ATP into the lumen of the rat urinary bladder. *J. Physiol.* **593**, 1857–1871 (2015).

198. Cea, L. A., Riquelme, M. A., Vargas, A. A., Urrutia, C. & SÃ¡ez, J. C. Pannexin 1

channels in skeletal muscles. *Front. Physiol.* **5**, 139 (2014).

199. Poon, I. K. H. *et al.* Unexpected link between an antibiotic, pannexin channels and apoptosis. *Nature* **507**, 329–34 (2014).

200. Garg, C. *et al.* Trovafloxacin attenuates neuroinflammation and improves outcome after traumatic brain injury in mice. *J. Neuroinflammation* **15**, 42 (2018).

201. Moremen, K. W., Tiemeyer, M. & Nairn, A. V. Vertebrate protein glycosylation: diversity, synthesis and function. *Nat. Rev. Mol. Cell Biol.* **13**, 448–462 (2012).

202. Aebi, M. N-linked protein glycosylation in the ER. *Biochim. Biophys. Acta - Mol. Cell Res.* **1833**, 2430–2437 (2013).

203. Roth, J. & Zuber, C. Quality control of glycoprotein folding and ERAD: the role of N-glycan handling, EDEM1 and OS-9. *Histochem. Cell Biol.* **147**, 269–284 (2017).

204. Penuela, S., Bhalla, R., Nag, K. & Laird, D. W. Glycosylation regulates pannexin intermixing and cellular localization. *Mol. Biol. Cell* **20**, 4313–23 (2009).

205. Sang, Q. *et al.* A pannexin 1 channelopathy causes human oocyte death. *Sci. Transl. Med.* **11**, eaav8731 (2019).

206. Gehi, R., Shao, Q. & Laird, D. W. Pathways Regulating the Trafficking and Turnover of Pannexin1 Protein and the Role of the C-terminal Domain. *J. Biol. Chem.* **286**, 27639–27653 (2011).

207. Weilinger, N. L. *et al.* Metabotropic NMDA receptor signaling couples Src family kinases to pannexin-1 during excitotoxicity. *Nat. Neurosci.* **19**, 432–442 (2016).

208. DeLalio, L. J. *et al.* Constitutive SRC-mediated phosphorylation of pannexin 1 at

tyrosine 198 occurs at the plasma membrane. *J. Biol. Chem.* **294**, 6940–6956 (2019).

209. Lohman, A. W. *et al.* Pannexin 1 channels regulate leukocyte emigration through the venous endothelium during acute inflammation. *Nat. Commun.* **6**, 7965 (2015).

210. Billaud, M. *et al.* Pannexin1 regulates α1-adrenoreceptor-mediated vasoconstriction. *Circ. Res.* **109**, 80 (2011).

211. Riquelme, M. A. *et al.* The ATP required for potentiation of skeletal muscle contraction is released via pannexin hemichannels. *Neuropharmacology* **75**, 594–603 (2013).

212. Rose, A. J., Alsted, T. J., Kobberø, J. B. & Richter, E. A. Regulation and function of Ca2+-calmodulin-dependent protein kinase II of fast-twitch rat skeletal muscle. *J. Physiol.* **580**, 993–1005 (2007).

213. Poornima, V., Vallabhaneni, S., Mukhopadhyay, M. & Bera, A. K. Nitric oxide inhibits the pannexin 1 channel through a cGMP–PKG dependent pathway. *Nitric Oxide* **47**, 77–84 (2015).

214. Xiao, F. *et al.* Lipoapoptosis induced by saturated free fatty acids stimulates monocyte migration: a novel role for Pannexin1 in liver cells. *Purinergic Signal.* **11**, 347–59 (2015).

215. Xiao, F., Waldrop, S. L., Khimji, A. & Kilic, G. Pannexin1 contributes to pathophysiological ATP release in lipoapoptosis induced by saturated free fatty acids in liver cells. *Am. J. Physiol. Cell Physiol.* **303**, C1034-44 (2012).

216. Lauber, K., Blumenthal, S. G., Waibel, M. & Wesselborg, S. Clearance of Apoptotic

Cells: Getting Rid of the Corpses. *Mol. Cell* **14**, 277–287 (2004).

217. Straub, A. C. *et al.* Compartmentalized Connexin 43-Nitrosylation/Denitrosylation Regulates Heterocellular Communication in the Vessel Wall. *Arterioscler. Thromb. Vasc. Biol.* **31**, 399–407 (2011).

218. Asada, K., Kurokawa, J. & Furukawa, T. Redox- and calmodulin-dependent S-nitrosylation of the KCNQ1 channel. *J. Biol. Chem.* **284**, 6014–20 (2009).

219. Yoshida, T. *et al.* Nitric oxide activates TRP channels by cysteine S-nitrosylation. *Nat. Chem. Biol.* **2**, 596–607 (2006).

220. Aracena-Parks, P. *et al.* Identification of cysteines involved in S-nitrosylation, S-glutathionylation, and oxidation to disulfides in ryanodine receptor type 1. *J. Biol. Chem.* **281**, 40354–68 (2006).

221. Takahashi, H. *et al.* Hypoxia enhances S-nitrosylation-mediated NMDA receptor inhibition via a thiol oxygen sensor motif. *Neuron* **53**, 53–64 (2007).

222. Lohman, A. W. *et al.* S-nitrosylation inhibits pannexin 1 channel function. (2012). doi:10.1074/jbc.M112.397976

223. Thompson, R. J. Pannexin channels and ischaemia. *J. Physiol.* **593**, 3463 (2015).

224. Lai, C. P. K. *et al.* Tumor-Suppressive Effects of Pannexin 1 in C6 Glioma Cells. *Cancer Res.* **67**, 1545–1554 (2007).

225. Song, B. *et al.* Identify lymphatic metastasis-associated genes in mouse hepatocarcinoma cell lines using gene chip. *World J. Gastroenterol.* **11**, 1463–72 (2005).

226. Derangère, V. *et al.* Liver X receptor β activation induces pyroptosis of human and murine colon cancer cells. *Cell Death Differ.* **21**, 1914–24 (2014).

227. Largo, C. *et al.* Identification of overexpressed genes in frequently gained/amplified chromosome regions in multiple myeloma. *Haematologica* **91**, 184–91 (2006).

228. Boyd-Tressler, A., Penuela, S., Laird, D. W. & Dubyak, G. R. Chemotherapeutic Drugs Induce ATP Release via Caspase-gated Pannexin-1 Channels and a Caspase/Pannexin-1-independent Mechanism. *J. Biol. Chem.* **289**, 27246–27263 (2014).

229. Schalper, K. A., Carvajal-Hausdorf, D. & Oyarzo, M. P. Possible role of hemichannels in cancer. *Front. Physiol.* **5**, 237 (2014).

230. Xiang, X. *et al.* Oncogenesis Pannexin 1 inhibits rhabdomyosarcoma progression through a mechanism independent of its canonical channel function. **7**, 89 (2018).

231. Bao, B. A., Lai, C. P., Naus, C. C. & Morgan, J. R. Pannexin1 drives multicellular aggregate compaction via a signaling cascade that remodels the actin cytoskeleton. *J. Biol. Chem.* **287**, 8407–16 (2012).

232. Dean, D. M. & Morgan, J. R. Cytoskeletal-Mediated Tension Modulates the Directed Self-Assembly of Microtissues. *Tissue Eng. Part A* **14**, 1989–1997 (2008).

233. Wicki-Stordeur, L. E., Dzugalo, A. D., Swansburg, R. M., Suits, J. M. & Swayne, L. A. Pannexin 1 regulates postnatal neural stem and progenitor cell proliferation. *Neural Dev.* **7**, 11 (2012).

234. Liu, H. *et al.* In vitro effect of Pannexin 1 channel on the invasion and migration of I-

10 testicular cancer cells via ERK1/2 signaling pathway. *Biomed. Pharmacother.* **117**, 109090 (2019).

235. Langlois, S. *et al.* Pannexin 1 and pannexin 3 channels regulate skeletal muscle myoblast proliferation and differentiation. *J. Biol. Chem.* **289**, 30717–31 (2014).

236. Langlois, S. *et al.* Membrane type 1-matrix metalloproteinase induces endothelial cell morphogenic differentiation by a caspase-dependent mechanism. *Exp. Cell Res.* **307**, 452–464 (2005).

237. Solan, J. L. & Lampe, P. D. Connexin43 phosphorylation: structural changes and biological effects. *Biochem. J.* **419**, 261–272 (2009).

238. Palacios-Moreno, J. *et al.* Neuroblastoma tyrosine kinase signaling networks involve FYN and LYN in endosomes and lipid rafts. *PLoS Comput. Biol.* **11**, e1004130 (2015).

239. Penuela, S., Bhalla, R., Nag, K. & Laird, D. W. Glycosylation Regulates Pannexin Intermixing and Cellular Localization. *Mol. Biol. Cell* **20**, 4313–4323 (2009).

240. Skrenkova, K. *et al.* N-Glycosylation Regulates the Trafficking and Surface Mobility of GluN3A-Containing NMDA Receptors. *Front. Mol. Neurosci.* **11**, 188 (2018).

241. Boassa, D. *et al.* Pannexin1 Channels Contain a Glycosylation Site That Targets the Hexamer to the Plasma Membrane * Downloaded from. *NUMBER 43 J. Biol. Chem.* **282**, 31733–31743 (2007).

242. Penuela, S. *et al.* Pannexin 1 and pannexin 3 are glycoproteins that exhibit many distinct characteristics from the connexin family of gap junction proteins. *Cell Sci.*

120, 3772–3783 (2007).

243. Liefhebber, J. M., Punt, S., Spaan, W. J. & van Leeuwen, H. C. The human collagen beta(1-O)galactosyltransferase, GLT25D1, is a soluble endoplasmic reticulum localized protein. *BMC Cell Biol.* **11**, 33 (2010).

244. Baumann, S. & Hennet, T. Collagen Accumulation in Osteosarcoma Cells lacking GLT25D1 Collagen Galactosyltransferase. *J. Biol. Chem.* **291**, 18514–24 (2016).

245. Ferris, S. P., Jaber, N. S., Molinari, M., Arvan, P. & Kaufman, R. J. UDP-glucose:glycoprotein glucosyltransferase (UGGT1) promotes substrate solubility in the endoplasmic reticulum. *Mol. Biol. Cell* **24**, 2597 (2013).

246. Takeda, Y. *et al.* Both isoforms of human UDP-glucose:glycoprotein glucosyltransferase are enzymatically active. *Glycobiology* **24**, 344–350 (2014).

247. O'Shaughnessy, J., Deseau, V., Amini, S., Rosen, N. & Bolen, J. B. Analysis of the c-src gene product structure, abundance, and protein kinase activity in human neuroblastoma and glioblastoma cells. *Oncogene Res.* **2**, 1–18 (1987).

248. Matsunaga, T. *et al.* Neuronal src and trk a protooncogene expression in neuroblastomas and patient prognosis. *Int. J. cancer* **79**, 226–31 (1998).

249. Navarra, M. *et al.* Antiproliferative and pro-apoptotic effects afforded by novel Src-kinase inhibitors in human neuroblastoma cells. *BMC Cancer* **10**, 602 (2010).

250. Bieerkehazhi, S. *et al.* Novel Src/Abl tyrosine kinase inhibitor bosutinib suppresses neuroblastoma growth via inhibiting Src/Abl signaling. *Oncotarget* **8**, 1469–1480 (2017).

251. Haura, E. B., Turkson, J. & Jove, R. Mechanisms of Disease: insights into the emerging role of signal transducers and activators of transcription in cancer. *Nat. Clin. Pract. Oncol.* **2**, 315–324 (2005).

252. Jorcyk, C., Tawara, K. & Jorcyk, C. L. Clinical significance of interleukin (IL)-6 in cancer metastasis to bone: potential of anti-IL-6 therapies. *Cancer Manag. Res.* **3**, 177 (2011).

253. Bollrath, J. *et al.* gp130-Mediated Stat3 Activation in Enterocytes Regulates Cell Survival and Cell-Cycle Progression during Colitis-Associated Tumorigenesis. *Cancer Cell* **15**, 91–102 (2009).

254. Yang, F. *et al.* Sorafenib inhibits endogenous and IL-6/S1P induced JAK2-STAT3 signaling in human neuroblastoma, associated with growth suppression and apoptosis. *Cancer Biol. Ther.* **13**, 534–541 (2012).

255. Tackett, B. C. *et al.* P2Y2 purinergic receptor activation is essential for efficient hepatocyte proliferation in response to partial hepatectomy. *Am. J. Physiol. Gastrointest. Liver Physiol.* **307**, G1073-87 (2014).

256. Song, S. *et al.* ATP promotes cell survival via regulation of cytosolic [Ca2+] and Bcl-2/Bax ratio in lung cancer cells. *Am. J. Physiol. Cell Physiol.* **310**, C99-114 (2016).